12-2009

Bartonella Henselae Inhibits Cellular Apoptotic Regulators to Ensure Survival

Jeffery Todd Parker
Georgia State University

BARTONELLA HENSELAE INHIBITS CELLULAR APOPTOTIC REGULATORS TO ENSURE SURVIVAL

By

JEFFERY TODD PARKER

Under the Direction of Barbara R. Baumstark

ABSTRACT

Human pathogens survive anti-pathogen host immune assault by either circumventing or evading the host immune response. *Bartonella henselae*, an intracellular pathogen previously shown to disrupt intrinsic apoptotic messengers to enhance its survival, exploits multiple facets of the cellular apoptotic mechanisms.

Cellular pathways affected by apoptotic processes were assessed using real-time reverse-transcriptase-polymerase-chain-reaction (rRT-PCR) to measure the effect of *B. henselae* on cell regulator gene expression (TRADD, FADD, caspase-8 and caspase-3), caspase activity, DNA cell cycle analysis, cell regulator protein expression and overall cell viability and morphology. The presence of *B. henselae* suppresses overall gene expression for TRADD and FADD and it dramatically suppresses ceramide-induced TRADD and FADD gene expression. The presence of *B. henselae* has a noticeable effect on ceramide-induced caspase-8 and caspase-3 gene expression. Only caspase-3 enzymatic activity was ceramide-induced and likewise supressed by

the presence of *B. henselae*, whereas caspase-6 and caspase-8 were unaffected and equivalent to controls. The presence of *B. henselae* inhibits ceramide-induced DNA fragmentation, maintains overall cell morphology and enhances host cell viability. Lastly, *B. henselae* inhibits the time-dependant ceramide-induction of TRADD protein and suppresses ubiquitous FADD protein expression.

We demonstrated that *B. henselae* inhibits apoptotic induction in a systematic manner following exogenous apoptotic induction. *B. henselae* protection of microvascular endothelial cells from apoptosis induction begins at the modulation of cell surface receptor-dependent signaling. *B. henselae* minimizes, but does not completely abrogate, the cytotoxic effect of the apoptogenic shingolipid ceramide on human microvascular endothelial cells (CDC.EU.HMEC-1).

Broadening our understanding of the sequence of cell regulator suppression events by intracellular pathogens will provide insight into disease manifestation. Further, understanding how infected cells initiate and conclude apoptosis will open new avenues into the study of disease treatment.

INDEX WORDS: *Bartonella henselae*, Apoptosis, Ceramide, TRADD, FADD, Caspase, Real-time RT-PCR

BARTONELLA HENSELAE INHIBITS CELLULAR APOPTOTIC REGULATORS TO ENSURE SURVIVAL

by

JEFFERY TODD PARKER

A Dissertation Submitted in Partial Fulfillment of the Requirements for the Degree of

Doctor of Philosophy

in the College of Arts and Sciences

Georgia State University

2009

BARTONELLA HENSELAE INHIBITS CELLULAR APOPTOTIC REGULATORS TO ENSURE SURVIVAL

By

JEFFERY TODD PARKER

Committee Chair: Barbara R. Baumstark

Committee: Julia Hilliard
Zehava Eichenbaum

Electronic Version Approved:

Office of Graduate Studies
College of Arts and Sciences
Georgia State University
December 2009

To my wife, Irene, and daughter McKenna….this is as much yours as mine.

To the late Mr. Steve Sisson, you were such an inspiration.

To my late grandfather Joe….to someday becoming the man you always were.

ACKNOWLEDGEMENTS

I thank my Lord for giving me the strength to see this through.

I thank the following people for their support and contributions, My wife Irene for standing by me through it all, my daughter M^{c}Kenna for being so patient, Anne Whitney my partner-in-arms and *compadré*, Dr. Michael Bowen for scientific wisdom, Dr. Jonas Winchell for being the best “devil’s advocate”, Erin Black for the “mountain of ways” you’ve helped, Bill Morrill for enduring my endless gripe sessions, Kathy Thurman for your insight, Dr. Mark Rigler for your guidance to persevere. To all my other friends for your prayers and support-- I can never thank you enough.

To my committee members, Dr. Zehava Eichenbaum and Dr. Julia Hilliard for your critiques, and a special thank you to Dr. Barbara Baumstark--the best teacher ever. Thanks for all the great stories.

TABLE OF CONTENTS

ACKNOWLEDGEMENTS v

LIST OF TABLES viii

LIST OF FIGURES ix

LIST OF ABBREVIATIONS xi

CHAPTER

1. GENERAL INTRODUCTION 1

Overview 1

Apoptosis Pathways of Induction 2

The Extrinsic Pathway 3

Caspase-8 Activation 4

Activation of Other Caspases 7

The Intrinsic Pathway 8

Ceramide and Ceramide Signaling 12

Bartonella and Host Cell Survival 14

Bartonella and Apoptosis Suppression 15

Summary 17

2. BARTONELLA HENSELAE INHIBITION OF APOPTOSIS MODULATORS 18

Introduction 18

Materials and Methods 20

Results 26

Discussion 47

3. BARTONELLA INHIBITS GENE EXPRESSION OF APOPTOSIS MODULATORS 58

Introduction 58

Materials and Methods 59

Results 62

Discussion 80

4. CONCLUSION 92

Role of This Study 92

Gram-negative Bacterial Infection and LPS 93

B. henselae Infection 94

Bartonella Protein Factors and Their Role in Intracellular Survival 95

B. henselae Disrupts Gene and Protein Expression of Extrinsic and Intrinsic Apoptotic Pathway Modulators Following Apoptogenic Ceramide Treatment 97

B. henselae Disrupts Extrinsic Pathway Receptor Mediated Apoptosis in Order to Ensure Its Survival 98

B. henselae Suppresses Caspase-3 100

Summary 102

Future Directions 103

BIBLIOGRAPHY 104

LIST OF TABLES

Table 1. Apoptogenic Agents 19

Table 2. Gene Targets Tested 64

Table 3. TRADD Gene Expression Summary 75

Table 4. FADD Gene Expression Summary 78

Table 5. Caspase-8 Gene Expression Summary 81

Table 6. Caspase-3 Gene Expression Summary 84

LIST OF FIGURES

Figure 1. Phosphotidylserine Translocation 3

Figure 2. Formation of the TNF-receptor Death-inducing-signaling-complex (DISC) 5

Figure 3. c-FLIP L Is a Caspase-8 Antagonist and/or Activator 7

Figure 4. Intrinsic Apoptosis Pathway 10

Figure 5. Mechanism of Action of Bid 11

Figure 6. Invasome 16

Figure 7. FADD Western Blot 27

Figure 8. Cytotoxic Effect of Apoptogenic Agents 28

Figure 9. Cell Morphology—Controls and Two-hour Ceramide Treatment 31

Figure 10. Classic Morphology of Early Apoptosis Event 32

Figure 11. Cell Morphology—Four- and Six-hour Ceramide Treatment 33

Figure 12. Cell Morphology—Eight- and Twelve-hour Ceramide Treatment 34

Figure 13. Cell Viability by Trypan Blue Exclusion 35

Figure 14. TRADD Protein Expression Analysis by Flow Cytometry—Thirty Minute and One-hour Ceramide Treatment 37

Figure 15. TRADD Protein Expression Analysis by Flow Cytometry—Two- and Three-hour Ceramide Treatment 38

Figure 16. TRADD Protein Expression Analysis by Flow Cytometry—Four-hour Ceramide Treatment 39

Figure 17. FADD Protein Expression Analysis by Flow Cytometry—Thirty Minute and One-hour Ceramide Treatment 40

Figure 18. FADD Protein Expression Analysis by Flow Cytometry—Two- and Three-hour Ceramide Treatment 41

Figure 19. FADD Protein Expression Analysis by Flow Cytometry—Four-hour Ceramide Treatment 42

Figure 20. Caspase Activity Assay 43

Figure 21. Multicaspase Fluorescent Substrate: B+C Cells 44

Figure 22. Multicaspase Fluorescent Substrate: Cer Cells 45

Figure 23. DNA Cell Cycle Analysis 46

Figure 24. Supplemental Magnesium Titration and Multiple RT-PCR Primer/Probe Sets 65

Figure 25. Reproducibility of Multiplex RT-PCR Requires tRNA 65

Figure 26. Primer and Probe Titration 66

Figure 27. Standard Curve of TRADD Gene Expression 67

Figure 28. Standard Curve of FADD Gene Expression 68

Figure 29. Standard Curve of Caspase-8 Gene Expression 69

Figure 30. Standard Curve of Caspase-3 Gene Expression 70

Figure 31. Multiplex Real-time RT-PCR for TRADD Gene Expression 73

Figure 32. TRADD Gene Expression 74

Figure 33. Multiplex Real-time RT-PCR for FADD Gene Expression 76

Figure 34. FADD Gene Expression 77

Figure 35. Multiplex Real-time RT-PCR for Caspase-8 Gene Expression 79

Figure 36. Caspase-8 Gene Expression 80

Figure 37. Multiplex Real-time RT-PCR for Caspase-3 Gene Expression 82

Figure 38. Caspase-3 Gene Expression 83

Figure 39. Multiplex Real-time RT-PCR for TRADD Controls 85

Figure 40. Multiplex Real-time RT-PCR for FADD Controls 85

Figure 41. Multiplex Real-time RT-PCR for Caspase-8 Controls 86

Figure 42. Multiplex Real-time RT-PCR for Caspase-3 Controls 86

LIST OF ABBREVIATIONS

B+C-*B. henselae*-infected ceramide treated HMEC-1 cells

Cer-Ceramide treated uninfected HMEC-1 cells

TRADD-TNF-associated Death Domain

FADD-Fas-associated Death Domain

NF-κB-Nuclear factor kappa B

ICAM-1-Intercellular adhesion molecule-1

VCAM-1-Vascular cell adhesion molecule-1

ELAM-1-Endothelial cell leukocyte adhesion molecule-1

c-kit-Cytokine receptor (CD117)

RT-PCR-Reverse-transcriptase polymerase chain reaction

E-selectin-Cellular adhesion molecule CD62E

TNF-α-Tumor necrosis factor-alpha

HMEC-1-Human microvascular endothelial cell line

HUVEC-Human umbilical vein endothelial cells

FasL-Fas ligand

DD-Death domain

DED-Death effector domain

CHAPTER 1

GENERAL INTRODUCTION

Overview

Cell death is an essential process in the growth and maintenance of all multicellular organisms. Cells are constantly being replaced as they age or become damaged. Since the human body typically produces about 10 billion new cells each day, it must have some way to rid itself of senescent, functionally impaired, or otherwise unwanted cells. One way to accomplish this is through apoptosis.

Apoptosis is a well-ordered process of programmed cell death. Cells undergoing apoptosis show a distinct set of morphological changes, including shrinking of the cytoplasm, condensation of chromatin in the nucleus, and membrane blebbing. The last stages of apoptosis are accompanied by the disintegration of the cell into small vesicles called apoptotic bodies. Apoptotic processes play a number of beneficial roles during the life cycle of the organism, including the removal of infected and neoplastic cells, and the elimination of superfluous cells during differentiation and development. Apoptotic processes have also been implicated in the cellular destruction associated with a number of disease states, including Parkinson's Disease (Schulz 2008), Alzheimer's Disease (Dickson 2004), and AIDS (de St Groth and Landay 2008).

The highly structured mechanisms underlying apoptotic processes can be distinguished from necrosis, a form of death resulting from direct injury to the cell. Necrosis involves the release of degradative lysosomal enzymes into the cytoplasm, where they cause massive destruction of cellular components. Cell lysis then ensues, resulting in the release of harmful chemicals into the proximal extracellular environment. This in turn induces an inflammatory

response, precipitating the destruction of surrounding tissues. In contrast, cellular debris accumulating in the late stages of apoptosis is rapidly ingested by tissue macrophages in a manner that does not induce the inflammatory response (Moreira and Barcinski, 2004). The signal for phagocytic ingestion of apoptotic bodies is the translocation of phosphatidyl serine (PS) from the inner to the outer leaflet of the plasma membrane (Figure 1). The process by which PS is moved to the external surface of the cell is not fully understood, but its role as a marker triggering phagocytic digestion allows apoptotic bodies to be eliminated without eliciting the inflammatory responses that cause damage to nearby cells (van England *et al.*, 1998).

Apoptosis Pathways of Induction

There are two general mechanisms of apoptotic induction. The extrinsic pathway, as its name implies, is triggered by a signal from outside the cell. Specific signaling ligands initiate the apoptotic sequence by interacting with a transmembrane receptor located on the cell surface. Trimerization of this receptor in response to ligand binding then precipitates a cascade of events that leads to the sequential activation of several cysteine-aspartate-specific proteases (caspases). Activated caspases degrade cellular components directly or indirectly through their proteolytic activation of other cellular proteases. Induction of the caspase cascade results in the eventual death of the cell (Salvesen and Dixit 1999). The intrinsic pathway is induced by internal stressors, such as DNA damage, heat shock, or by products of the extrinsic pathway. The intrinsic pathway involves the permeabilization of mitochondrial membranes and the resulting release of mitochrondrial proteins into the cytoplasm, where they set in motion a caspase cascade that eventually merges with that of the extrinsic pathway (Giacca 2005).

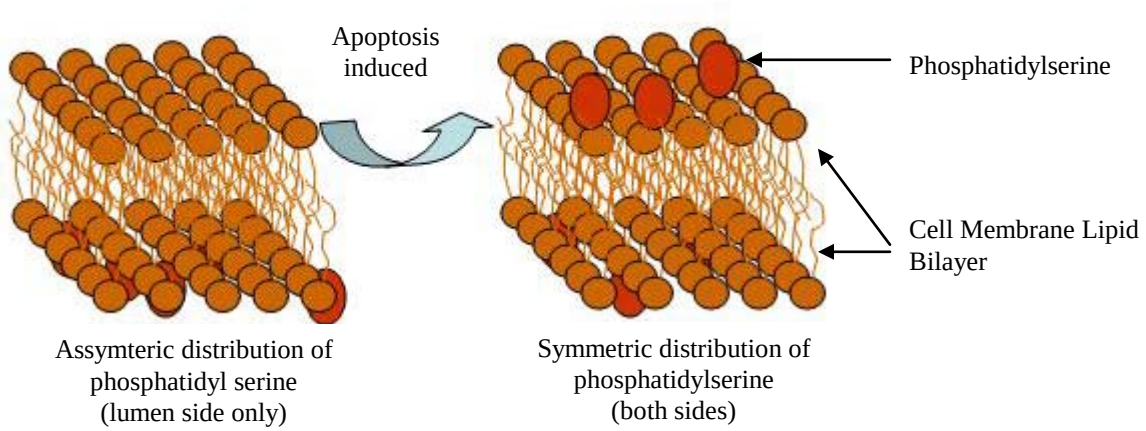

Figure 1 Phosphotidylserine Translocation. Translocation of phosphotidyl serine (PS) is an early indicator of apoptosis. Following apoptosis induction, PS translocates to the outer membrane and marks the cell for ingestion by phagocytic cells.

The Extrinsic Pathway

The initial stages of extrinsic induction have been well characterized, and are mediated by the action of several tumor necrosis factors (TNF), or "death receptors". Tumor necrosis factor (TNF) receptors are members of a superfamily of membrane-spanning proteins that includes TNF-receptor-1 (TNFR1), TNF-receptor-2 (TNFR2) and Fas (Ware, 2003). Activation of the TNF receptors is believed to occur when a trimerized ligand such as FasL or TNF-α induces the trimerization of three TNF receptor monomers at the cell surface (Dempsey *et al.*, 2003). TNF receptor proteins contain a highly conserved 80-amino-acid region that is localized to the cytoplasmic side of the membrane (Thorburn, 2004). This region of the protein is referred to as the "death domain" (DD). Through interactions between their death domains, trimerized TNF receptors cluster together in lipid rafts (ceramide-rich regions of the plasma membrane) to form a signal transduction complex (Grassme *et al.*, 2003; Ruvuolo, 2003). The receptor trimers attract specific adaptor proteins that bind to the receptors through their own DD sequences (Walsh *et*

al., 2003). Adaptor proteins in turn recruit procaspase-8 (an "initiator" caspase) to the TNF-receptor complex, acting directly or indirectly through a second adaptor protein. Binding by procaspase-8 to the adaptor protein occurs at a region of homology shared by the two proteins called the Death Effector Domain (DED). Association of receptor, adaptor(s), and procaspase-8 produces a complex on the membrane called the Death Inducing Signaling Complex (DISC; Ashkenazi and Dixit, 1998).

The process of DISC formation can be illustrated by the interactions between TNFR1 and its adaptor proteins. Following binding of the ligand to the receptor, TNFR1 trimers form a complex with the adaptor molecule TRADD (TNF-receptor-associated death domain) through interactions between the death domains of the two proteins. TRADD in turn recruits a second adaptor molecule, FADD (Fas-associated death domain), which also binds to TRADD through DD interactions (Green, 2003). The DED region of FADD then interacts with the homologous region of procaspase-8; (Thorburn *et al*., 2003) to form the DISC (Figure 2). Procaspase-8 exists within this complex as a dimer and undergoes a process of self-activation. Activated caspase-8 subsequently recruits and activates an "executioner" caspase (caspase-3), and this process sets in motion a cascade that ultimately results in the digestion of about 100 proteins (Creagh *et al.*, 2003).

Caspase-8 Activation

Caspases function as "messengers" by relaying apoptotic signals from adaptor proteins to cellular target proteins. To prevent unscheduled cell suicide, each caspase is translated as a zymogen containing a pro-domain and a catalytically active domain (Green, 2003; Boatright and Salvesen, 2003). Early studies on the mechanism of caspase-8 activation revealed that the two

procaspase-8 molecules recruited to the DISC are able to undergo cross-proteolysis *in trans*, with one digesting the other (Zimmerman and Green, 2001). This caused investigators to equate activation with autoproteolysis, and led them to propose that proteolytic cleavage is an essential component of the caspase-8 activation process (Shi, 2002).

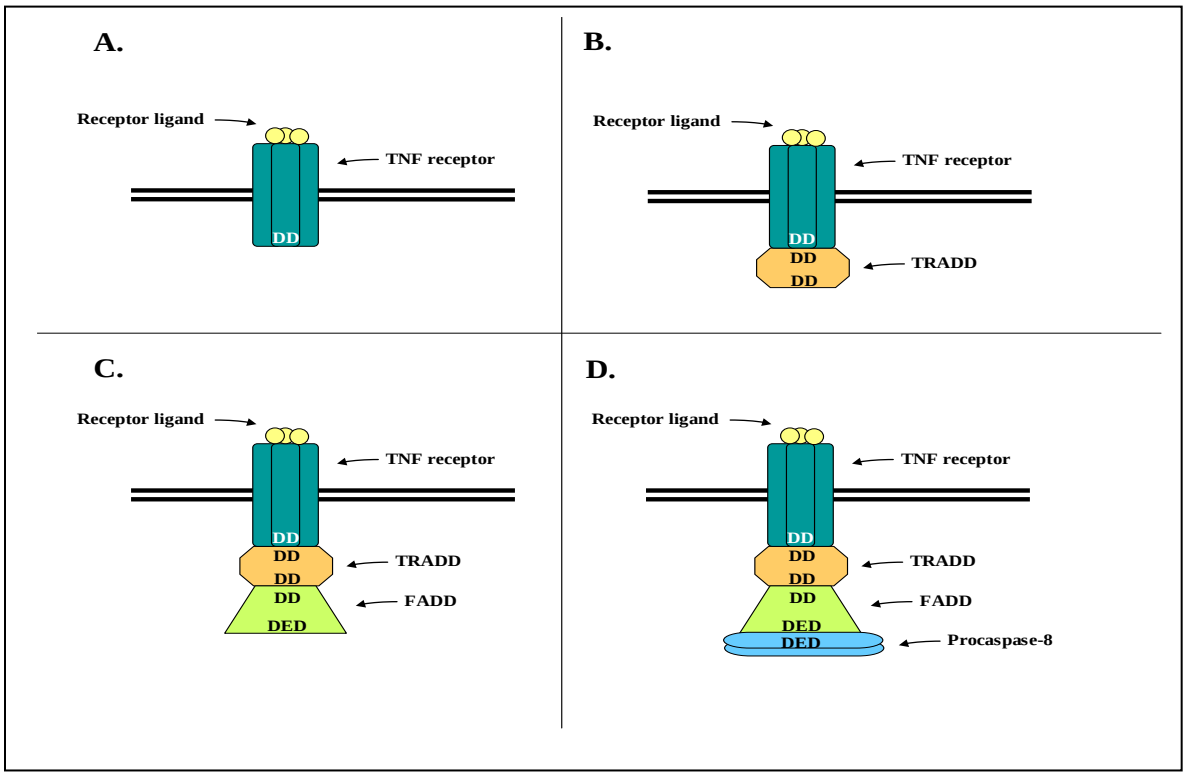

Figure 2. Formation of the TNF-receptor Death-inducing-signaling-complex (DISC). The trimeric ligand trimerizes the TNF receptor (A). The trimeric receptor recruits the primary adaptor protein, TRADD (B). The primary adaptor recruits the secondary adaptor protein, FADD. Interaction of adaptors is through the Death Domain (DD) of the adaptor proteins (C). The Death-Effector-Domain (DED) of the secondary adaptor protein interacts with the DED of the recruited initiator caspase, procaspase-8 (D).

However, the results of more recent studies suggest that proteolysis is not in itself necessary for the generation of caspase-8 activity (Thorburn 2004). This conclusion is based on investigations into the role played by naturally occurring inactive caspase-8-like molecules in the regulation of

death-receptor induced apoptosis. These regulatory molecules are called *cellular FLICE-like-inhibitory proteins,* or c-FLIP. FLICE stands for FADD-like-interleukin-converting-enzyme, the name previously assigned to caspase-8 (Day *et al.*, 2006). .

c-FLIP proteins can exist in two isoforms, a long form (c-FLIP-L) and a short form (c-FLIP-S). c-FLIP-L contains two DED domains plus a region homologous to the catalytic domain of caspase-8 (Kataoka 2005). c-FLIP-S also contains two DED domains, but lacks the caspase-8 catalytic domain region. c-FLIP-L can dimerize with caspase-8, but is not an active protease because it contains several sequence differences that affect the catalytic domain of the protein (Longley *et al.*, 2006).

By interacting through their DED regions with adaptor molecules such as FADD, c-FLIP proteins compete with procaspase-8 for binding at the DISC (Figure 3). Based on this observation, c-FLIP proteins were initially believed to act solely as inhibitors of apoptosis. Subsequent evidence, however, suggested that under certain circumstances the recruitment of c-FLIP-L to the DISC can actually promote apoptosis by activating caspase-8 (Sohn *et al.*, 2006). Recent studies have demonstrated that the formation of a heterodimer between c-FLIP-L and procaspase-8 is enough to induce caspase-8 activity, even though c-FLIP-L is unable to catalyze the cross-proteolysis of its partner. This has led investigators to conclude that caspase-8 is enzymatically active in its unprocessed form. Processing may stabilize the caspase-8 dimer, but is neither necessary nor sufficient for catalytic activation (Boatright and Salvesen 2003; Salvesen and Dixit 1999; Zimmerman and Green 2001).

The demonstration that dimerization alone is sufficient for caspase-8 activation has raised questions as to the role of processing in caspase-8 activity. Recent evidence indicates that caspase-8 is recruited to the cytosolic complex of TRADD and FADD (Micheau and Tschopp,

2003). The caspase-8 dimer is capable of self activation by cleavage of internal residues. Within the cytosol the processed caspase-8 is available to interact with substrates in close proximity (Harper *et al.*, 2003).

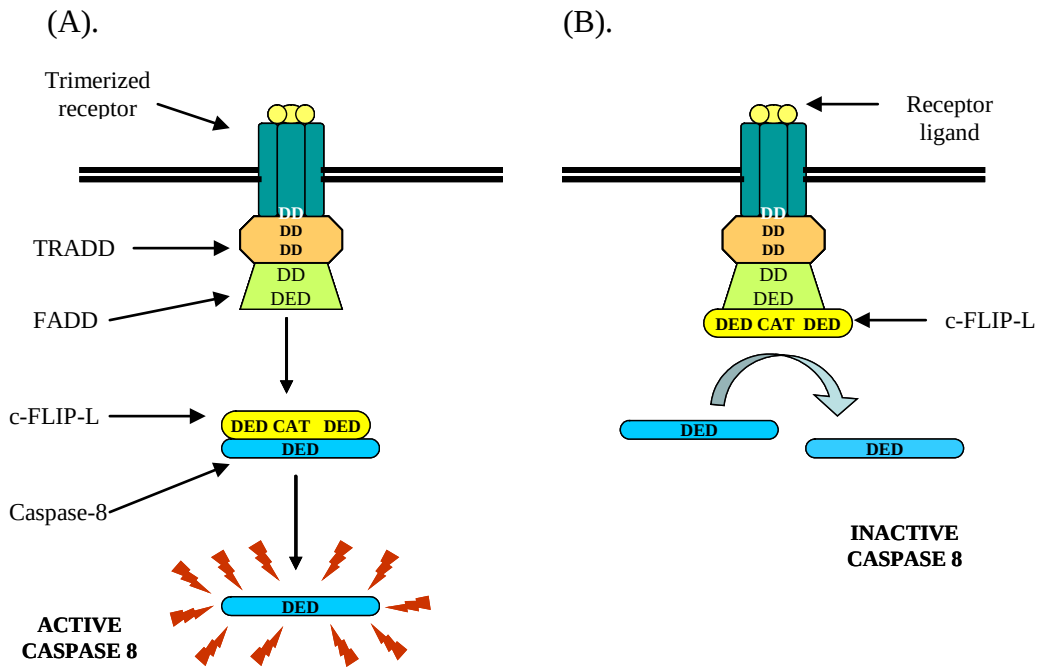

Figure 3. c-FLIP L Is a Caspase-8 Antagonist and/or Activator. The long form of cellular FLICE-like inhibitory protein c-FLIP L interacts with FADD and Caspase-8. (A). c-FLIP L dimerizes with caspase-8 (proform), inducing its activation. (B). c-FLIP L competes with caspase-8 for FADD death-effector-domain (DED).

Activation of Other Caspases

Following its activation, caspase-8 cleaves caspase-3, setting off a cascade of proteolytic events that result in the activation of several downstream caspases. Once activated, "executioners" caspases such as caspase-3 (Feng, Y. *et al.*, 2005), caspase-6 (MacLachlan and El-Deiry, 2002) and caspase-7 (Xia, Y. *et al.*, 2007; Slee *et. al.*, 2001) cleave key cellular components, thereby precipitating cell death. Each executioner caspase can exist as an inactive

dimer in its zymogen form. The executioner caspases reside primarily in the cell cytosol. Caspase-3 is the most abundant caspase in the cytosol, and acts as an executioner for both extrinsic and intrinsic pathways (Chickova *et al.*, 2004). Caspase-3 cleaves caspase-6 and poly-ADP-ribosyl polymerase as well as other cellular proteins. Activation of these targets ultimately leads to the cleavage of lamin proteins and the fragmentation of nuclear DNA (Hirata *et al.*, 1998).

The Intrinsic Pathway

As mentioned previously, internal cellular stress such as DNA damage or oxidative stress can act as a trigger for apoptosis. The response to internal stress is mediated by the intrinsic pathway. Intrinsic induction of apoptosis leads to an increased permeability of the mitochondrial outer membrane, which results in the release of cytochrome c and other mitochondrial proteins that trigger a caspase cascade. Regulation of membrane permeability is achieved by members of a large protein superfamily called Bcl-2, derived from B-Cell Lymphoma, the cell lineage from which it was originally identified (Yang *et al.*, 1997). Included within the Bcl-2 superfamily are proteins that stimulate apoptosis (pro-apoptotic proteins) and those that suppress it (anti-apoptotic proteins; Cory and Adams, 2002). All Bcl-2 family members share one or more of four BH (Bcl-2 Homology) domains that promote protein-protein interactions and are required for protein function. Anti-apoptotic proteins contain all four domains (BH1 – BH4), while pro-apoptotic proteins contain from one to three domains (Cory *et al.*, 2003).

Induction of the intrinsic pathway begins with a disruption of the balance between pro- and anti-apoptotic factors. The two primary anti-apoptotic proteins, Bcl-2 and Bcl-X_L, are located in the outer membrane of the mitochondria. Two additional Bcl-2 family members, Bax (Bcl-2

associated X protein) and Bak (Bcl-2 homologous antagonist/killer protein), also reside in the mitochondrial membrane (Figure 4). Based on their resemblance to bacterial pore forming channel proteins, Bax and Bak are believed to be involved in production of the pores through which mitochondrial components are leaked into the cytoplasm (Desagher *et al.*, 1999). Thus, they play a pro-apoptotic role within the cell. There are also several cytoplasmic pro-apoptotic proteins that act as sensors of cellular stress. These proteins typically contain only the BH-3 homology domain, and therefore are sometimes referred to as BH-3-only proteins. If they are activated by apoptotic signals, they travel to the surface of the mitochondria where they interact with membrane-associated Bcl-2 family members (Ashkenazi, 2008).

The BH3-only proteins can be divided further into three subgroups. One group, represented by proteins such as Bim (Bcl-2 interacting mediator of cell death), can bind directly to the pro-apoptotic proteins Bax and Bak, activating them to produce pores in the membrane. The second group, represented by proteins such as Bik (Bcl-2 interacting killer protein) and Bad (Bcl-2 associated death promoter), are believed to exert their effect primarily by binding to anti-apoptotic proteins such as Bcl-2 and Bcl-X_L (Bcl-2 extra-long protein) (Ashkenazi, 2008). In this way, they displace other pro-apoptotic proteins that might be bound to the anti-apoptotic proteins, thereby freeing proteins such as Bax and Bak to oligomerize with each other and form pores. The third group, represented by Bid (BH3 Interacting Domain death agonist), can induce pore formation through direct binding to Bak/Bax or through binding to the anti-apoptotic proteins (Goping *et al.,* 1998). The mechanism of action of the pro-apoptotic protein Bid (Figure 5) provides a well-documented example of the steps leading to induction of the intrinsic pathway, and illustrates how the apoptotic switch depends on a delicate balance between the pro- and anti-apoptotic proteins at the mitochondrial membrane (Lessene *et al*., 2008).

Under non-apoptotic conditions, Bid is located in the cytosol in its inactive form (Tang *et al.*, 2000). In response to cellular stress, however, Bid can be activated by caspase-8, which cleaves it into a truncated form known as tBid (Ogretum and Hannun, 2004). tBid then migrates to the surface of the mitochondrion, where it interacts directly with Bak, causing the protein to undergo a conformational change that induces Bax/Bak pore formation (Cory *et al.*, 2003). In addition to its effect on Bak, tBid can also interact with anti-apoptotic proteins such as $BclX_L$. If the anti-apoptotic proteins are in excess, they can bind to tBid, thereby sequestering it so that it cannot interact with and activate Bak; conversely, if tBid is in excess, it can inactivate anti-apoptotic proteins and directly activate Bak simultaneously.

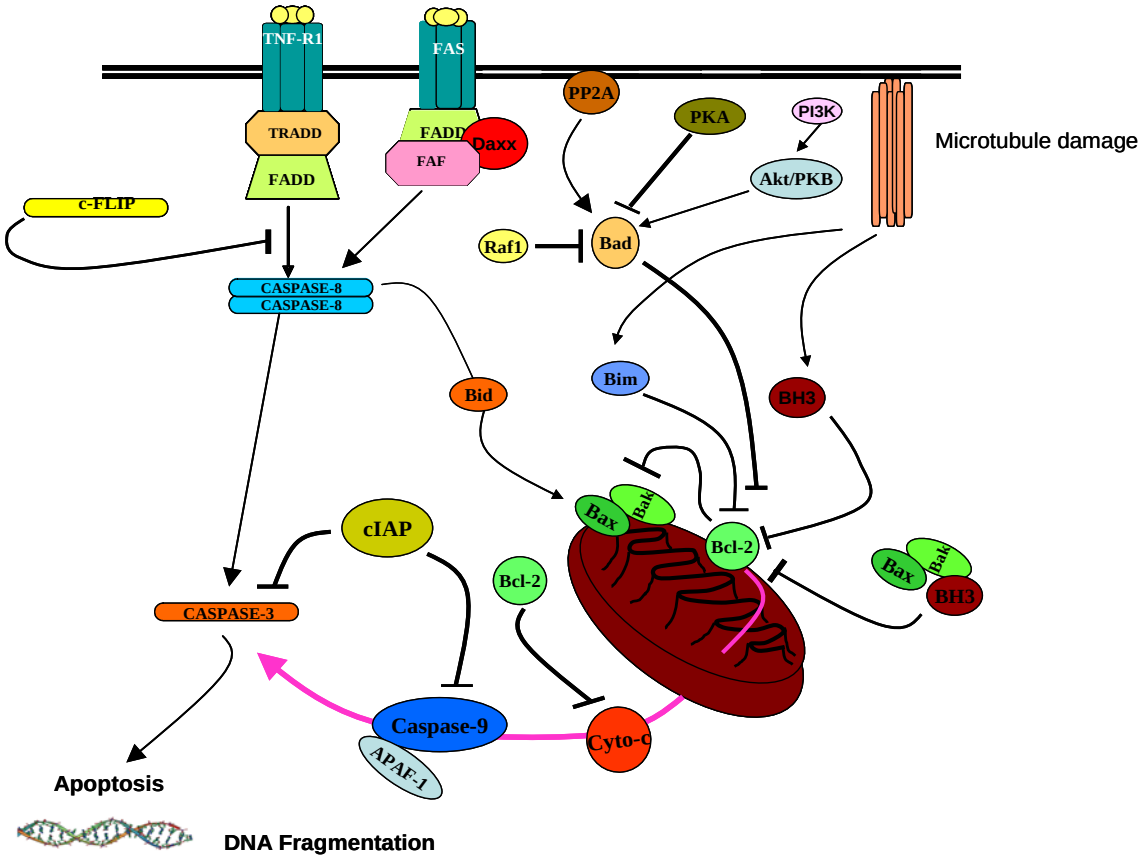

Figure 4. Intrinsic Apoptosis Pathway. The intrinsic pathway demonstrates the interaction of the caspase cascade and the bcl-2 proteins. Mitochondrial proteins interplay in the formation of the apoptosome leading to activation of executioner caspase-3. Image adapted from www.proteinlounge.com

It has been reported (Grinberg *et al*., 2002), that a mutant Bid that lacks a functional BH3 domain is still able to induce cyctochrome c release and apoptosis in the absence of direct interactions with either Bak or the Bcl-2 anti-apoptotic proteins. To explain these observations, the investigators proposed the tBid forms homo-oligomers through a BH3-independent mechanism to create pores in the mitochondrial membrane. Thus, it is possible that Bid plays multiple roles in the apoptotic process.

Cytochrome c, a heme-binding protein that is loosely associated with the inner mitochondrial membrane, is an integral component of the mitochondrial electron transport chain.

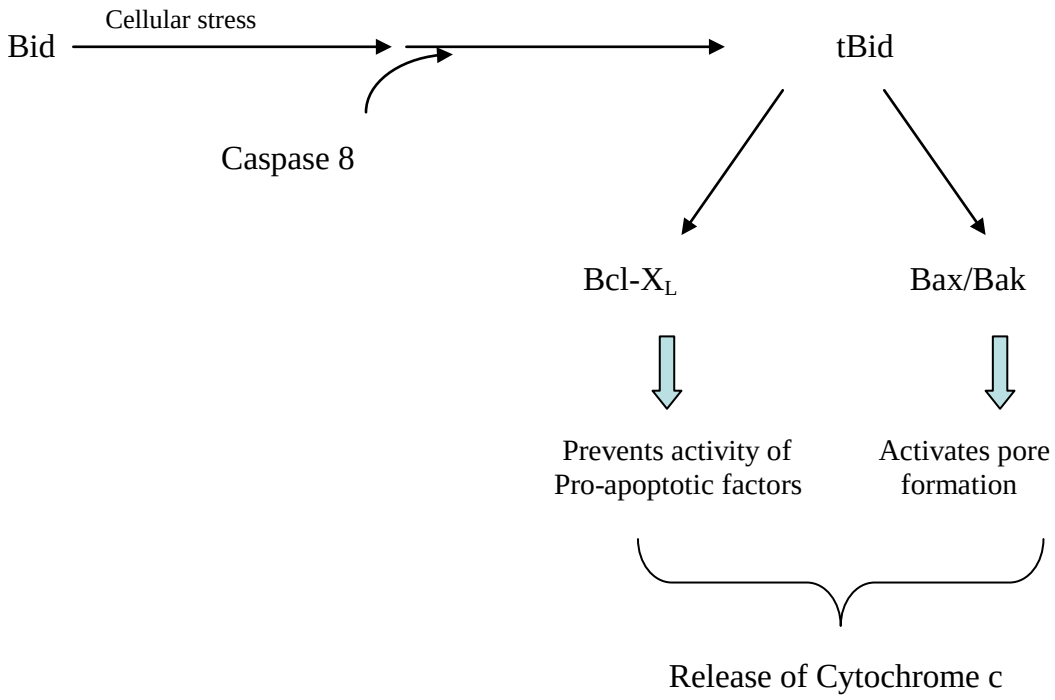

Figure 5. Mechanism of Action of Bid. Bid is activated by caspase-8 cleavage to generate the truncated (t-Bid) form. tBid can interact with both anti-apoptotic proteins (Bcl-X_L) or pro-apoptotic proteins (Bax/Bak). Excess of Bcl-X_L will lead to sequestering of tBid. Excess of tBid leads to inactivation of Bcl-X_L and activation of Bax/Bak.

With the destruction of mitochondrial membrane integrity following an apoptotic stimulus, however, cytochrome c is quickly released into the cell cytosol (Kluck *et al.*, 1997; Yang *et al.*, 1997), where it binds to and activates APAF-1 (apoptosis protease activating factor-1), a receptor protein located at the outer mitochondrial membrane. The APAF-1/cytochrome c complex then associates with dATP to form a complex called the apoptosome (Wang, 2001). The caspase recruitment domain (CARD) of APAF-1 recruits caspase-9 to the apoptosome complex (Rodriguez and Lazebnik, 1999). Apoptosome-bound caspase-9 initiates the activation of terminal effector proteins (e.g., caspase-6) through the cleavage and activation of other executioner caspases (caspase-3 and -7) (Tao *et al.*, 1998). Through its proteolytic activation of caspase-3, caspase-9 initiates the cleavage of multiple cellular targets, which ultimately results in an orderly disintegration of the cell (Wang, 2001; Nakazawa *et al*., 2003). However, mitochondrial induced apoptosis does not necessarily require caspase-9 (King, 2005).

Ceramide and Ceramide Signaling

Ceramides are lipid molecules consisting of sphingosine and a fatty acid. They constitute part of the structure of sphingomyelin, one of the major components of the lipid bilayer, and as a consequence are present in high amounts in the plasma membrane. The classic cell membrane model, originally depicted by Singer (Singer and Nicholson, 1972), proposes a random distribution of lipids and proteins in the cell membrane. However, recent studies indicate that the lipid distribution in the cellular membrane is anything but random. Until recently, ceramides were believed to function predominantly as structural components in the membrane. In the past few years, however, a number of studies have revealed that these compounds also play a role in cell signaling, participating in several processes, including cell differentiation, cellular

senescence, and the growth of cancer cells (Browne and London, 1998). Moreover, it is becoming increasingly evident that ceramides play a pivotal role in apoptosis (Davis *et al.*, 2006).

It has been shown that clustering of Fas and members of the TNF receptor superfamily triggers the conversion of sphingomyelin into ceramide (Gulbins and Li, 2006). The newly generated ceramide then becomes a major component of the lipid rafts that serve as the anchor points for the association of TNF receptors and other proteins with pro-caspase-8 to form the DISC complex used in the extrinsic apoptotic pathway. Recent studies also demonstrate that ceramide is essential for the formation of these lipid rafts. In doing so it serves as an essential signaling component for the aggregation of receptor death domains (Gulbins *et al.*, 2000; Grassme *et al.*, 2001). Ceramide also plays a role in the intrinsic apoptotic pathway by activating the kinase suppressor of Ras (KSR). Activation of KSR initiates a phosphorylation cascade that ultimately inhibits Akt, a kinase whose substrates include the Bcl-2 pro-apoptotic protein Bad (Datta *et al.*, 1997; Schubert *et al.*, 2000). Phosphorylation by Akt converts Bad into its inactive form. Thus, the indirect inhibition of Akt by ceramide leads to the accumulation of unphosphorylated, active Bad at the mitochondrial membrane, and thereby promotes cell death (Basu *et al.*, 1998).

Ceramides are classified by the length of their fatty acid chains. Natural ceramides typically have fatty acid chains of ~16-carbon atoms. Cultured cells are permeable to exogenous short-chain (two to six carbons) ceramides, but are not permeable to longer carbon chain molecules. Still, ceramides greater than six carbons can translocate between the leaflets of the cells plasma membrane. Exogenously supplied ceramides mimic their natural analogues to

induce anti-proliferative responses, cell-cycle arrest, differentiation, and apoptosis (Obeid *et al.*, 1993).

Exogenously added C_2-ceramides have been reported to increase the permeability of mitochondrial membranes. However, it can also induce NFκB, which subsequently induces a number of genes responsible for cell survival (Ruvulo, 2001). In cells of cancer origin, C_2-ceramides lead to transient caspase-3 activation following 24 hours of ceramide treatment (Fillet *et al.*, 2003). The mode and severity of cellular response to ceramide are cell type specific.

Bartonella **and Host Cell Survival**

Bartonella henselae is the causative agent of Cat-Scratch Disease (CSD), an illness characterized by low-grade fever, malaise, and swelling of the lymph nodes (Emmons *et al.*, 1976). The bacterium is usually transmitted through the bite or scratch of an infected cat or kitten. Symptoms appear between one and two weeks after infection (Bass *et al.*, 1997). In many patients, a small cutaneous lesion is noted at the site of the bite or scratch a few days after the injury (Slater *et al.*, 1993). *B. henselae* infects endothelial, epithelial, erythrocyte and macrophage cells in cats and humans (Minnick and Anderson, 2000; Kempf *et al.*, 2005). In immunocompetent individuals, CSD is typically a self-limiting disease, lasting from six to 12 weeks. In contrast, immunocompromised individuals such as AIDS patients can be persistently infected by *B. henselae*. Persistent *B. henselae* infection can trigger endothelial cell proliferation, resulting in Bacillary Angiomatosis (BA). Patients with BA have multiple vasculoproliferative lesions on their skin. Vascular tumors can also appear in response to organ infection, a process known as Bacillary Peliosis (BP). The bacterial factor(s) responsible for this proliferation have not been fully characterized, although they are known to be proteinaceous and require bacterial

synthesis following infection (Maeno *et al.*, 1999; Dehio 2003). Upon infection of endothelial cells, the bacteria induce the formation of an adhesion-molecule-rich cell membrane protrusion called an invasome (Dehio 1999).

The formation of the invasome is an actin-dependent and microtubulin-independent process. Aggregated bacteria are trapped in the actin and phosphotyrosine-rich tips of the protrusion and drawn into the cell (Figure 6). The tips of the invasome are also enriched in caps of intracellular adhesion molecule-1 (ICAM-1) and other adhesion molecules (Dehio, 2003). Gene expression of most adhesion molecules, including ICAM-1, VCAM-1 and ELAM-1 molecules is regulated by the nuclear factor NF-κB (Clifton *et al*.1998; True *et al.*, 2000). Vascular endothelial cells either ubiquitously express or are induced to express adhesion molecules following cytokine treatment (Ades *et al.*, 1992). In addition to adhesion molecules, NF-κB regulates cell proliferation factors including vascular endothelial growth factor, VEGF (Kirby 2004; Kempf *et al.*, 2001).

Enhanced expression of host-encoded growth factors via a paracrine loop has been demonstrated following *B. henselae* infection of several cell types. The presence of the bacteria is not necessary for either enhanced endothelial cell proliferation or enhanced growth factor expression but direct contact between *B. henselae* and endothelial host cells does potentiate an enhanced proliferative effect (Fuhrmann *et al.*, 2001). Growth factor expression is not sustained indefinitely following intracellular *B.* henselae infection (Kempf *et al.*, 2002).

***Bartonella* and Apoptosis Suppression**

Obligate intracellular pathogens, particularly viruses, often ensure their survival by either promoting host cell proliferation or by preventing the induction of programmed cell death (Lax

and Thomas, 2002; Mehock *et al.,* 1998; Hentschel *et al.,* 2000; Saini *et al.,* 1999). It has been shown previously that *B. henselae* infection upregulates cell surface adhesion molecule production and suppresses activity of both initiator and executioner caspases (Kirby and Nekorchuk, 2002). The upregulation of vascular cell endothelial growth factor (VEGF) and secretion of other apoptosis inhibitory proteins is considered to be the principal anti-apoptotic mechanism used by *Bartonella* (Kempf *et al.,* 2005). Recently, Bartonella encoded anti-apoptotic substrates have been described (Schmid *et al.,* 2004; Schmid *et al.,* 2006). Our studies were designed to investigate the multifaceted manner by which *B. henselae* exerts an anti-apoptotic effect by modifying both molecular expression and protein expression/activation of both extrinsic and intrinsic apoptosis modulators.

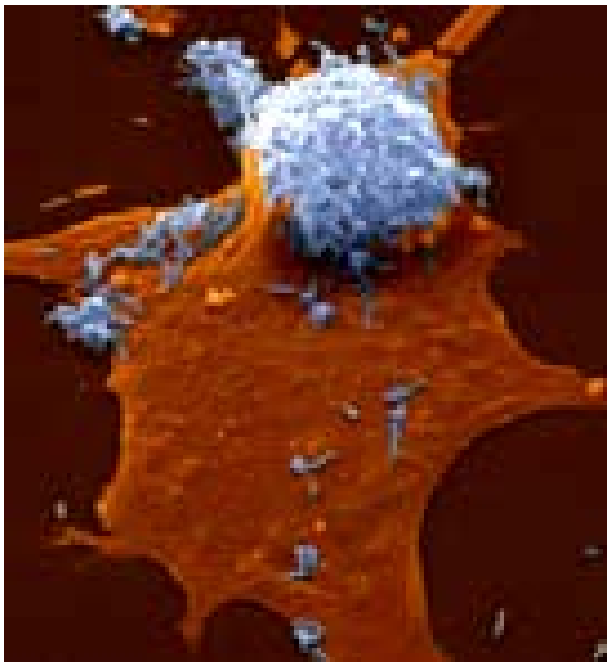

Figure 6. Invasome. The "invasome" is characterized by membrane protrusions which entrap an aggregate of bacteria. The invasome facilitates *B.* henselae invasion of endothelial cells through adhesion molecule rich membrane protrusions (reproduced with permission, Cristoph Dehio).

Summary

The mechanisms whereby *B. henselae* establishes and maintains a successful infection have not been fully characterized. However, it has been demonstrated that neither host cell growth nor a paracrine loop of endogenous growth factors are the sole mechanisms for ensuring *B. henselae* intracellular survival (Anderson, 2001; Resto-Ruiz *et al.*, 2002). The reports that *B. henselae* affects the expression of genes that are known to be involved in cell death suggest that this bacterium may use an additional survival mechanism: the prevention of apoptotic processes that would ultimately lead to the death of its host cell. Activation of cell growth and suppression of apoptosis are two seemingly opposite pathways with the same net effect. This study addresses the observations that *B. henselae* ensure its survival by processes that extend beyond a simple manipulation of cell proliferation. Rather, *B. henselae* preserves its safe haven by inhibiting the initial intrinsic apoptotic pathway and, further, preventing the induction of executioner caspases targeted by the apoptogenic agent C_2-ceramide. The cellular factors inhibited by *B. henselae* provide a comprehensive restraint on the intrinsic apoptosis pathway modulators.

CHAPTER 2

BARTONELLA HENSELAE INHIBITION OF APOPTOSIS MODULATORS

Introduction

Intracellular pathogens and tumor cells enhance their ability to survive by circumventing host apoptosis. Tumor cells accomplish this by inducing the over-expression of anti-apoptotic proteins, such as Bcl-2 (Apakama *et al.*, 1996). However, pathogens first mitigate the immune assault against them before successfully infecting the competent host cells. The tropism of *B. henselae* for endothelial cells is an intriguing evolutionary adaptation due to 1.) the presence of Gram negative bacterial LPS on *B. henselae*, 2.) the endothelial cell role in excreting TNF-α following exposure to bacterial LPS and 3.) the endothelial cell expression of NF-κB genes following paracrine-loop exposure to TNF-α (Dehio, 2001; Kyong-Bok *et al.*, 1998; Imaizumi *et al.*, 2000). *B. henselae* seems to exploit all of these features to permit the tropism for an intracellular safe haven in microvascular endothelial cells.

To ensure chronic intracellular infection, *B. henselae* is capable of inhibiting apoptosis. Our study was designed to investigate the ability of *B. henselae* to inhibit apoptosis following direct apoptogenic challenge. A variety of apoptogenic agents were screened for their ability to induce apoptosis. Among these agents were camptothecin, staurosporine, C_2-ceramide, ricin toxin and abrin toxin. The mode of action of these agents spans protein kinase activation, inhibition of protein kinase DNA binding, inhibition of DNA packaging enzymes and inhibition of ribosomal activity. We chose C_2-ceramide not only because it was capable of inducing dose dependent apoptosis, but also because it mimics the mechanism of LPS induced inflammatory

pathways. The addition of C_2-ceramide alters the membrane bilayer to induce the formation of lipid rafts.

Table 1. Apoptogenic Agents.

	Mode of action	Effect on HMEC-1 cells
TNF-α	Induces extrinsic apoptosis pathway, causes release of in vivo ceramide	Ineffective with HMEC-1
C_2-ceramide	Increases protein kinase activity	Concentration and time-dependent morphological effect
Staurosporine	Inhibition of protein kinase ATP binding	Required high concentration before effective
Camptothecin	Quinoline alkaloid inhibits DNA topoisomerase I	Low concentration obliterated cells, media cloudy
ET-18 (etoposide)	Topoisomerase II inhibitor	Low concentration obliterated cells, media cloudy
Ricin toxin	Depurination of eukaryotic ribosomal sarcin-ricin loop	Effective at low confluency and low serum
Abrin toxin	Depurination of eukaryotic ribosomal sarcin-ricin loop	Effective at low confluency and low serum
Serum starvation	Varied: G_0/G_1 cycle arrest, downregulation of ERK2 activity	≤5% serum has "serum starvation effect"

A variety of apoptogenic agents were tested for their ability to induce apoptosis. Mechanism of apoptosis for agents tested was varied. Agents were tested on uninfected cells for 4 hours incubated at 35^{o}C at 95% humidity.

Lipid raft formation provides a mechanism for intrinsic apoptosis pathway receptors to cross link, thereby initiating the intrinsic apoptosis pathway. The presence of *B. henselae* interferes with the C_2-ceramide stimulated expression of intrinsic pathway proteins such as TNF-

associated death domain (TRADD) and Fas-associated death domain (FADD) inhibiting the initiating stage of apoptosis induction. Further, the presence of intracellular *B. henselae* inhibits C_2-ceramide stimulated expression of caspase proteins and caspase enzymatic activity. Lastly, the presence of *B. henselae* inhibits DNA fragmentation and the protective effect attributed to the bacteria is visible by changes in gross cellular morphology.

Materials and Methods

Western Blot

HMEC-1 cells were lysed using PBS-TDS (0.01M PBS with 1% Triton X-100, 0.5% sodium deoxycholate, 0.1% SDS, 1% protease inhibitor cocktail (Pierce, Rockford, IL; Burnette, 1980). Twenty micrograms of cell lysates were mixed 1:5 with 5X Loading Buffer (Bio-Rad, Richmond, CA). Cell lysates were loaded using an SDS-PAGE precast (12% resolving gel, 4% stacking gel) minigel system (Bio-Rad, Richmond CA). Gels were run at 20 mA following dilution of 10X Tris/Glycine/SDS Buffer (Bio-Rad, Richmond, CA). Proteins were transferred onto Immuno-Blot PVDF Membrane (Bio-Rad, Richmond, CA) at 250 mA for 1 hour.

Blot membranes were blocked using 10X Blocking Agent (Bio-Rad, Richmond, CA) in TBS overnight at 4^{o}C. PVDF membranes were incubated with primary Rabbit anti-FADD antibody (Santa Cruz) at 1:1000 in Blocking Buffer for 1 hour at room temperature while shaking gently. Blots were washed 3x 10 minutes in Wash Buffer (TBS supplemented with 0.1% Tween 20). Blots were incubated with phosphatase-labeled anti-Mouse IgG (H+L) secondary antibody (KPL, Gaithersburg, MD) at 1:10,000 in Blocking Buffer for 1 hour at room temperature while shaking gently. Blots were washed 3x 10 minutes in Wash Buffer while shaking. Blots were

developed by incubating for 10 minutes with PhosphaGLO Reserve AP Substrate (KPL, Gaithersburg, MD). Excess substrate was drained and blots were inserted into a plastic sheet cover. Blots were visualized using a Bio-Rad documentation System.

Bacterial Culture

Bartonella henselae 882-str was cultured on Brain Heart Infusion (BHI) agar supplemented with 5% rabbit blood and 50 μg/mL streptomycin (Invitrogen, Carlsbad, CA). To obtain pure cultures of *B. henselae,* bacterial cultures were streaked for isolation and allowed to grow for 3 days at 37 ^{o}C and 5% CO_2. Cultures used for infection were prepared by streaking *B. henselae* onto a plate of BHI with 5% rabbit blood and 50 μg/mL streptomycin (Lee and Falkow, 1998).

Cultures were grown for 3 days post-inoculation to ensure that log-phase bacteria were used for all experiments. The zone of inoculum was scraped with a 10 μL loop and resuspended in BHI broth. Bacterial cells were resuspended to an $O.D._{600}$ of 0.5, an optical density that corresponds to approximately 1×10^9 cfu/mL. The concentration of bacteria was determined by triplicate plate counts of serial bacteria dilutions, as described previously (Kirby and Nekorchuk, 2002).

Cell Culture

CDC.HMEC-1 (HMEC-1) cells were obtained by Material Transfer Agreement (F.J. Candal, E.W. Ades, CDC, Atlanta, GA; T. Lawley, Emory University, Atlanta, GA.). HMEC-1 endothelial cells were grown at 37 ^{o}C and 5% CO_2 using MCDB-131 (GIBCO BRL) media supplemented with 15% fetal bovine serum (Hyclone, Ogden, UT), 25 μg/mL streptomycin and 1% L-glutamine (Invitrogen, Carlsbad, CA). HMEC-1 cells were seeded at 1.5×10^5 cells/mL for both stock subcultures and experimental cultures. HMEC-1 cells were grown for 3 days to 70%+

confluency prior to experimental use. Cells were subcultured every 7 days or as needed. For optimal performance and stability, HMEC-1 cells were used at passages T16 to T25.

Chemicals and Antibodies

C_2-ceramide (*N*-acetyl-*D*-erythrosphingosine) was dissolved in absolute ethanol at a concentration of 20 mM (Avanti Polar Lipids, Alabaster, AL). Murine anti-human TRADD and FADD were obtained from BD/Pharmingen (San Diego, CA). Secondary 488 conjugated goat anti-mouse IgG was obtained from Molecular Probes (Eugene, OR). Staurosporine and camptothecin were obtained from Sigma (St. Louis, MO). RNAase H was obtained from Epicentre (Madison, WI).

Ricin and abrin toxin were prepared from whole beans. One gram of beans was macerated to generate pulp mass and expressed toxin "mother liquor." PBS (0.01M, pH 7.2-7.4) was added to provide 1 mL of aqueous phase. Total material was centrifuged for 3 minutes at 3000 xg at 25^{o}C. The aqueous phase was decanted and centrifuged again for 3 minutes at 3000 xg at 25^{o}C. The respective toxins were semi-quantified using CDC LRN immunoassays for the detection of ricin or abrin toxin compared to a known toxin standard.

Intracellular Infection with B. henselae and Ceramide Treatment

HMEC-1 cells were grown to 70%+ confluency prior to infection. *B. henselae* bacteria were harvested and resuspended at 1×10^7 cfu/mL in serum-free MCDB-131 media (Invitrogen, Carlsbad, CA). An absorbance of 0.5 at 600 nm yields 1×10^9 cells/mL (McCord *et al.*, 2005). The cell culture medium was replaced with reduced serum (3% serum) media prior to *B. henselae* infection. HMEC-1 cells were infected at an MOI of 10 by adding 100 μL of a 1×10^9 cfu/mL bacterial suspension to HMEC-1 cells cultures approximately 70%+ confluent. HMEC-1

cultures were grown in 6-well Costar culture plates. *B. henselae*-infected cells were allowed to incubate overnight and then media replaced with MCDB-131 supplemented with 15% FBS for the remainder of the 36 hours at 37 ^{o}C and 5% CO_2 (Liberto *et al.*, 2003). C_2-ceramide was added to a total concentration of 20 μM to both *B. henselae*-infected and uninfected endothelial cells. Uninfected and untreated cells were used as experimental controls.

Endothelial Cell Viability Assay

Cell viability was determined by Trypan Blue (Invitrogen, Carlsbad, CA) exclusion (Bird and Forrester, 1981). Cells were harvested by collecting trypsinized cells following standard trypsinization procedures. Trypsinized cells were briefly centrifuged for 3 minutes at 100 xg at 4 ^{o}C. The supernatant from centrifuged cells was carefully aspirated to remove cellular debris. Collected cells were resuspended in a minimal volume of 100 μL. Trypan Blue was added at a 1:1 ratio with resuspended cells and viability was determined by a standard protocol using a Seitz cell counting chamber (Sigma, St. Louis MO).

Flow Cytometric Intracellular Protein Analysis

HMEC-1 endothelial cells were infected and treated with ceramide as described here. Cells were harvested by gentle agitation with 100 μM glass beads (Corning Glass, Corning, NY) as described here. Harvested cells were washed 2x with 0.01M PBS, pH 7.4, and pelleted by centrifugation at 100 xg for 3 minutes. Pelleted cells were resuspended and fixed by adding 10% EM-grade formalin (Polyscience, Warrington, PA) in 0.01M PBS, pH 7.4, to a final concentration of 1.5% formaldehyde. Cells were incubated in fixative for 10 minutes at 4^{o}C. Fixed cells were washed 2x with 0.01M PBS, pH 7.4, and pelleted by centrifugation at 100 xg for 3 minutes. Cells were then resuspended and permeabilized in 1X Perm II solution (BD, San Jose, CA) in 0.01M PBS, pH 7.4 (Invitrogen, Carlsbad, CA) for 10 minutes at 4 ^{o}C (Belloc *et al.*,

2000). Cells were washed 2x with FACS Wash Buffer (0.01M PBS, pH 7.4 (Invitrogen, Carlsbad, CA) supplemented with 2% human AB+ serum (Irvine Scientific, Irvine, CA.) + 0.01% NaN_3). Cells were pretreated with excess unlabeled anti-TRADD or FADD antibodies (BD, San Jose) for 1 hour at 4 ^oC and washed 2x with FACS Wash.

Cells were stained using 0.5 μg/sample of anti-TRADD (BD, San Jose, CA), 0.5 μg of anti-FADD (BD, San Jose, CA) in 0.01M PBS, pH 7.4 at 4^oC overnight. Cells were washed 2x with FACS Wash and centrifuged at 100 xg. Secondary Alexa 647 goat anti-mouse antibodies (Molecular Probes, Eugene OR) were used at a working dilution of 1:5,000. Samples were analyzed on a FACSCaliber cytometer (BD, San Jose CA), calibrated daily with Calibrite beads (BD, San Jose) supplied with lasers operating at 488 and 633 nm (Krutzik and Nolans, 2003) Data were acquired using the FL4 channel excited at 633 nm and 668 emission.

Caspase Enzymatic Activity Assay

Samples were analyzed for activity of caspase-3, 6 and 8 using Trupoint^{TM} Caspase Assays (Perkin-Elmer, Boston, MA), according to the manufacturers' protocol. Briefly, cells were washed in the well 2x with physiological saline and lysed using a 1:10 dilution of 10X Lysis Buffer. Cells were homogenized by rapid pipetting and collected into 1.7 mL eppendorf tube. The caspase sample wells consist of 10 μL caspase-DTT Buffer, 5 μL (800 nmol/L) caspase substrate and 5 μL cell lysate. Background wells consist of 15 μL caspase-DTT Buffer and 5 μL caspase substrate (Karvinen *et al.,* 2002). Lysates and caspase substrates were incubated at 37^oC, 95% relative humidity for a minimum of 2 hours prior to reading. Caspase assays were read using a Victor^3 plate fluorometer at 615 nm according to the manufacturers' protocol (Wallac, Turku, Finland).

Multicaspase Fluorescent Assay

To a 100 μL aliquot of cells ($1x10^5$/mL), 4 μL of 20X SR-VAD-FMK (Millipore/Guava) reagent were added, and to each sample or control tube was mixed by gentle vortexing and incubated for 1 hour at 37°C in 5% CO2 incubator. The cells were resuspended once during the incubation period. Approximately 1 mL of 1X Apoptosis Wash Buffer (Millipore/Guava) was added to each tube, vortexed and centrifuged at 300 to 400xg for 5 minutes to pellet the cells. The supernatant was removed and the cell pellet was retained. The cells were washed twice more as described. Each cell pellet was resuspended in 100 μL of 1X Apoptosis Wash Buffer (Millipore/Guava). Approximately 50 μL of stained cells were air dried on glass slides. Slides were examined directly using a Nikon fluorescent microscope with a 565 nm excitation and 615nm emission filter

Flow Cytometric DNA Cell Cycle Analysis

Cell supernatants were collected and pelleted by centrifugation at 100 xg for 3 minutes. Pelleted cells were added to harvested cells described below. Cell monolayers were washed 2x with 0.01M PBS, pH 7.4 (Invitrogen, Carlsbad, CA) prior to harvesting. Cells were harvested from culture plates by gentle agitation with 100 μM glass beads (Corning Glass, Corning, NY). HMEC-1 cells were prepared for ethanol fixation by washing 2x with excess 0.01M PBS, pH 7.4 (Invitrogen, Carlsbad, CA) and centrifuged for 3 minutes at 100 xg. Cells were fixed by the addition of 0.5 mL 70% ethanol (Pharmco, Brookfield, CT) in sterile deionized water (Mediatech, Richmond VA).

Ethanol fixed cells were washed 2x with excess 0.01M PBS, pH 7.4 (GIBCO/BRL, Grand Island NY) and centrifuged for 3 minutes at 100 xg. Following fixation, cells were resuspended in 200 μL of 0.01M PBS, pH 7.4 (Invitrogen, Carlsbad, CA) with 2 μg/mL RNAse

A (Epicentre, Madison, WI). Cells were incubated for 30 minutes at 37 ^{o}C, washed 2x with excess 0.01M PBS, pH 7.4, and subsequently resuspended at approximately 1×10^{6} cells/mL in 0.01M PBS, pH 7.4, containing 5 μg/mL propidium iodide (PI, Sigma, St. Louis, MO.). DNA cell cycle analysis was performed on a FACSCAliber (Becton-Dickinson, San Jose, CA). DNA cell cycle data were assessed by log range FL-2 height for PI staining (Abraham *et al.*, 2003).

Statistics

The data presented herein are the means± S.D. of three independent experiments with experimental samples performed in triplicate. Statistical significance was determined using the Student's "two-tailed" *t*-test. A *P* value of <0.05 was considered significant.

Results

Analysis of FADD by Western Blot

Western blot analysis of Fas-associated Death Domain (FADD) was conducted to determine whether *B. henselae* altered FADD protein expression. By two hours post-infection, the levels of FADD are undetectable (Figure 7). From these observations, we conclude that there is a significant and rapid decline in FADD protein expression during the course of *B. henselae*-infection relative to their uninfected counterparts.

Apoptogenic Agents

Apoptogenic agents were tested for their ability to alter cell viability following 3 hours' treatment of HMEC-1 endothelial cells. Apoptogenic agents were serially diluted and cell viability determined using Trypan Blue exclusion for HMEC-1 cells grown at 4^{o}C and 95% humidity. Percent viability is presented in Figure 8. Among the apoptogenic agents tested, only C_2-ceramide was cytotoxic in a titratable dose-dependent manner. Further, several of the other

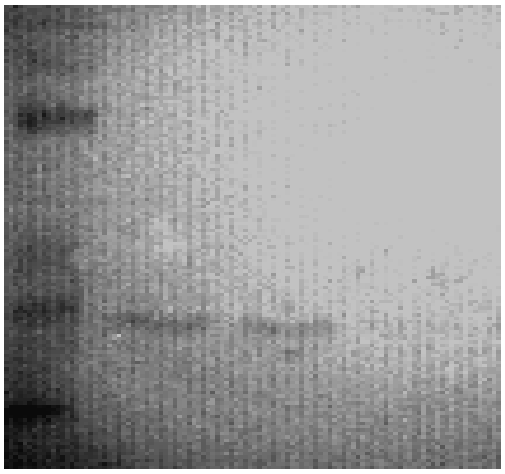

Figure 7. FADD Western Blot. HMEC-1 cells were incubated with *B. henselae* for 1 hr at 37oC. Growth media was added and cells were harvested at 1 and 2 hour post-infection timepoints. Control cells were harvested at timepoint of 2 hour post-infection identical manner in the absence of *B. henselae*.

agents tested were cytotoxic, but did not produce the distinguishable morphological effects on the endothelial cells that are characteristic of apoptosis (data not shown). For these reasons, C_2-ceramide was the apoptotic agent of choice for all subsequent experiments involving the induction of apoptosis.

Cellular Morphology under Apoptotic Conditions

To determine the response of cells infected with *B. henselae* to signals inducing apoptosis, we compared the effect of infection on HMEC-1 cells that were treated with ceramide for varying periods of time. Prior to ceramide treatment, uninfected and *B. henselae*-infected cells

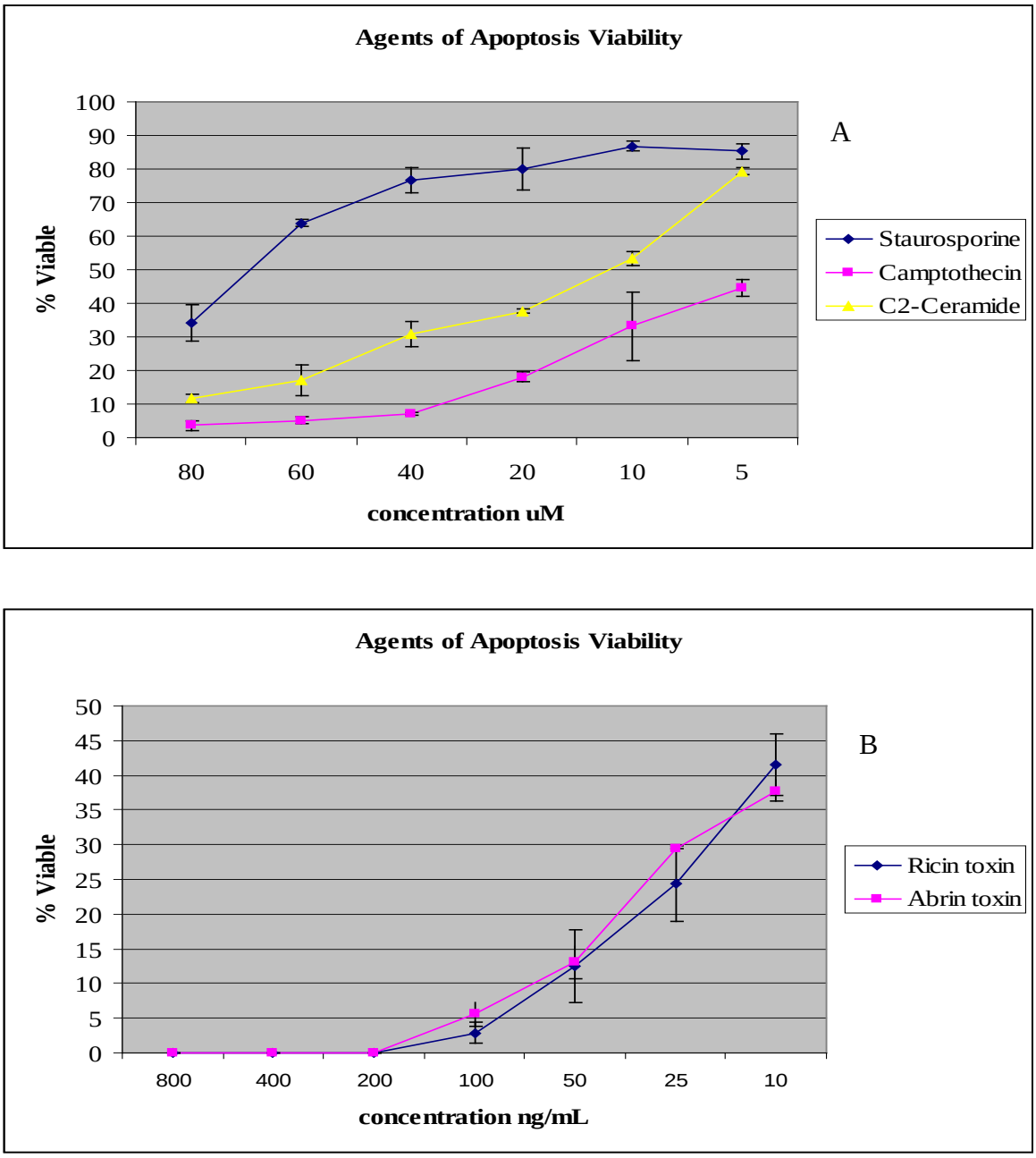

Figure 8. Cytotoxic Effect of Apoptogenic Agents. Commercially available apoptogenic agents were titrated using dilutions of 100 µM stock (A). Ricin and Abrin toxin were prepared from natural source. Concentrations were determined by LRN immunoassay reactivity compared to standards (B). HMEC-1 cells were treated with apoptogenic agents for 3 hours. Viability was assessed using Trypan Blue exclusion.

both produce a confluent monolayer (Figure 9A and 9B). Some cell rounding is apparent in the infected culture, which we ascribe to an overgrowth of the cells. Little change in gross morphology is observed for both uninfected (Cer) and infected (B + C) cells following two hours of ceramide treatment (Figure 9C and 9D). Uninfected cells demonstrate a higher refractive index, but overall the effect on the cell monolayer is minimal for both cultures. A higher magnification does reveal some remarkable differences between infected and uninfected cells after two hours of ceramide treatment, however. Uninfected ceramide-treated cells exhibit cytoplasmic membrane blebbing (Figure 10A), a classic characteristic of early apoptosis events (Green, 2003). *B. henselae*-infected cells treated with ceramide for the same amount of time exhibit no cytoplasmic membrane blebbing (Figure 10B).

After four hours of treatment with ceramide, uninfected cells began to show pronounced rounding of the cells and sloughing of cells from the monolayer, characteristics that become more apparent at six hours of exposure (Figure 11A and 11C). During this same time period, ceramide treatment has little visible effect on the appearance of the *B. henselae*-infected culture (Figure 11B and 11D). By eight hours of treatment, the uninfected culture exhibits a pronounced loss of monolayer integrity (Figure 12A), while the *B. henselae*-infected culture exhibits modest rounding of the cells and sloughing of the monolayer (Figure 12B). Following 12 hours of ceramide exposure the uninfected cells have lost nearly all adherent properties and nearly half of the *B. henselae*-infected cells are rounding (Figure 12C and 12D). During this same time period, ceramide treatment has little visible effect on the appearance of the *B. henselae*-infected culture (Figure 11B and 11D).

***Cell Viability under Conditions Inducing Apoptosis*.**

The uptake of the vital dye Trypan Blue is associated with a loss of nuclear membrane integrity, and is thus considered to be a reliable gross indicator of cell viability. Figure 13 illustrates the changes in cellular viability following ceramide treatment of both *B. henselae*-infected (B+C) and uninfected (Cer) endothelial cells, as compared to controls that are not exposed to ceramide. Ceramide exposure results in a steady decline in viability for both infected and uninfected cells relative to the untreated controls; however, the decrease in viability is much more pronounced in the uninfected culture, suggesting that *B. henselae* infection is providing a protective effect against cell death.

Intracellular Expression of TRADD and FADD

Previous results (Figure 7) indicated that the levels of FADD in cells infected by *B. henselae* are significantly reduced in comparison to their uninfected counterparts. To determine the concentrations of TRADD and FADD in infected and uninfected cells under apoptotic conditions, flow cytometric analysis was conducted on cells that had been visualized by treatment with anti-TRADD and anti-FADD antibodies followed by incubation with a secondary goat anti-mouse antibody. Following thirty minutes of ceramide treatment, TRADD producing cells are minimal in both uninfected and infected cells (13% and 13.2% of the total cells, respectively, Figure 14A and B). Following one hour ceramide treatment, TRADD-producing cells remain low in the infected sample (14.9%, Figure 14C) but have begun to show an increase in the uninfected cells (23.1% of total cells, Figure 14D). TRADD protein production spikes for uninfected cells at 2 hours (75.94%, Figure 15A) and is still elevated at 3 hours (69.04%, Figure 15C) after ceramide treatment

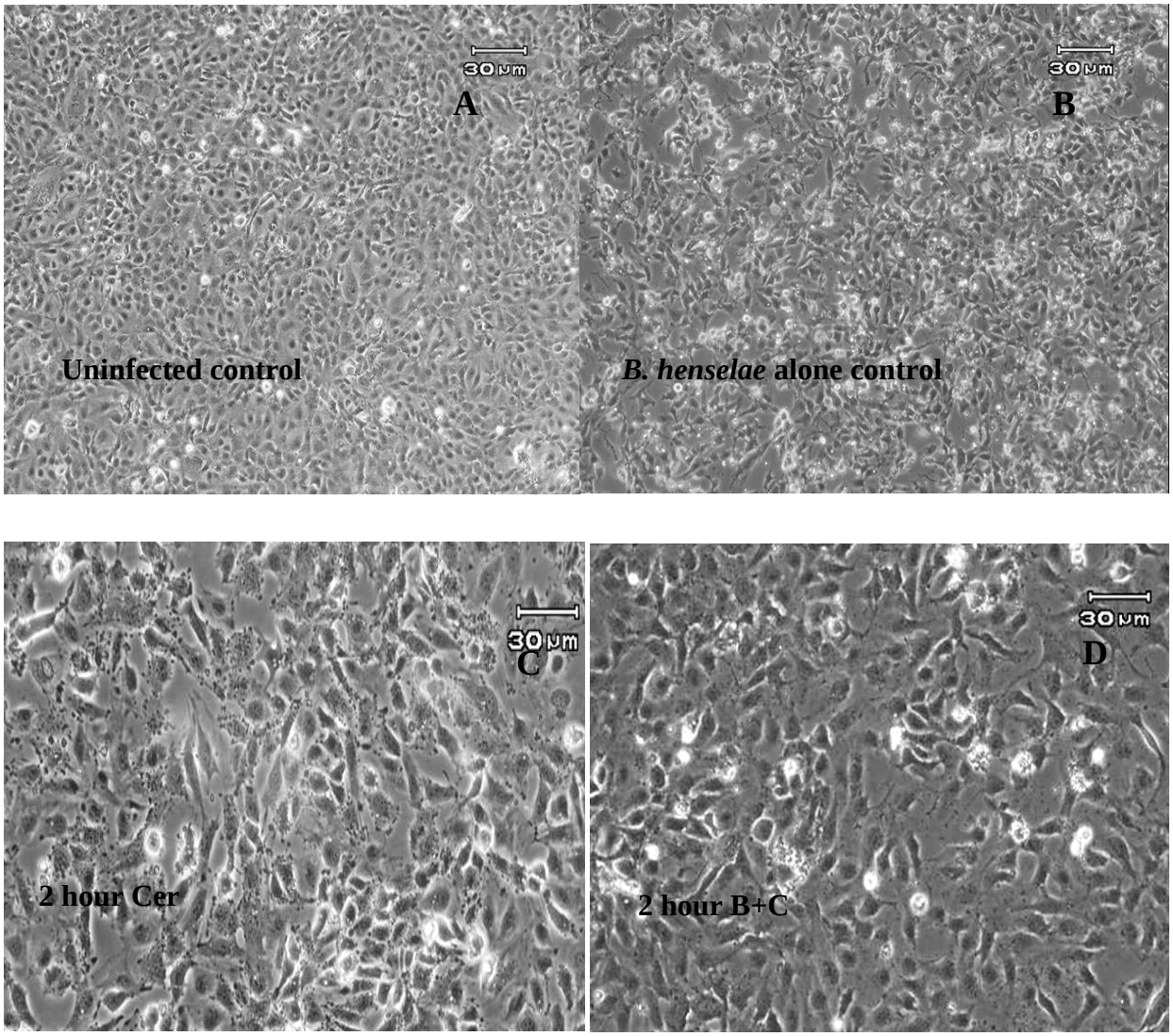

Figure 9. Cell Morphology—Controls and Two-hour Ceramide Treatment. Changes in cell morphology with ceramide treatment. Uninfected of *B. henselae*-infected cells were exposed to 20 μM C_2-ceramide for varying periods of time. A. Uninfected control cells prior to ceramide exposure. B. *B. henselae*-infected control cells prior to ceramide exposure. C. Uninfected cells after 2 hour exposure to ceramide. D. *B. henselae*-infected cells after 2 hour exposure. Figures are representative of multiple independent experiments (n=3). After four hours of treatment with ceramide, uninfected cells began to show pronounced rounding of the cells and sloughing of cells from the monolayer, characteristics that become more apparent at six hours of exposure (Figure 11A and 11C).

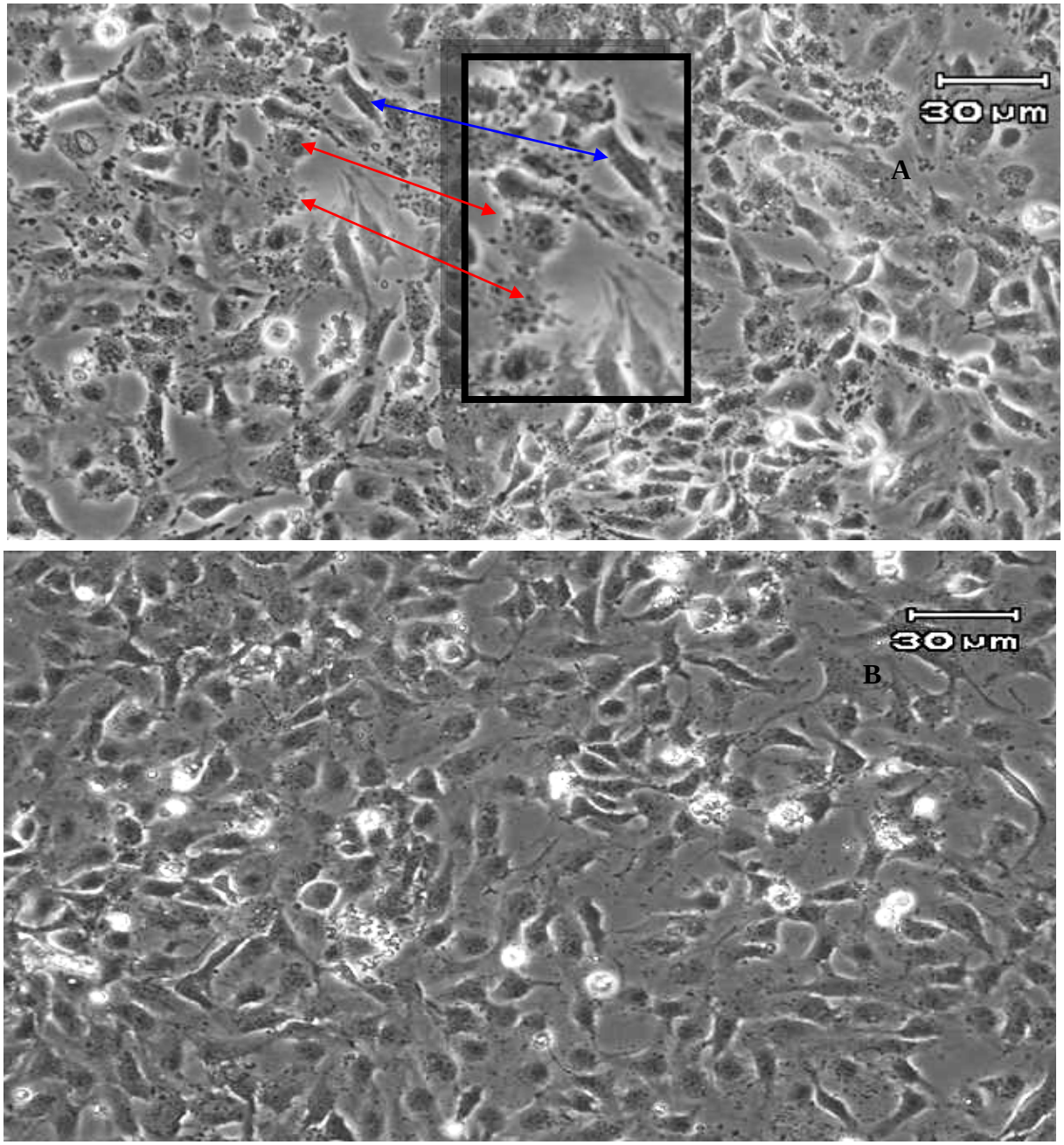

Figure 10. Classic Morphology of Early Apoptosis Event. Enlarged view of 2 hour 20 µM C_2-ceramide treatment. A. Uninfected cells after 2 hour exposure. Cytoplasmic blebbing is highlighted in picture inset (red arrows) as compared to no blebbing (blue arrows). B. *B. henselae*-infected cells after 2 hour exposure view after two hour ceramide exposure.

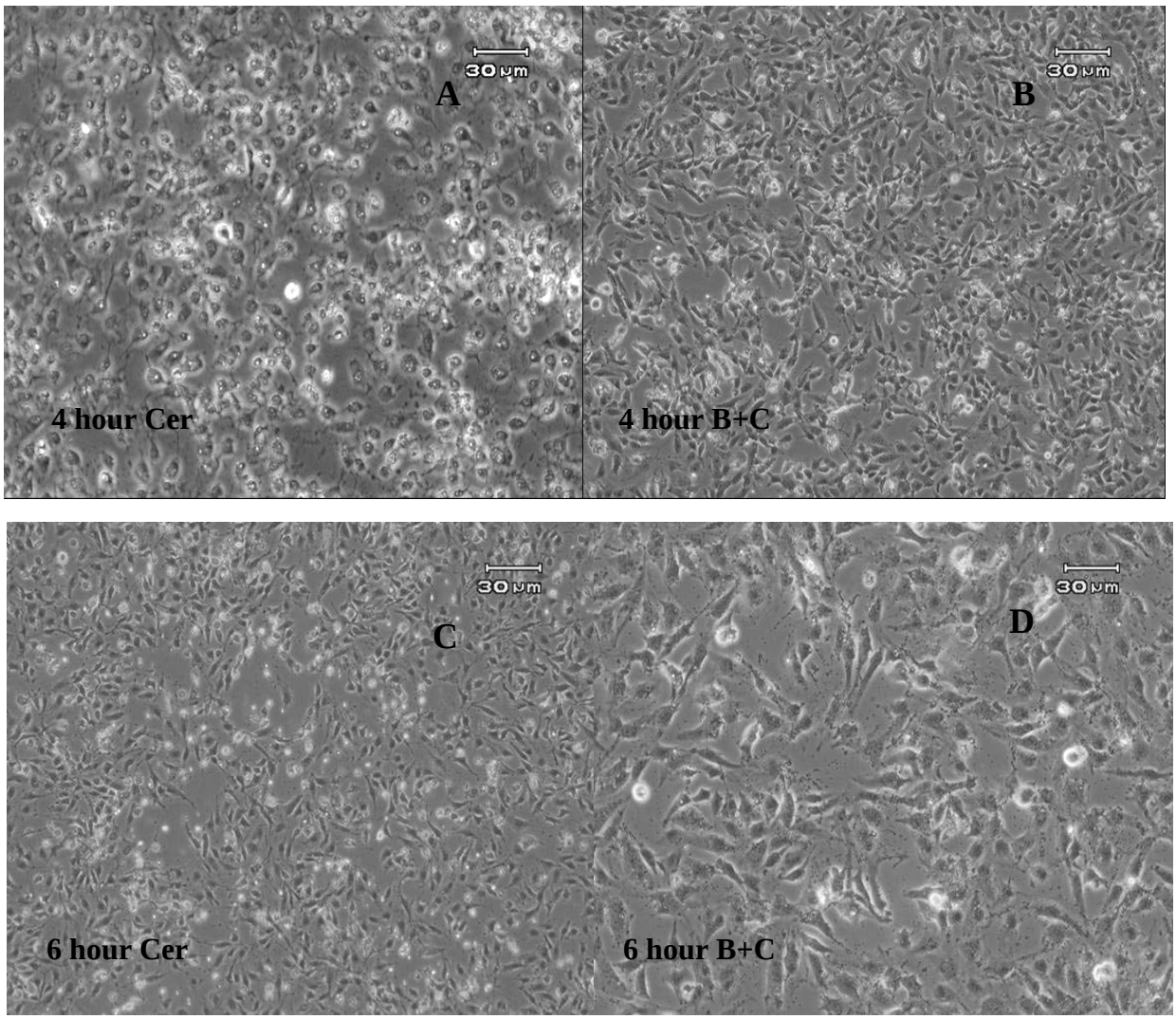

Figure 11. Cell Morphology—Four- and Six-hour Ceramide Treatment. Change in cell morphology with ceramide treatment. Uninfected of *B. henselae*-infected cells were exposed to 20 μM C_2-ceramide for varying periods of time. A. Uninfected cells after 4 hour exposure to ceramide. B. *B. henselae*-infected cells after 4 hour exposure. C. Uninfected cells after six hour exposure to ceramide. D. *B. henselae*-infected cells after 6 hour exposure. Figures are representative of multiple independent experiments (n=3).

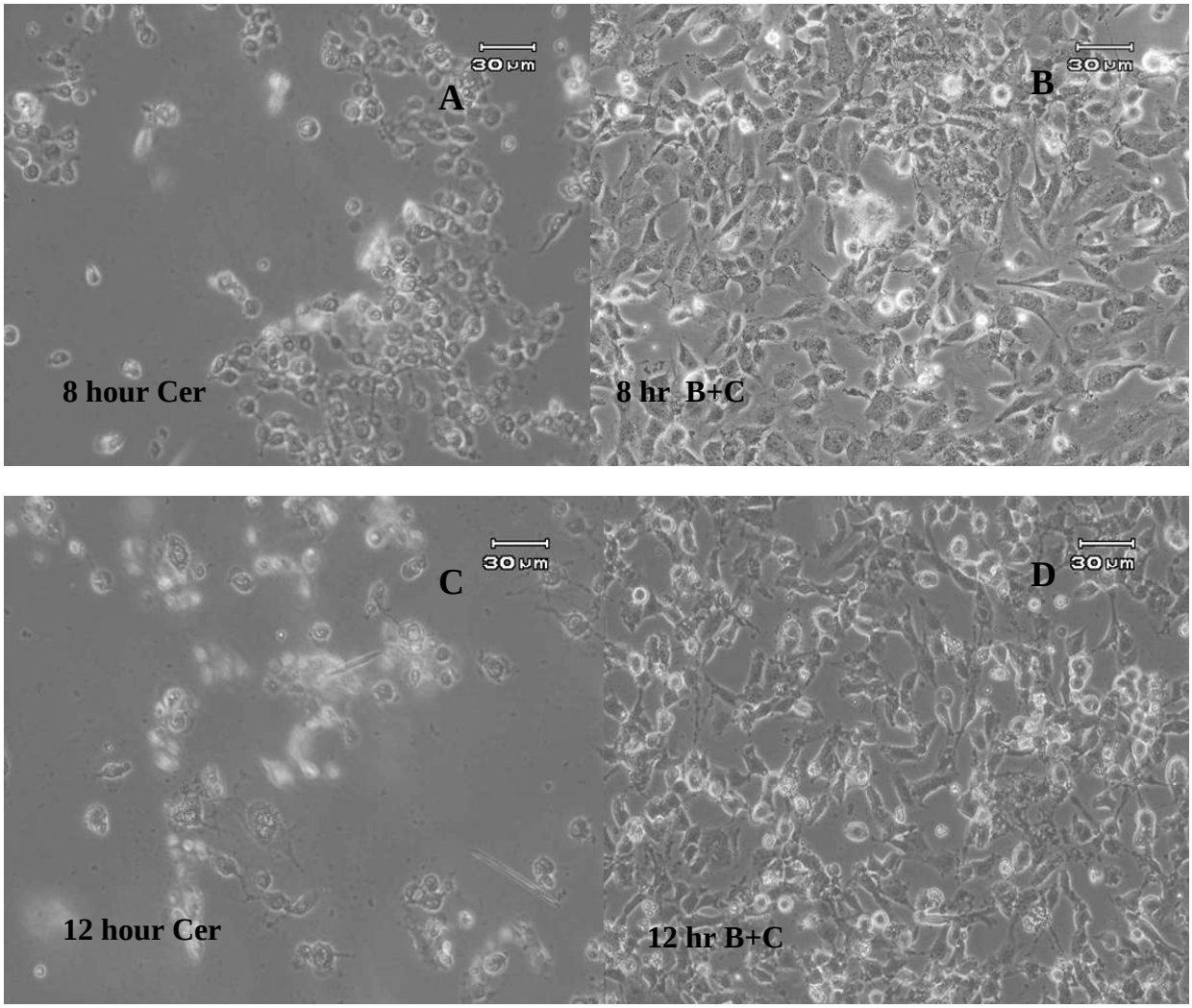

Figure 12. Cell Morphology—Eight- and Twelve-hour Ceramide Treatment. Change in cell morphology following ceramide treatment. Uninfected of *B. henselae*-infected cells were exposed to 20 μM C_2-ceramide for varying periods of time. A. Uninfected cells after 8 hour exposure to ceramide. B. *B. henselae*-infected cells after 8 hour exposure. C. Uninfected cells after 12 hour exposure to ceramide. D. *B. henselae*-infected cells after 12 hour exposure. Figures are representative of multiple independent experiments (n=3).

Among infected cells the proportion producing TRADD is only marginally enhanced at 2 hours (28.70%; Figure 15B) and remains low at 3 hours (22.30%, Figure 15D). The proportion of TRADD-positive cells in the uninfected sample has reached a plateau following 4 hours ceramide treatment (69.81%, Figure 16A), while TRADD production in the infected cells is still seen in only a small proportion of infected cells (16.13%, Figure 16B).

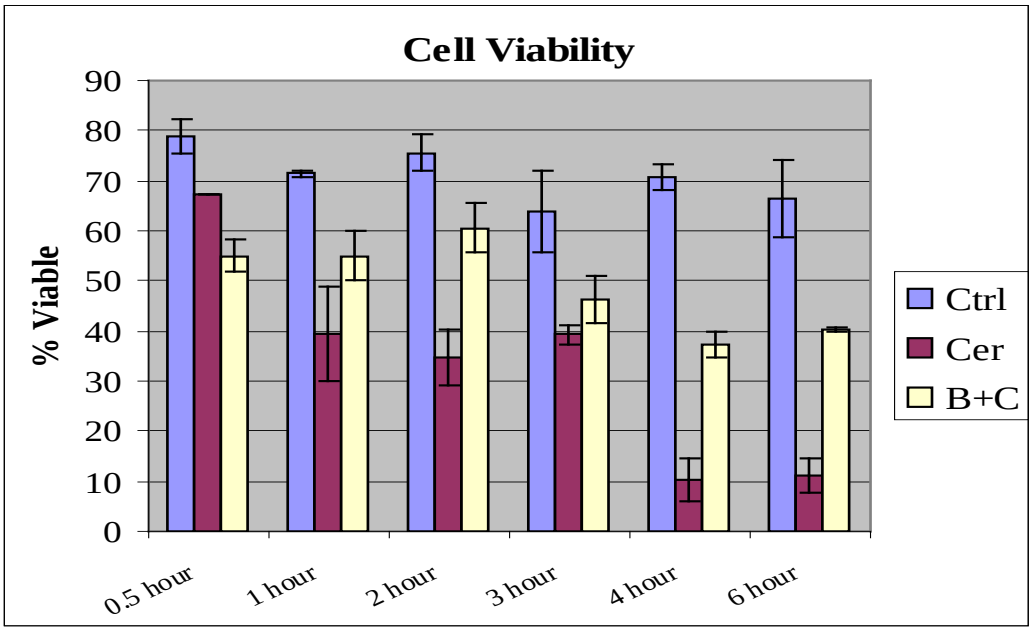

Figure 13. Cell Viability by Trypan Blue Exclusion. Cell counts were determined in triplicate. Uninfected cells treated with ceramide (Cer), *Bartonella henselae*-infected cells treated with ceramide (B+C), and normal control cells (Ctrl) were assessed for cellular viability by Trypan blue exclusion. Mock experimental controls for B+C and Cer were 69.16±4.67% and 65.04±1.41%. Graphs are representative of multiple independent experiments (n=3).

Thus, *B. henselae* infection is associated with a reduction in TRADD production under conditions favoring apoptosis. Like TRADD, FADD is produced in more uninfected cells treated with ceramide than in their *B. henselae*-infected counterparts. Even at thirty minutes of ceramide treatment, the proportion of cells producing FADD in the uninfected cell population (60.7%; Figure 17A) is significantly higher than that seen in the infected sample (40.2%; Figure 17B). The numbers of FADD- producing cells in the uninfected sample increase further at one hour of ceramide treatment (75.1%; Figure 17C), while FADD production is waning in the infected sample (32%; Figure 17D) at the same time point. Over the next three hours, the proportion of FADD-producing cells in the uninfected sample remains high (70% at 2 hours, Figure 18A; 64% at 3 hours, Figure 18C), and 81% at 4 hours (Figure 19A) of ceramide treatment). During the

same time period, the levels remain fairly static in the infected cell population, decreasing slightly after 4 hours (30.3% at 2 hours (Figure 18B, 30.8% at 3 hours (Figure 18D), and 24.7% at 4 hours, Figure 19B). Thus, as with TRADD, infection by *B. henselae* is correlated with lower levels of FADD following the induction of apoptosis.

Inhibition of Caspase Activity in B. henselae Infected Cells

The effect of B. henselae infection on caspase activity was initially measured using the Trupoint assay system (Perkin-Elmer). Controls using both normal control cells and untreated *B. henselae*-infected cells were used for comparison. The results (Figure 20) reveal that the enzymatic activity for caspase-8 and caspase-6 are enhanced in both *B. henselae*-infected and ceramide-treated cells, as compared to their uninfected counterparts. Caspase-6 is significantly increased in B+C cells, as compared to Cer cells, only following prolonged ceramide treatment. Caspase-3 enzymatic activity, as seen in Figure 20A, is enhanced in Cer cells, as compared to B+C cells or control cells. Enzymatic activity for caspase-3 rapidly increases following 1 to 4 hours of ceramide treatment.

Multicaspase Fluorescent Peptide Assay for Detection of Caspase Activity

The multicaspase fluorescent peptide assay makes use of a peptide substrate that can be cleaved by caspases to yield fluorescent products. Although the assay does not differentiate between a spectrum of caspases (caspase-2, -3, -6, -7, -8, and -10), it does provide a picture of the overall levels of caspase activity, and hence the apoptotic condition of the cell (Slee *et al.*, 1999). Use of this assay indicates that *B. henselae*-infected cells demonstrate a rapid induction of caspase activity following 2 and 3 hours of ceramide treatment (Figure 21A and 21C).

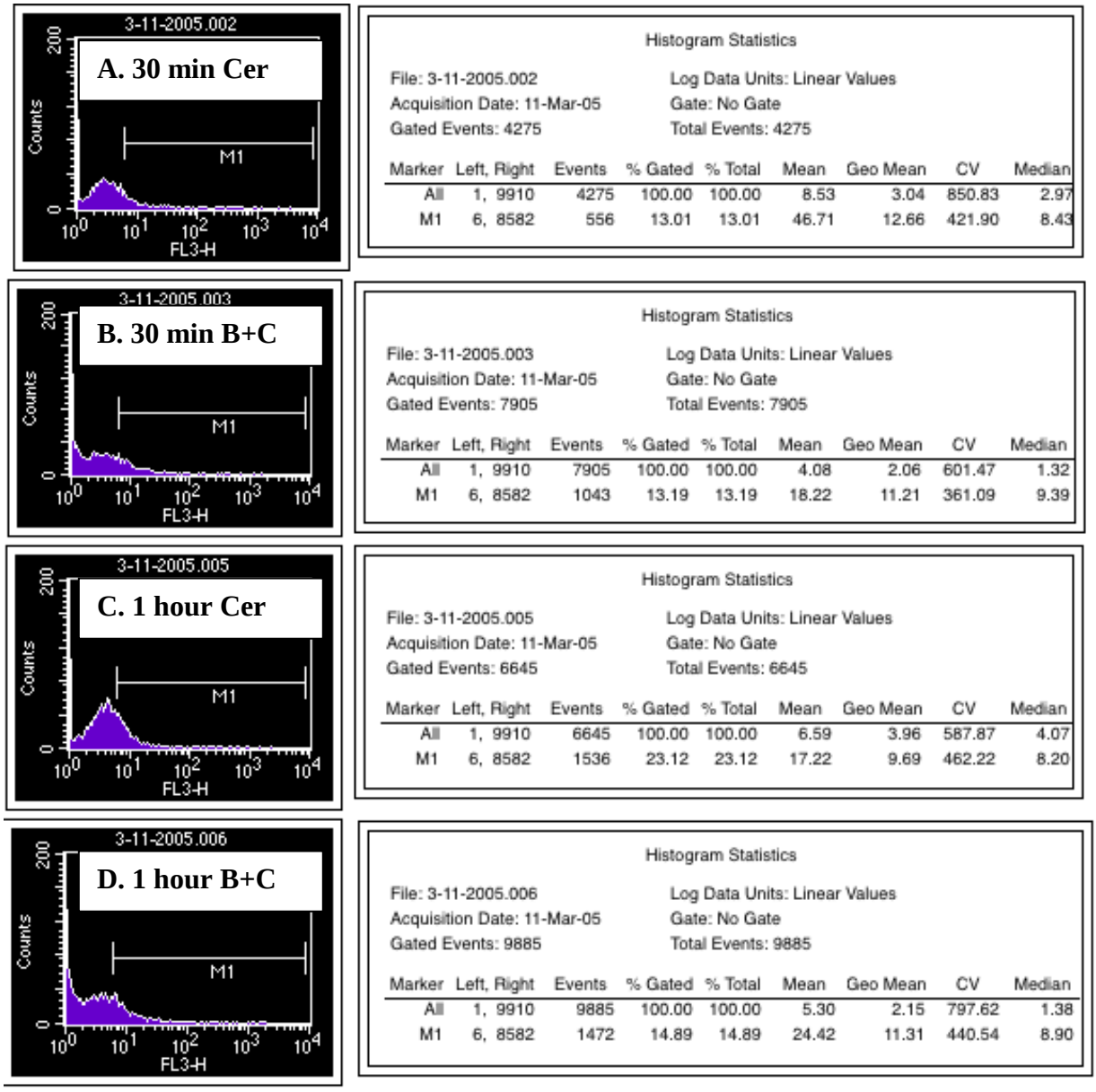

Figure 14. TRADD Protein Expression Analysis by Flow Cytometry—Thirty minute and One-hour Ceramide Treatment. TRADD protein expression for Cer and B+C cells following 30 minutes (A and B, respectively) and 1 hour (C and D, respectively) following ceramide treatment. TRADD protein expression is baseline for both Cer cells (13.01%) and B+C cells (13.19%) following 30 minutes ceramide treatment. Following 1 hour ceramide treatment, TRADD protein expression increases for Cer cells (23.12%, C) as compared to B+C cells (14.89%, D). Figures are representative of two independent experiments (n=2).

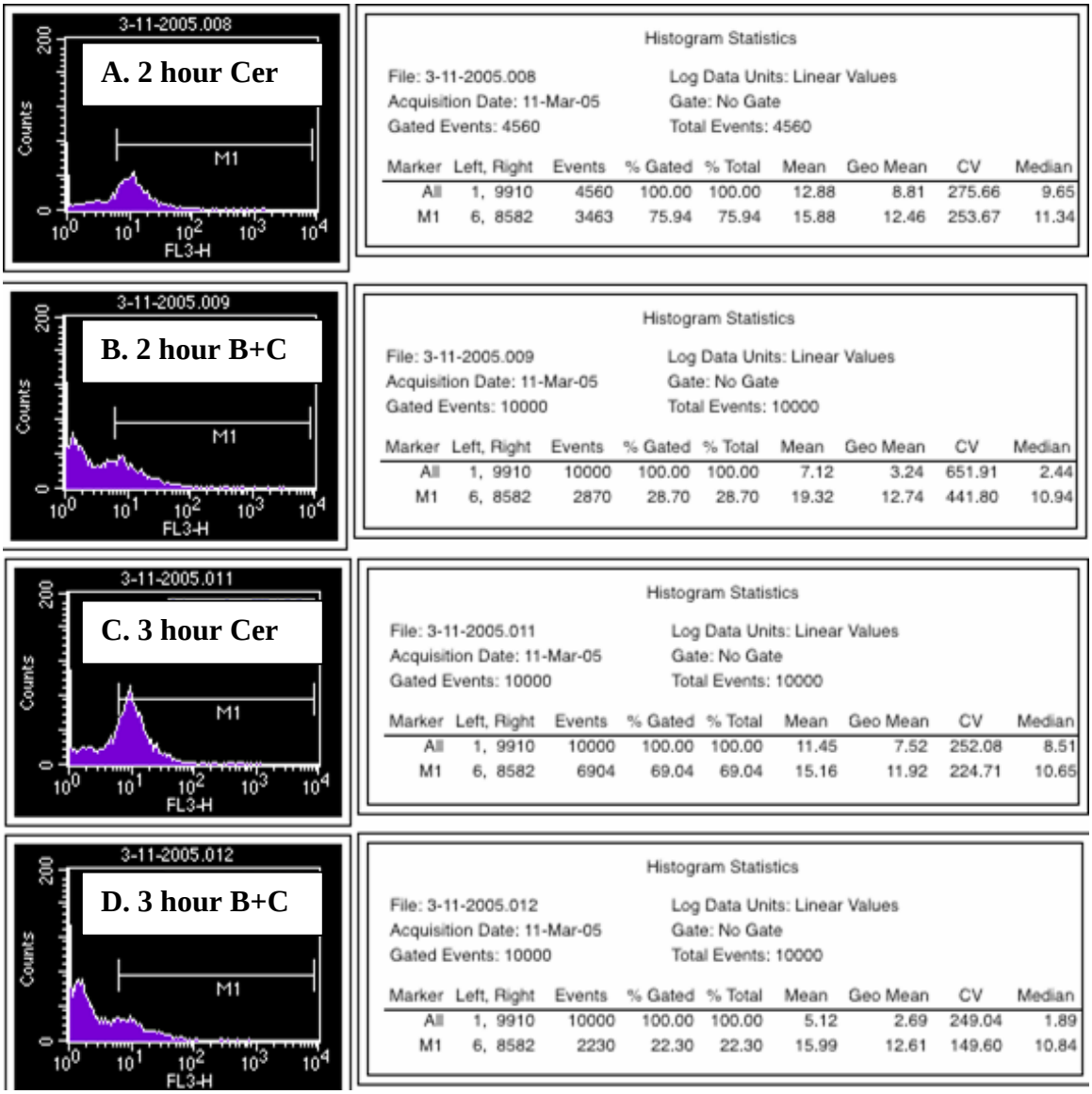

Figure 15. TRADD Protein Expression Analysis by Flow Cytometry—Two- and Three-hour Ceramide Treatment. TRADD protein expression for Cer and B+C cells following 2 (A and B, respectively) and 3 hour (C and D, respectively) ceramide treatment. TRADD protein expression is enhanced for Cer cells following 2 hour ceramide (75.94%, A) as compared to B+C cells (26.70%, B). Following 3 hour ceramide treatment, TRADD protein expression decreases for Cer cells (69.04%, C) and is relatively unchanged for B+C cells (22.30%, D). Figures are representative of two independent experiments (n=2).

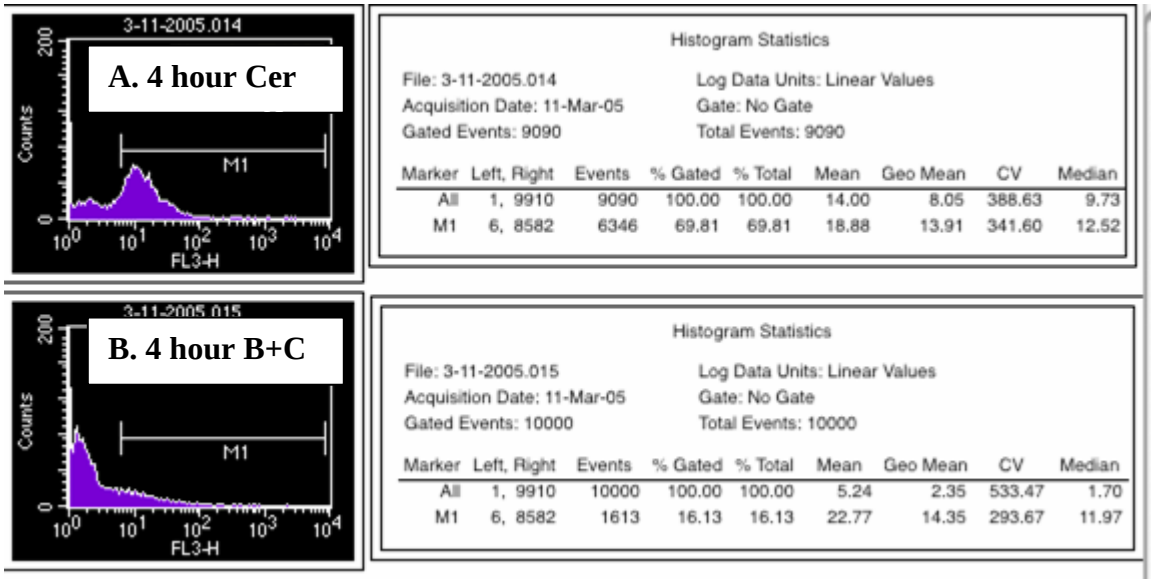

Figure 16. TRADD Protein Expression Analysis by Flow Cytometry—Four-hour Ceramide Treatment. TRADD protein expression is still enhanced for Cer cells following 4 hours ceramide treatment (69.81%, A) as compared to slight decrease in B+C cells (16.13%, B). Figures are representative of two independent experiments (n=2).

Multicaspase activation in these cells wanes following 4 hours of ceramide treatment, and continues to decline following 6 hours of treatment (Figure 21E and G). Uninfected cells also exhibit a rapid overall induction of caspase activity between 2 and 3 hours of ceramide treatment (Figure 22A and 22C), but unlike their infected counterparts, they continue to demonstrate induced caspase activity, as indicated by the maintenance of high fluorescence levels extending after 4 and 6 hours of treatment (Figure 22E and 22G). Taken together, these results suggest that *B. henselae* suppresses overall caspase induction under apoptotic conditions.

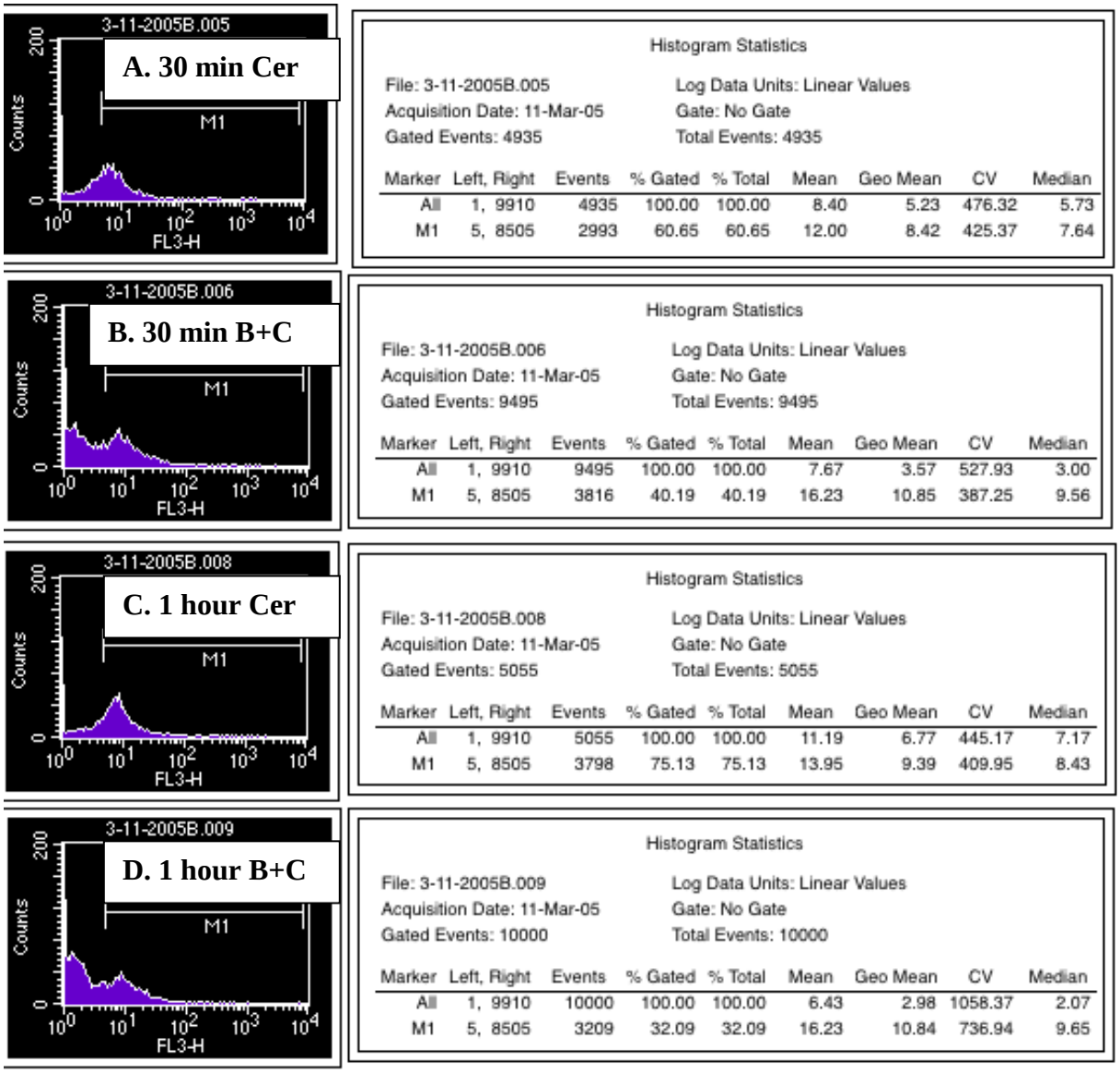

Figure 17. FADD Protein Expression Analysis by Flow Cytometry—Thirty Minute and One-hour Ceramide Treatment. FADD protein expression for B+C and Cer cells following 30 minutes (A and B, respectively) and 1 hour (C and D, respectively), following ceramide treatment. FADD protein expression is enhanced for Cer cells following 30 minutes ceramide (60.65%, A) as compared to B+C cells (40.19%, B). Following 1 hour ceramide treatment, FADD protein expression increases for Cer cells (75.13, C) as compared to a decrease in FADD protein expression for B+C cells (32.09%, D). Figures are representative of two independent experiments (n=2).

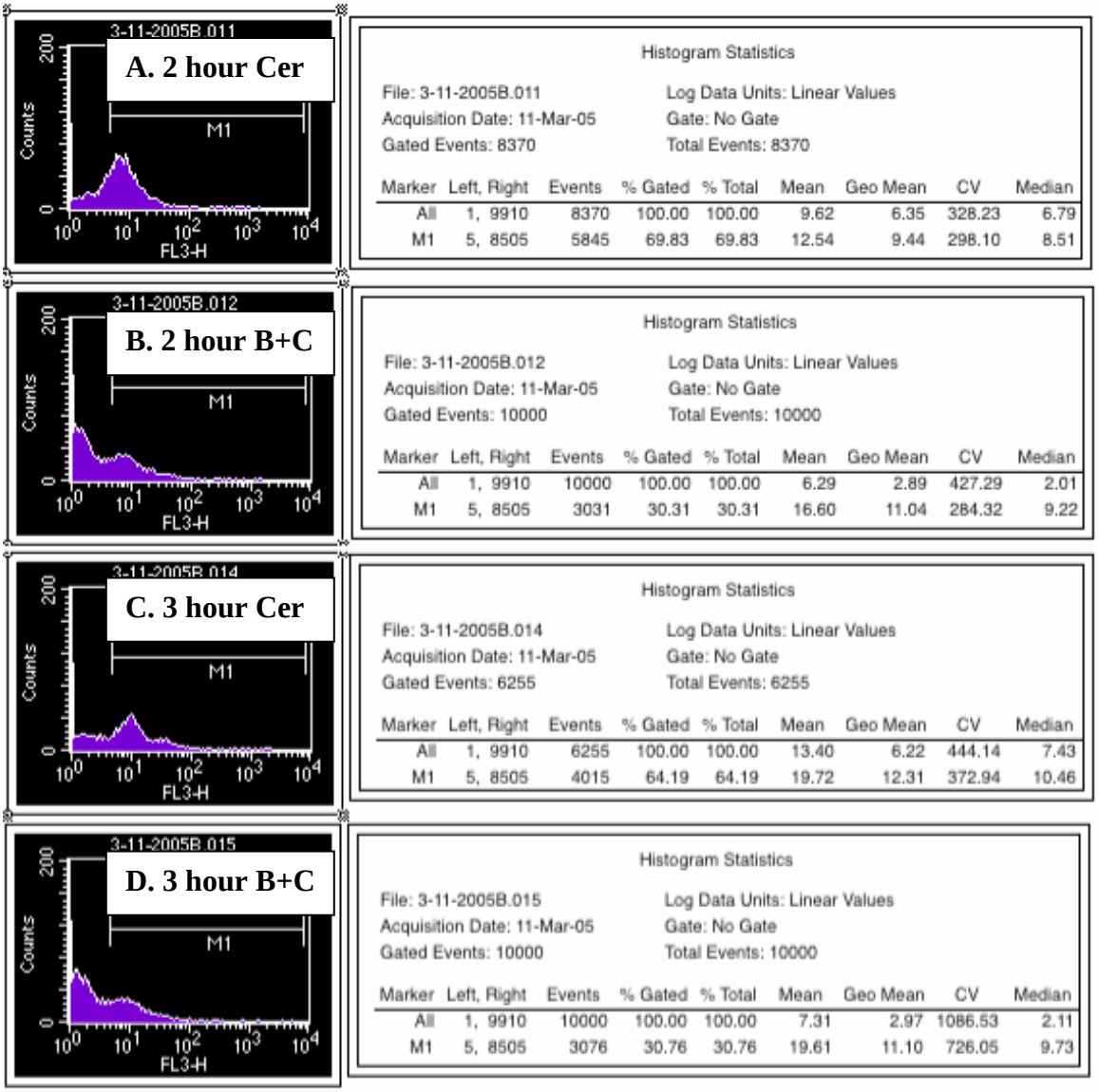

Figure 18. FADD Protein Expression Analysis by Flow Cytometry—Two- and Three-hour Ceramide Treatment. FADD protein expression for B+C and Cer cells, following 2 hour (A and B, respectively) and 3 hour (C and D, respectively) ceramide treatment. FADD protein expression is enhanced for Cer cells following 2 hour ceramide (69.83%, A) as compared to B+C cells (30.31%, B). Following 3 hour ceramide treatment, FADD protein expression decreases for Cer cells (64.19%, C), while FADD protein expression remained unchanged for B+C cells (30.76%, D). Figures are representative of two independent experiments (n=2).

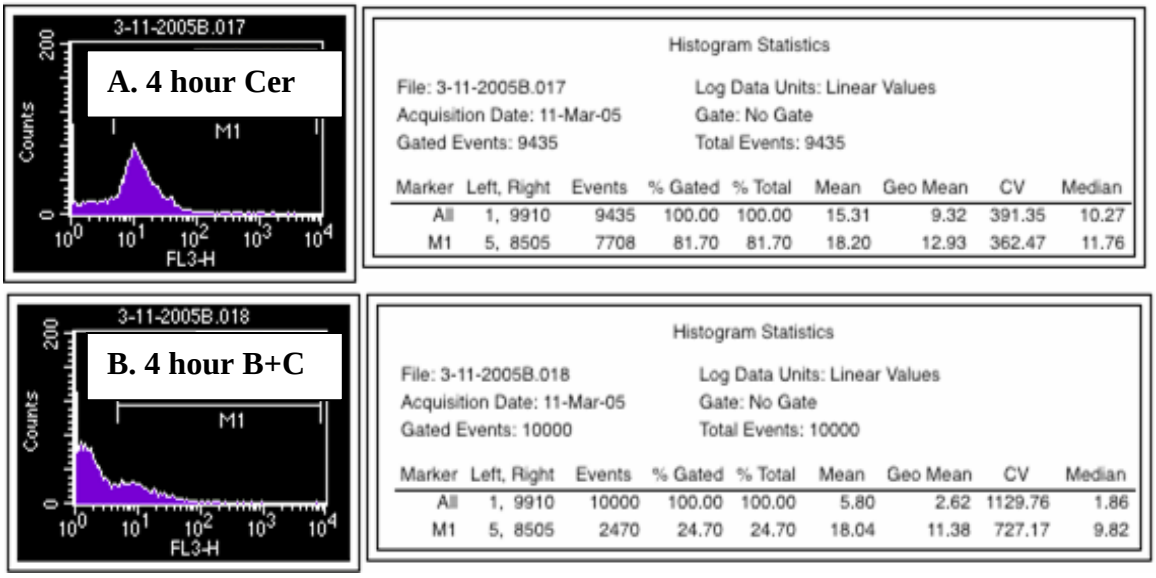

Figure 19. FADD Expression Protein Analysis by Flow Cytometry—Four-hour Ceramide Treatment. FADD protein expression for both Cer and B+C cells, following 4 hour (A and B, respectively) ceramide treatment. FADD protein expression is enhanced for Cer cells following 4 hour ceramide (81.70%, A) and decreases for B+C cells (24.70%, B). Figures are representative of two independent experiments (n=2).

Effect of B. henselae infection on Ceramide-induced DNA Fragmentation

Flow cytometry was conducted in order to assess the effect of infection on DNA fragmentation, which is an indicator of apoptotic conditions. The fluorescent intercalating dye propidium iodide (PI) was used for cell staining. The DNA cell cycle was determined by FL-2 height (FL2-H) on a log scale: actively growing cells are expected to sort at positions corresponding to G_1 (1X DNA) through S and G_2 (2X DNA), while cells in a resting state, G_1/G_0, or those undergoing DNA fragmentation, sub G_1/G_0, should exhibit correspondingly less fluorescence than their active counterparts (Elzbieta *et al*., 1998). Untreated *B. henselae*-infected and uninfected cells demonstrate a typical DNA histogram distribution (Figure 27A and B respectively), with cells distributed between G_1, S and G_2.

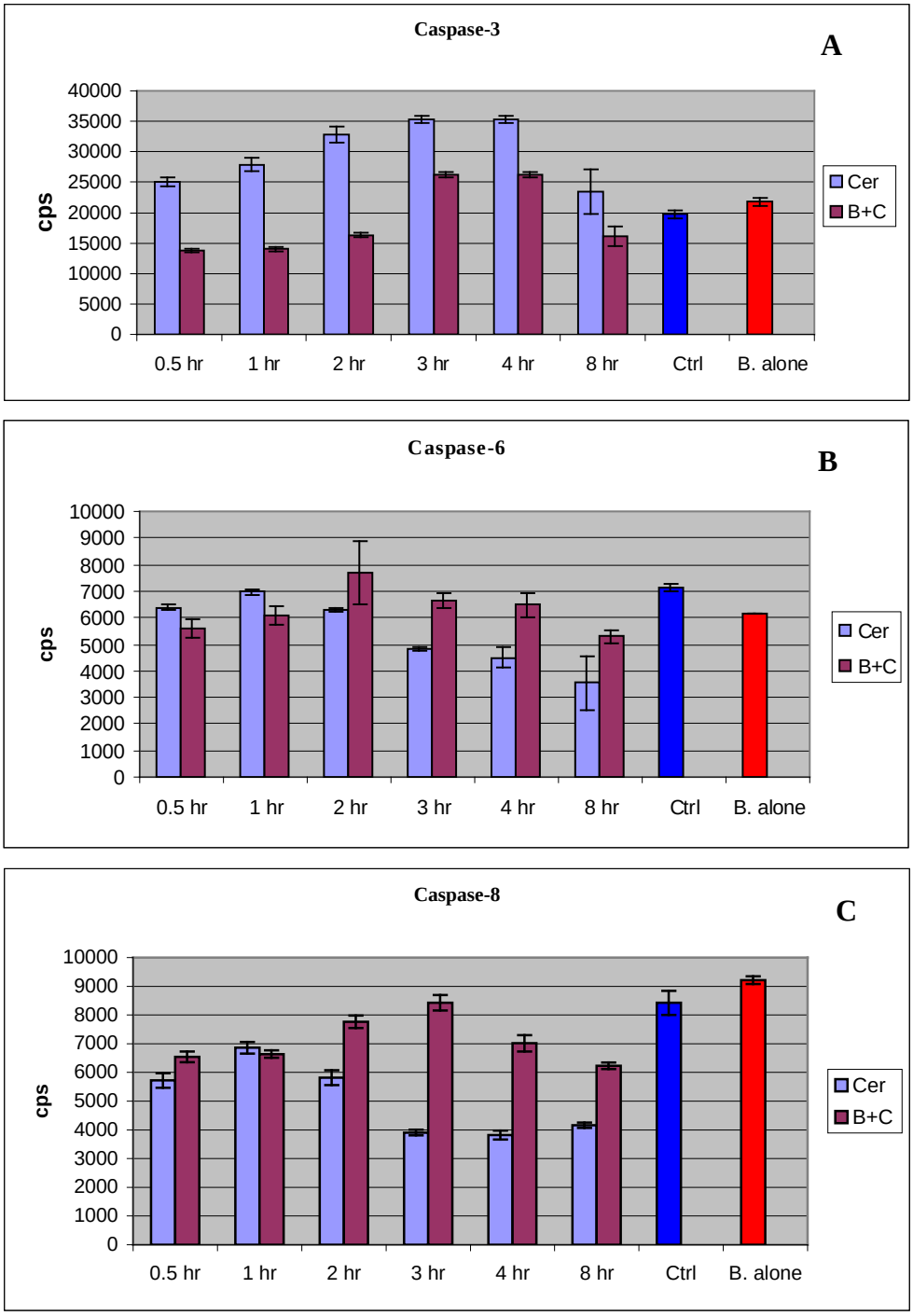

Figure 20. Caspase Activity Assay. Caspase-3 enzymatic activity is suppressed for B+C cells as compared to Cer treated cells (A). Both caspase-6 (A) and caspase-8 (C) enzymatic activity are enhanced for B+C cells as compared to Cer cells. Enhanced enzymatic activity of caspase-6 and caspase-8 for B+C cells is not over that of control (Ctrl) cells. However, caspase-6 and-8 activity is similar to that of untreated B. henselae infected controls (B. alone). Significant enhanced expression above controls is denoted by asterick ($p<0.05$). Values represent mean ±S.D of multiple independent experiments (n=3).

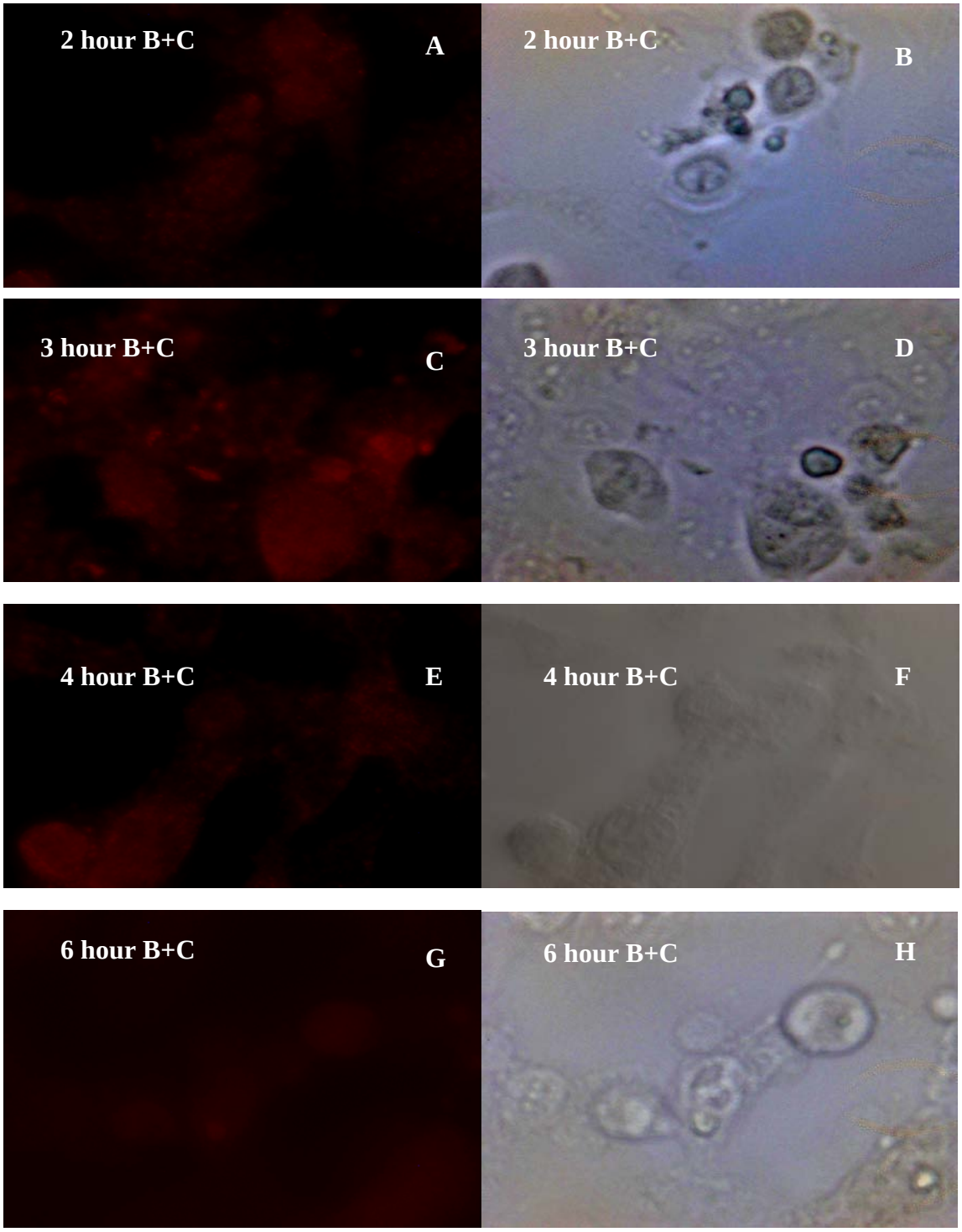

Figure 21. Multicaspase Fluorescent Substrate: B+C Cells. The cell permeable caspase substrate is reactive to cleavage by caspase-2, 3, -8, -9, -10. Enhanced fluorescence indicates increasing levels of overall caspase activity. Caspase fluorescence is baseline following 2 hours (A), enhanced following 4 hours (E) and wanes following 6 hour ceramide treatment (G), for *B. henselae* infected cells (B+C). Light micrographs demonstrate the presence and position of endothelial cells.

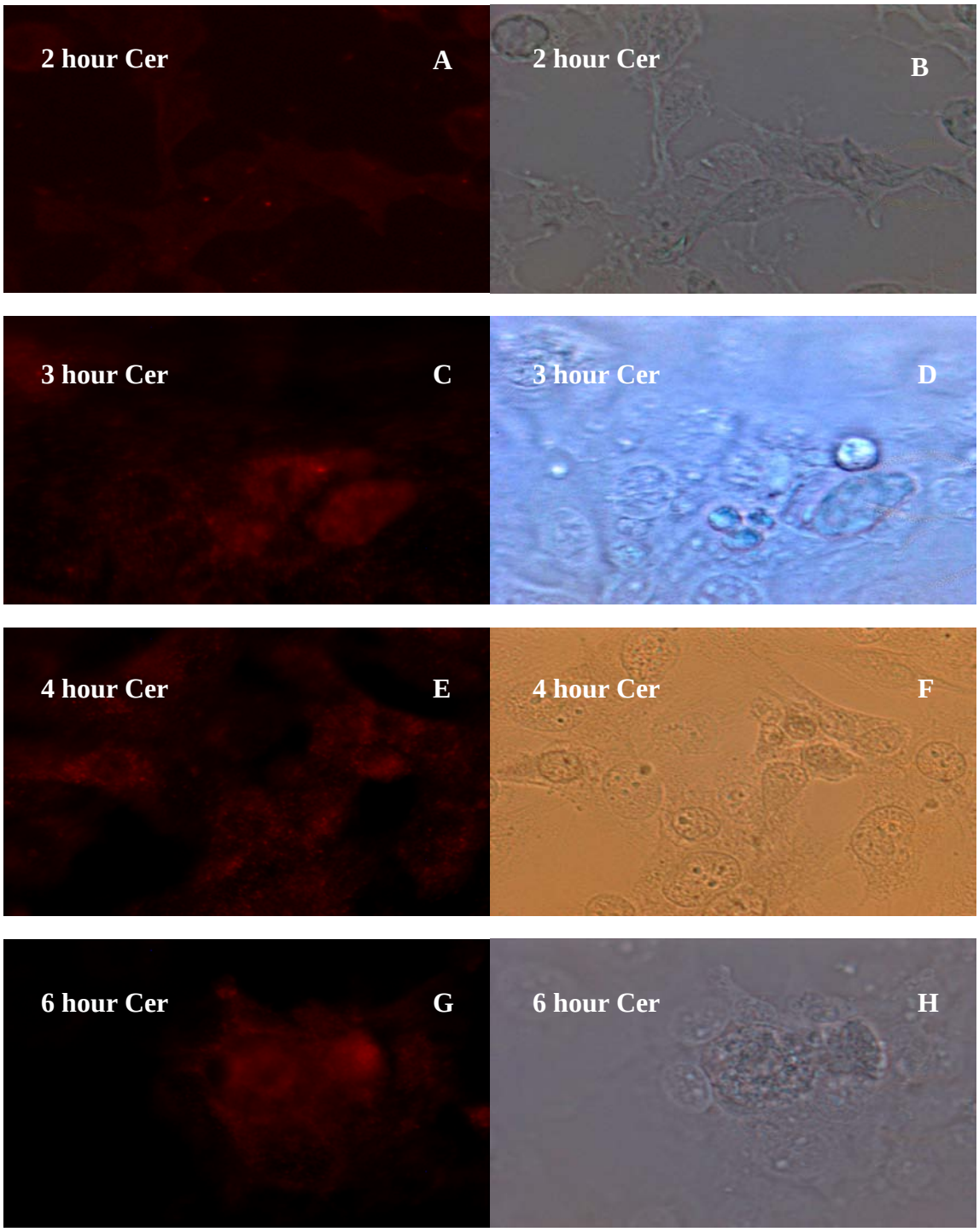

Figure 22. Multicaspase Fluorescent Substrate: Cer Cells. The cell permeable caspase substrate is reactive to cleavage by caspase-3, -8, -9, -10. Caspase fluorescence is at baseline following 2hours (A), but intensifying following 3 hours (C) and 4 hours (E) of ceramide treatment. Fluorescence remains steady following 6 hours ceramide treatment (G) for uninfected and ceramide treated cells (Cer). Light micrographs demonstrate the presence and position of endothelial cells.

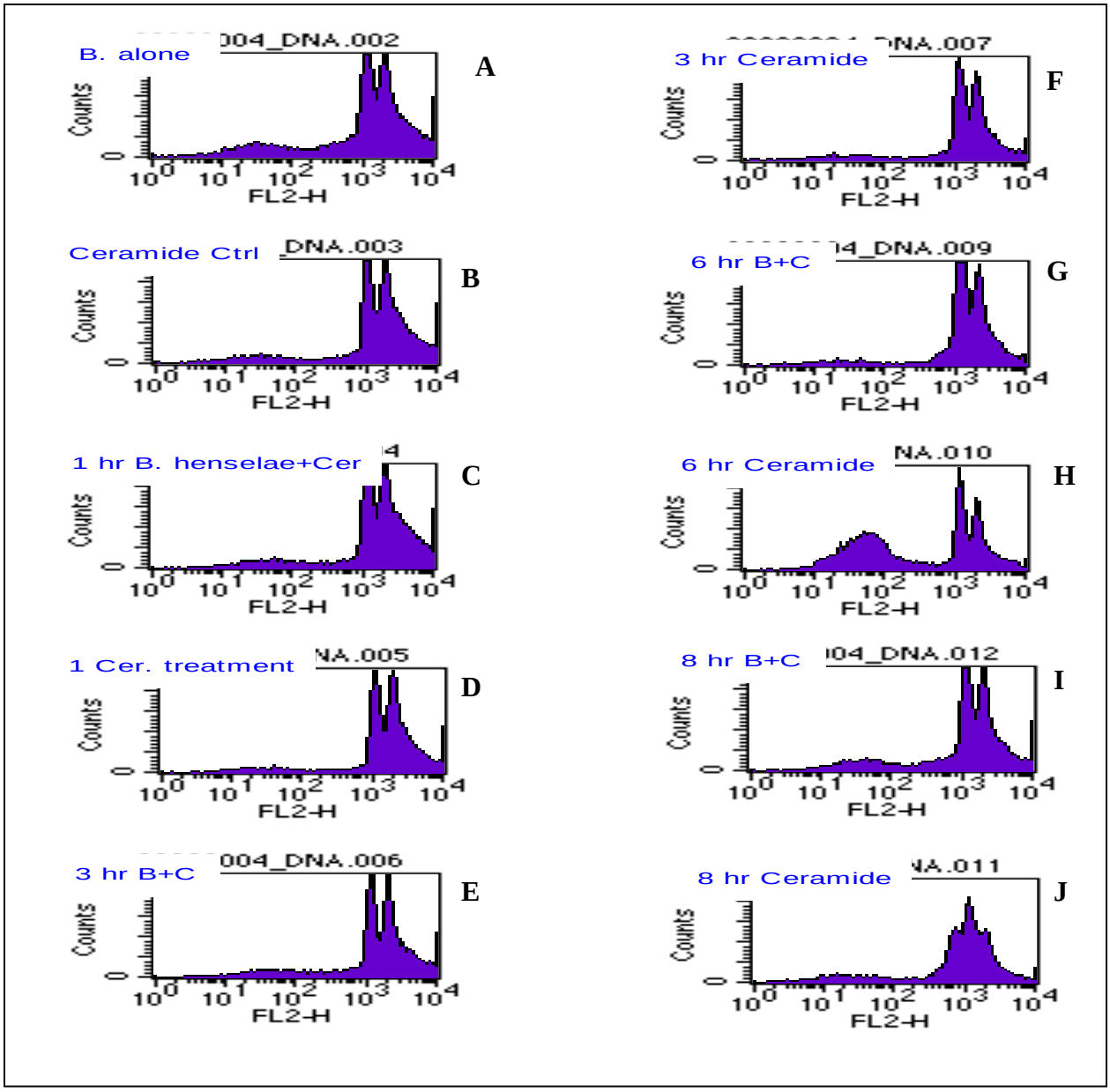

Figure 23. DNA Cell Cycle Analysis. DNA content and cell cycle is determined by PI staining of ethanol fixed cells. *B.henselae* alone control cells (A) has a small, but unsubstantial sub-G_1/G_0 population. Typical G_1/G_0, S, G_2M histogram is observed in ceramide negative control sample (B). Neither B+C nor Cer cells demonstrate significant sub-G_1/G_0 population for 1 hour (C and D, respectively) and 3 hour (E and F, respectively) ceramide treatment. Six hour ceramide-treated cells (H) demonstrate a remarkable sub-G_1/G_0 population as compared to 6 hr B+C cells (G). Following 8 hour ceramide B+C cells demonstrate a minimal sub-G_1/G_0 population (I) as compared to a breakdown of standard DNA cell cycle profile (J). Likewise, at no other timepoint is there a substantial sub-G_1/G_0 population. Histograms are representative of multiple independent experiments (n=3).

There is a small population of sub-G_1/G_0 cells in the infected sample, but the levels are not substantial. Similar patterns are seen following one and 3 hours' exposure to ceramide for both infected (Figure 27C and 27E, respectively) and uninfected cells (Figure 27D and 27F, respectively). Following six hours of ceramide treatment, the infected cells continue to be distributed among the G_1, S and G_2 cycles (Figure 27G), but a large sub-G_1/G_0 population, indicative of apoptosis, is clearly evident in the uninfected sample (Figure 27H). Only after 8 hours of ceramide treatment do any of the infected cells appear in the sub-G_1/G_0 stage, and their numbers are minimal. In contrast, by this time, the uninfected cell population reveals a distinct loss of the normal DNA cell cycle profile.

Discussion

Gram-negative Bacterial Infection and Apoptotic Response

Gram negative bacteria such as *B. henselae* are cloaked in lipopolysaccharide (LPS), and the presence of Gram-negative bacterial LPS initiates the host anti-bacterial immune response (Hu *et al*., 1998; Dauphinee and Karsan, 2006). The Gram-negative bacterial LPS are responsible for the host pyrogenic response that occurs during bacterial sepsis (Hotchkiss *et al.*, 2002; Rudiger *et al*., 2008), and LPS alone is a known apoptosis agonist (Hull *et al*., 2002). Other studies have shown that bacterial LPS induce apoptosis in HMEC-1 cells, provided there is an additional agonist (Kyong-Bok *et al*., 1998). The presence of bacterial LPS causes microvascular endothelial cells to excrete cellular TNF-α (Karsan *et al*., 1996). Excretion of TNF-α, in turn promotes infiltration of immune system cells, particularly neutrophils (Bartee *et al*., 2008). Likewise, TNF-α specifically upregulates NF-κB genes in HMEC-1 cells (Ades *et al*, 1992; Candal *et al*, 1996). Microvascular endothelial cells, as mentioned earlier, are resistant to the

cytolytic effect of TNF-α. However, TNF-α does induce a variety of other cell types to undergo apoptosis via extrinsic apoptosis pathways (Haimovitz-Friedman, 1997). While microvascular endothelial cells are resistant to the apoptogenic effect of TNF-α, the TNF-α-responsive genes such as IL-8, VEGF, E-selectin and VCAM-1 are upregulated by its presence in the HMEC-1 endothelial cell line (Xu *et* al., 1994; Ades *et al.*, 1992).

We assayed *B. henselae*-infected HMEC-1 cells for endotoxin concentration using a standard limulus amoebacyte lysate (LAL) assay (FDA Guidelines, 1987). *B. henselae* endotoxin (212±4 EU/mL) was not effective at inducing cell death alone following 12 hour incubation, a time period that resulted in significant cell death in cultures containing an analogous quantity of purified E. coli LPS (data not shown). Based on previous comparative studies correlating bacterial colony forming units (c.f.u.) and endotoxin units (E.U.), this quantity of endotoxin would correspond to approximately $1x10^6$ cfu/mL (Huntington *et al.*, 2007).

Other researchers have noted that apoptosis induced by bacterial LPS is potentiated by the addition of exogenous TNF-α-or a protein synthesis inhibitor (Hull *et al.*, 2002). During natural Gram-negative infection, the presence of bacterial Gram-negative LPS is an important factor for inducing host cell sphingolipid conversion (Franchi *et al.*, 2006). Sphingolipid conversion leads to the generation of ceramide at the cell membrane. The use of ceramide as an apoptogenic agent is discussed in detail later.

Bartonella henselae **Infection and Death Receptors**

Our early experiments revealed a rapid downregulation of Fas-associated death domain (FADD) protein in HMEC-1 cells during the course of *B. henselae* infection (Figure 7). This downregulation of FADD protein expression indicates that either Fas or TNF-receptor-1 (TNF-R1) pathway is affected by the presence of *B. henselae*.

Our initial observation of *B. henselae*-induced FADD protein downregulation was made in the absence of any additional exogenous apoptosis inducer. It was this early revelation that led to two important developments in our experimental design: 1) determination of *B. henselae's* ability to circumvent apoptogenic actions on the part of the cell following a direct challenge with an apoptotic agent and 2) molecular characterization of pathways that utilize FADD as an integral apoptotic modulator (TNF-R1 and Fas-receptor dependent pathways). We therefore sought to determine if *B. henselae* were capable of "protecting" infected cells from apoptotic challenge. To this end we examined a cadre of apoptogenic agents and conditions with divergent modes of action (Table 2). Among these were exogenous TNF-α (Wesche-Soldato, *et al*. 2007; Guoqing and Goeddel, 2002), C_2-ceramide (Smith and Schuchman, 2008), Staurosporine (Zhang *et al.*, 2004), Camptothecin (Rath *et al*., 2008), etoposide/ET-18 (Torrecillas *et al.*, 2006), Ricin toxin (Korcheva *et al*., 2007; Rao *et al.*, 2005), Abrin toxin (Qu and Qing, 2004) and Serum starvation (Ajeno, *et. al*, 2004). Our examination of apoptosis inducing agents determined that C_2-ceramide was most desirable for our experimental model (Zhang *et al.*, 2002) for the following reasons: 1) camptothecin and etoposide yielded obliterated cell monolayers even at low concentrations, 2) staurosporine had the inverse effect, causing endothelial cell death only at higher concentrations but requiring a much longer time to exert its effect, and 3) ricin and abrin toxin effectively killed endothelial cells with no morphological evidence of apoptosis.

True serum starvation is difficult to demonstrate with HMEC-1 cells and maintain microvascular endothelial characteristics (Xu *et al.,* 1994; Velma George personal communication). The normal culture media contains 15% serum and historical information demonstrates that HMEC-1 cells undergo substantial loss of viability with as little as 5% serum.

C_2-ceramide was the only apoptosis agonist we examined that provided a clear concentration-dependent cytotoxic effect (Figure 2; Table 1), so it was the agent of choice for our experiments.

C_2-ceramide is a short-chained, cell permeable exogenous apoptosis inducer that is optimal for use with microvascular endothelial cell cultures (Fillet *et al.*, 2003). First, exogenous ceramide treatment mimics the normal cellular responses to the presence of Gram-negative LPS exposure (Barber *et al.*, 1996). Second, ceramide conversion plays an integral role in extrinsic pathway signaling. Lastly, of the apoptogenic agents tested, C_2-ceramide demonstrates a linear dose and time dependence (Samadi, 2007; Figure 8).

Sphingolipids and Their Role in Death Receptor Apoptosis Induction

Metabolism of cell membrane sphingolipids generates endogenous ceramide in response to early apoptosis signaling events (Kolesnick, 2002; Ogretum and Hannun, 2004). A cellular function of ceramide is to modulate protein kinase pathways, leading to activation of downstream cellular apoptosis modulators (Basu *et al.*, 1998). Another function of ceramide is in aiding in the formation of lipid rafts (Gulbins *et al*., 2004; Browne and London, 1998). Lipid raft formation facilitates the clustering of cell surface transmembrane receptors, including death receptors (Gulbins, 2003). Clustered death receptors, specifically TNF-receptor-1 or Fas, are the initial signal for extrinsic apoptosis pathways (Gulbins and Li, 2006).

Effect of B. henselae on Ceramide-induced Changes in Cellular Morphology

Ceramide has a progressive effect on microvascular endothelial cell integrity, as demonstrated by gross cellular morphology for both ceramide-treated uninfected cells (Cer) and ceramide-treated *B. henselae*-infected cells (B+C). Both control uninfected (Figure 9A) and control *B. henselae*-infected cells consist of confluent cell monolayers (Figure 9B). Control cell morphology represents the end of the experimental timeline. The presence of some rounded cells

in the *B. henselae* alone control may be attributed to overconfluence of the endothelial cell monolayer. The obvious toxic effect of ceramide is more pronounced for Cer cells following longer ceramide treatment duration (Figure 9C, Figures 11A and C, Figures 12A and C). The appearance of Cer cells stands in stark contrast to their *B. henselae*-infected counterparts (B+C) withstanding the same ceramide challenge (Figure 9D, Figures 11B and D, Figures 12B and D). The progression of cellular damage emphasizes that ceramide is time-dependent in its cytotoxic morphological manifestation for microvascular endothelial cells.

Previous research suggests that the presence of *B. henselae* allows the host cells to circumvent apoptosis progression (Kirby and Nekorchuk, 2002.; Minnick *et al.*, 2003). It is important to note that the efficiency of *B. henselae* infection of cultured cells is approximately 40% (Dr. Russell Regnery, personal communication). Our experience using Gimenez staining of *B. henselae*-infected HMEC-1 cells is in agreement with that estimate. In our model, the proximity of *B. henselae* to uninfected cells within the infected cellular monolayer did not alleviate cell death. Therefore, we postulate that some loss of viability for B+C cells is due to uninfected cells within the B+C culture monolayer succumbing to the apoptogenic effect of ceramide. We observed no overriding “bystander” protective effect for uninfected cells from proximal *B. henselae*-infected cells.

Trypan Blue was used to determine the cellular viability for both *B. henselae*-infected (B+C) and uninfected ceramide-treated cells (Cer) and control cells (Bird and Forrester, 1981). Trypan Blue determines viability due to exclusion of dye by the intact cellular outer membrane (Huggett and Suffolk, 1936). Assays that measure substrates of cellular respiration, such as those that use the tetrazolium salt 3-(4,5-dimethylthiazol-2-yl)-2,5-diphenyltetrazolium bromide (MTT), are desirable in some experimental models because their effects can be quantified. The

addition of bacteria (Gebran *et al.*, 1994) and high serum concentrations in the cellular assay pose obstacles regarding the reliability of MTT assay results, however (MTT Assay Technical Data Sheet, Promega, Madison, WI). As mentioned previously, HMEC-1 cells do not maintain their desired cell characteristics when subjected to low serum concentrations (Ades *et al*., 1992). In addition, the presence of bacterial NAD dehydrogenase in the endothelial cell model creates aberrant results using MTT. For these reasons, we employed the use of Trypan Blue as a more reliable means of assessing viability considering the experimental parameters we used. In short, while both B+C and Cer cells experienced loss of viability, *B. henselae*-infected cells were markedly more viable and the endothelial cells were resistant to the cytotoxic effect of ceramide. Viability of ceramide treated uninfected cells rapidly declines in the time interval between 30 minutes and 6 hours of treatment (Figure 13). While the presence of *B. henselae* in infected culture cells enhances overall cellular viability, there appears to be a level of cellular stress for the B+C cell culture as demonstrated by gross morphology when compared to uninfected- and untreated control cells. It is possible that the presence of *B. henselae* creates a competition for carbon sources in the cell culture media or more likely a mild shift in the media pH. Other researchers have demonstrated that prolonged exposure of endothelial cells to *B. henselae* promotes dramatic cell proliferation (Maeno *et al*., 1999; Dehio, 2003). Our research demonstrates that while *B. henselae* protects microvascular endothelial cells from apoptosis, it has little effect on cell proliferation within the experimental timeframe used here (data not shown). We assert that *B. henselae's* intracellular survival tactic does not rely on enhancing cell proliferation and overall viability alone. Full characterization of the endothelial cell genes modulated during *B. henselae* intracellular infection would help to address this issue.

TRADD and FADD Intracellular Protein Expression

Contrary to the induction of gene expression, described in Chapter 3, changes in the intracellular protein concentration of TRADD and FADD can be caused by multiple factors. The percentage of TRADD/FADD positive cells indicates that these proteins are available from cytoplasmic pools, and could arise either from new transcription or translation, or from translocation from organelle storage. Untreated and uninfected cells have a consistent baseline of TRADD intracellular expression for both B+C and Cer cells (~13% positive cells). Following prolonged ceramide treatment, the percentage of TRADD positive cells increases for both B+C and Cer cells. Following the initiation of elevated TRADD expression, Cer cells maintain a high level of TRADD thereafter. Intracellular TRADD protein concentrations are likewise elevated for B+C cells, although the percentage of positive cells is nearly three-fold lower at its peak.

An analysis of FADD concentrations reveals a pattern that is striking different from that of TRADD. The percentage of FADD positive Cer cells is elevated for all time-points. However, a comparison of B+C and Cer cells reveals two unique differences. First, the presence of *B. henselae* appreciably diminishes FADD levels at all time points. Second, the presence of *B. henselae* causes a suppression of FADD expression following prolonged ceramide treatment. In fact, the presence of *B. henselae* causes nearly a four-fold decrease in the percentage of FADD positive cells following 4 hours of ceramide treatment.

Unlike TRADD, the cellular pool of FADD is not known (Screaton *et al.*, 2003). FADD does possess a nuclear localization sequence. However, it has been demonstrated that in a single population FADD can be localized in either the cytoplasm or the nucleus (Gomez-Angelats and Cidlowski, 2003). TRADD is primarily stored in the endoplasmic reticulum. However, both nuclear import and export sequences for TRADD have been identified (Morgan *et al.*, 2002;

Farrando-May, 2005). The permeabilization technique used in our studies is not sufficient to efficiently solubilize nuclear or endoplasmic reticulum membranes. Therefore, we conclude that the increase in TRADD levels is due to either new transcription, or translocation from the ER.

Caspase Activity

Caspase activity was assessed by the ability of available caspase to proteolytically cleave target peptides. The designer target peptides, which utilize a Europium-labeled reporter and a QSY-7 quencher, are "specific" for a particular caspase. The target peptide includes a target sequence that the enzymatically active caspase will cleave. The close proximity of the reporter and quencher in the intact target peptide results in total quenching of emitted signal following exposure to excitation. Proteolytic cleavage of the target peptide results in emission of a "fluorescent" signal following excitation. The LANCE system uses a caged chelated lanthanide (Europium) as the reporter molecule.

The caspase-3 assay demonstrated that proteolytic activity was enhanced at all time points in Cer cells as compared to B+C cells. Additionally, caspase-3 activity was significantly enhanced for time points 1 to 4 hours over untreated control cells and untreated *B. henselae* infected cells. Caspase-3 enzymatic activity waned by 8 hours post ceramide treatment. As described previously, viability for both Cer and B+C cells is adversely affected by 8 hours ceramide treatment. This may account for the decline in caspase-3 activity. Additionally, all of the cellular substrates targeted by caspase-3 may be cleaved at this point, leading to a suppressive effect of caspase-3.

In contrast to the results observed with caspase-3, caspase-6 proteolytic activity was enhanced in ceramide treated *B. henselae*-infected cells as compared to their uninfected counterparts. This result is in direct conflict with previous reports of *B. henselae's* ability to

disrupt apoptosis (Kirby *et al.*, 2001). Still, at no time point was the proteolytic activity significantly greater than that of untreated uninfected control cells, or untreated *B. henselae*-infected control cells. The work of Kirby and Nekorchuk demonstrated that the presence of *B. henselae* suppressed caspase-3, caspase-8 and pan-caspase activity for control cells and serum-starvation induced cell death. Their research utilized umbilical vein endothelial cells which have different responses to apoptosis stimuli than microvascular endothelial cells. In addition, our results demonstrate that the mere presence of *B. henselae* does not suppress enzymatic activity of caspase-3 and caspase-8. In fact for both caspase-3 and -8, *B. henselae* infected untreated cells have equal to or higher caspase activity for the respective caspase. The difference could simply be the use of two different cell models. The dynamics of apoptotic response tends to be tissue and cell specific.

Like caspase-6, caspase-8 exhibited significantly enhanced activity in ceramide treated *B. henselae*-infected cells (B+C) relative to their uninfected counterparts, especially at the 3 and 4 hour time-points. Moreover, untreated and uninfected control cells and untreated *B. henselae*-infected control cells exhibited greater caspase-8 activity than either B+C or Cer cells. As mentioned previously, enzymatic activity of caspase proteins has been used as the empirical measure of caspase involvement. Caspase activation and caspase activity are not always synonymous (Kottke *et al*., 2001). We know that several caspase proteins do not need to be proteolytically active in order to carry out their function (Zimmerman and Green, 2001).

The enzymatic activity counts of caspase-3 were at least three times those of either caspase-6 or -8. This is probably because caspase-3 is both the most abundant caspase and the initiator of both intrinsic and extrinsic apoptotic pathways.

Suppression of Overall Caspase Induction by B. henselae

The Multicaspase™ fluorescent assay is a broad spectrum caspase substrate that targets caspases-1, -3, -6, -7, -8 and -9. Again, this assay uses cleavage of fluorescent pan caspase target peptide to assess overall caspase activity. As a pan-caspase assay, it does not differentiate between the activites of individual caspases. *B. henselae*-infected cells treated with ceramide (B+C) exhibited a rapid, but truncated induction of overall caspases activity. The multicaspase assay revealed less overall caspase enzymatic activity in B + C cells than for cells treated with ceramide alone. More importantly, enhanced overall caspase activity for Cer cells lasted for a longer time (up to 6 hours). From these results, we conclude that the presence of *B. henselae* inhibits overall caspase induction caused by the induction of apoptosis.

The work performed by Kirby and Nekorchuk did utilize a pan-caspase assay. In their research the presence of *B. henselae* suppressed pan-caspase activity. However their research employed a “pan-caspase” assay that is preferential for caspase-3 and -7 utilizing umbilical vein endothelial cells in the presence and absence of serum. Our data suggests that the presence of *B. henselae* suppresses pan-caspase activity (caspase-1, -3, -4, -5, -6, -7, -8 and -9) following ceramide-induced apoptsis using microvascular endothelial cell line.

B. henselae Suppresses Ceramide-induced DNA Fragmentation

Flow cytometric assessment of the DNA cell cycle utilizes propidium iodide (PI) as a DNA fluorescent intercalating dye to determine DNA content. Following cellular membrane permeabilization, PI intercalates into the DNA of any double-stranded DNA it encounters. Intercalated PI is stoichiometrically proportional to DNA content. The height of the fluorescent pulse is proportional to the intensity of the fluorescent signal, while the width of the signal is proportional to the time required for the permeabilized fluorescent cell to travel across the beam

of the laser. The area is calculated from the fluorescence integral to the cell that traveled across the laser. Fluorescence area is important if we were interested in discriminating DNA content of a cell doublet from the DNA content of a G_2/M cell (Nunez, 2001).

Considering the size of endothelial cells, the fluorescent height of a G_0 singlet is the same as that of a G_0 doublet because only one nucleus will occupy the laser space at a time. However, the width of a G_0 doublet will be twice that of a G_0 singlet because it will take twice as long to traverse the laser beam. Likewise, the fluorescent area of a G_0 doublet will be twice that of a G_0 singlet (Zibigniew Darzynkiewicz, personal communication). The data were acquired by gating on the population that correspond to $G_0/G_1/S/G_2M$ singlet cells, excluding doublets, triplets and so on. Normal cell cycle distribution includes a large G_1/G_0 peak followed by a plateau of S-phase cells and concludes with a G_2/M peak of nearly ½ the height of the G_1/G_0 peak. Any peaks to the left of or smaller than the G_1/G_0 peak are considered to be sub-G_1/G_0 peaks and therefore apoptotic.

We chose to display DNA content using FL-2 height because it allows us to display in a log scale, making all low molecular weight DNA visible. Most low molecular weight DNA is precluded from view when assessed in a linear FL-2 area histogram. However, a large sub-G_1/G_0 population is observed at six hours of ceramide treatment for the Cer cells (Figure 23H). Eight hours of ceramide treatment produces a complete loss of DNA cell cycle integrity for Cer cells, as determined by a flattening of peak height (Figure 28J). In contrast, the B + C cells show no significant apoptotic population up through six hours of ceramide treatment (Figure 23G). Only after eight hours of ceramide treatment does a small apoptotic peak begin to emerge.

CHAPTER 3

BARTONELLA INHIBITS GENE EXPRESSION OF APOPTOSIS MODULATORS

Introduction

Intracellular pathogens are known to influence gene expression in their host cells (Darby *et al.,* 2007). Genes whose expression is increased by these pathogens include proliferation associated genes, anti-apoptosis associated genes and in some cases apoptosis genes (Gao and Kwaik, 2000). It is well known that bacteria, in particular *Bartonella* species, influence the expression of NF-κB associated gene products (Dehio, 2001). *B. henselae* exploits all of the extrinsic genes within the TNF-R1 pathway. This is intriguing due to the fact that endothelial cells, the usual host for this bacterium, are not responsive to the apoptosis effects of TNF-α (Viemann *et al.,* 2006).

To ensure chronic intracellular infection, *B. henselae* must inhibit apoptosis. As previously described, *B. henselae* suppresses the protein expression and activity of several TNF-R1 dependent pathway modulators. The experiments described here were designed to determine the effect of *B. henselae* infection on gene expression following direct apoptotic challenge. Two commonly used methods designed to investigate changes in gene expression are microarray analysis and approaches involving real-time RT-PCR. The use of ceramide, our selected apoptogenic agent, precluded the use of expression microarray chips due to the fact that the cytotoxity of ceramide dramatically reduced the number of intact cells and thereby the total mRNA concentration (Nagata *et al*., 2003). Therefore, we chose to investigate the effect of *B. henselae* on gene expression using multiplex real-time PCR.

Real-time RT-PCR assays measure the amount of transcript that is present in a given sample under a defined set of conditions. Following reverse transcription of the targeted RNA, .the amount of gene product is monitored after each amplification cycle and the number of cycles required for the product concentration to reach a pre-defined threshold (C_T) is determined. The higher the C_T value (i.e., the longer it takes to reach the designated threshold concentration), the lower the initial concentration of the RNA in the original sample Thus, the C_T value provides an estimate of the "quantity" for the specific gene target. By comparing the C_T value for a gene-of-interest (GOI) to the C_T value of a benchmark or normalizing gene such as glyceraldehyde-6-phosphate dehydrogenase (GAPDH), the relative abundance of that GOI can be determined. Approximately 3.3 cycles change in the C_T value is equal to one log, or a 10-fold difference in gene expression. Multiplexing the real-time RT-PCR assay provides an added advantage, since it allows for simultaneous comparisons within a single reaction vessel.

Materials and Methods

RNA Extraction

Suspended and floating cells were pelleted from the media of 6-well culture dishes and spun for 3 minutes at 1,000 xg. Cell monolayers and pelleted cells were pooled together. Cells were lysed with 100 μL of Roche MagNApure RNA II Lysis Buffer (Roche, Indianapolis, IN.). RNA II Lysis Buffer, at a volume of 100 μL, was added to the sample processing tray for each sample. The total volume of lysed cells in the RNA II Lysis Buffer was added to the sample processing tray according to the manufacturers' protocol. RNA extraction was performed using the robotic MagNApure system using the RNA II kit following the High Performance RNA II protocol according to manufacturers' instructions.

RNA was pelleted by adding 100 µL 95% ethanol, then decanting off the ethanol. Contaminating DNA was removed by adding 5 µL RNase-Free DNase I and bringing the total volume up to 200 µL with 1X DNase Buffer (Epicentre, Madison, WI). The dissolved RNA was incubated for 30 minutes at 37 ^{o}C. A volume of 200 µL of 2x T and C Lysis Solution was added followed by vortexing for 5 seconds. A volume of 200 µL of MPC Protein was added and the solution was vortexed for 10 seconds and placed on ice for 5 minutes. Debris was pelleted by centrifugation at 10,000 xg in a microcentrifuge. The supernatant was transferred to an RNase-free microfuge tube, after which 500 µL of isopropanol was added and the tube inverted several times.

The purified RNA was pelleted by centrifugation at 4 ^{o}C for 10 minutes. The RNA pellet was washed 2x with 75% ethanol, in nuclease-free water, and centrifuged at 10,000 xg for 5 minutes. RNA pellet was dissolved in 200 µL TE buffer supplemented with tRNA added to a final concentration of 1 µg/100 µL (Ambion, Austin, TX). tRNA was also added to nuclease-free water (Promega, Madison, WI) at 10 µg/mL, for all RNA dilutions.

Real-time RT-PCR Primers

Primer sequences were as follows.

Glyceraldehyde-3-phosphate dehydrogenase

(GAPDH) forward 5’-TGGGCTACACTGAGCACCAG-3’

Glyceraldehyde-3-phosphate dehydrogenase

(GAPDH) reverse 5’-CAGCGTCAAAGGTGGAGGAG-3’

Caspase-8 (Cas8) forward 5’-GCCTGGACTACATTCCGCA-3’

Caspase-8 (Cas8) reverse 5’-CCTGGAGTCTCTGGAATAACATCA-3’

Caspase-3 (Cas3) forward 5’-TGTTCCATGAAGGCAGAGCC-3’

Caspase-3 (Cas3) reverse 5'-TGCGTATGGAGAAATGGGC-3'

FADD forward 5'-CTTCGGATGAGGCCCTCAT-3'

FADD reverse 5'-TCTAGGGCACTGCAGGGCT-3'

TRADD forward 5'-GATGGCAGCTGGGCAAAAT-3'

TRADD reverse 5'-GCGAGGACTCCACAAACAGG-3'.

Probes

Target probe sequences and chemistries are as follows.

GAPDH probe 5'FAM-TGGTCTCCTCTGACTTCAACAGCGACAC-3'BHQ;

Cas8 probe 5'YamY-AGGAAGCAAGAACCCATCAAGGATGCC-3'BHQ;

Cas3 probe 5'Cy5-TGGACCACGCAGGAAGGGCC-3'BHQ;

FADD probe 5'-YakY-CCCATTCGGGAGATCATGTCTCACTTCA-BHQ-3'

TRADD probe 5'-Cy5-CACGAAGAGTGGGTGGGCAGCG-BHQ-3';

Multiplex RT-PCR Conditions

Multiplex RT-PCR Master Mix contained the following components per reaction: 11.5 μL Quantitect™ Probe RT-Master Mix, 0.25 μL Quantitect™ RT Mix (Qiagen, Valencia, CA); 2.5 μL LC-FastStart Enzyme w/o $MgCl_2$ (Roche, Indianapolis, IN) and 0.125 μL nuclease-free water (Promega, Madison, WI). The multiplex RT-PCR Master Mix components were supplemented with an additional 0.5 mM $MgCl_2$ (Roche, Indianapolis, IN), 0.8 mM dNTPs (Promega, Madison, WI) and 5 U per reaction Platinum *Taq*™ (Invitrogen, Carlsbad, CA).

The Qiagen RT Mix contains a proprietary mixture of Omniscript™ and Sensiscript™ reverse transcriptases, and Hotstart™ *Taq* DNA polymerase and 4mM $MgCl_2$. Further, the Quantitect™ Probe RT-PCR Master Mix contains a proprietary mixture of dNTPs and buffers.

Primers/probes were used at the following concentrations: GAPDH primers/probe at 250nM/50nM; and FADD and TRADD primers/probe at 500nM/100nM and 1000 nM/200nM respectively. GAPDH, Cas8 and Cas3 primers/probe were used at 250nM/50nM, 500/100 nM and 1000nM/200nM, respectively. Cycling conditions were 48 ^{o}C for 30 minutes, 95 ^{o}C for 15 minutes followed by 45 cycles of 95 ^{o}C for 10 seconds and 60 ^{o}C for 90 seconds. Data were acquired (i.e., optics were on) during the 60 ^{o}C step.

Results

Real-time RT-PCR was used to determine the effect of *B. henselae* infection on the expression of selected apoptosis-associated genes. As an initial step, parameters optimizing the conditions for reproducible amplification were established. Development of real-time PCR assay conditions involves the selection of an optimal primer/probe set, the titration of primer/probe combinations to determine optimal concentration, the titration of the optimal $MgCl_2$ concentration, and determination of the need for supplemental components to ensure RNA template integrity. Several genetic targets were evaluated for assessing apoptosis induction (Table 2).

The panel of primer/probe sets described in Table 2 was designed using Primer Express^{TM} software. Complete mRNA sequences of the desired human apoptotic genes were analyzed by BLAST gene sequences available through GenBank. Targets that had multiple primer/probe options were further screened to determine the optimal primer/probe set (Figure 24). Different primer/probe sets directed against the same gene target can display variability in the efficiency of amplification and signal intensity for that gene target. For this reason each possible gene target primer/probe set is screened for amplification efficiency. For the sake of

simplicity, screening of primer probe sets is paired with $MgCl_2$ titration (Figure 24). The addition of supplemental yeast tRNA was determined at the onset to be necessary to ensure RNA stability and reproducible curves (Figure 25). tRNA was added to all RNA stocks and template diluent to both stabilize the target and ensure proper template recovery from frozen template.

Optimal primer/probe concentrations were determined by serial two-fold titration of primer/probes from 1μM/200nM to 250nM/50nM (Figure 26). The primer/probe set for a desired gene target that demonstrated: 1) a strong reproducible fluorescent signal, and 2) the absence of a no-template-controls (NTC) signal, was selected for further study (See Materials and Methods primer and probe sequences). Previous experience demonstrated that additional dNTP's and supplemental Platinum Taq™ were necessary for multiplexing a real-time PCR assay (data not shown).

Standard curves of RNA template verify both the efficacy and robustness for real-time RT-PCR assays under the conditions optimized above. A linear dilution series demonstrates that each real-time RT-PCR assay is reliable across a wide concentration range. The linearity of the C_T curve provides verification that amplification efficiency is maintained across a linear dilution series of input template for TRADD (Figure 27), FADD (Figure 28), Caspase-8 (Figure 29) and Caspase-3 (Figure 30). In addition to standard curves for each gene target using control cells, RNA templates were isolated from infected and uninfected cell samples after 1, 2, 3, 6 and 12 hours of ceramide treatment. The efficiencies of gene amplification ranged between 90% and 100% for all gene targets, all sample types and all time points (data not shown).

Table 2. Gene Targets Tested.

Target	**Number of primer/probe sets tested**	**Fluorophore**
18S rRNA	1	FAM
RNAse P	1	FAM
β-actin	1	FAM
GAPDH	2	FAM
TRADD	3	Cy5
FADD	2	Yak Yellow
Fas	2	Yak Yellow
Caspase-8	3	Yak Yellow
Caspase-3	2	Cy5
MDR-1	1	Yak Yellow
TGF-β	1	Yak Yellow

Several targets were selected for assessing apoptosis induction. The number of primer/probe sets was determined by Primer Express software blast of target gene sequences. Targets that had multiple primer/probe sequences were further screened to determine the optimal primer/probe set. Fluorophore listed is the dye used for the optimal primer/probe set.

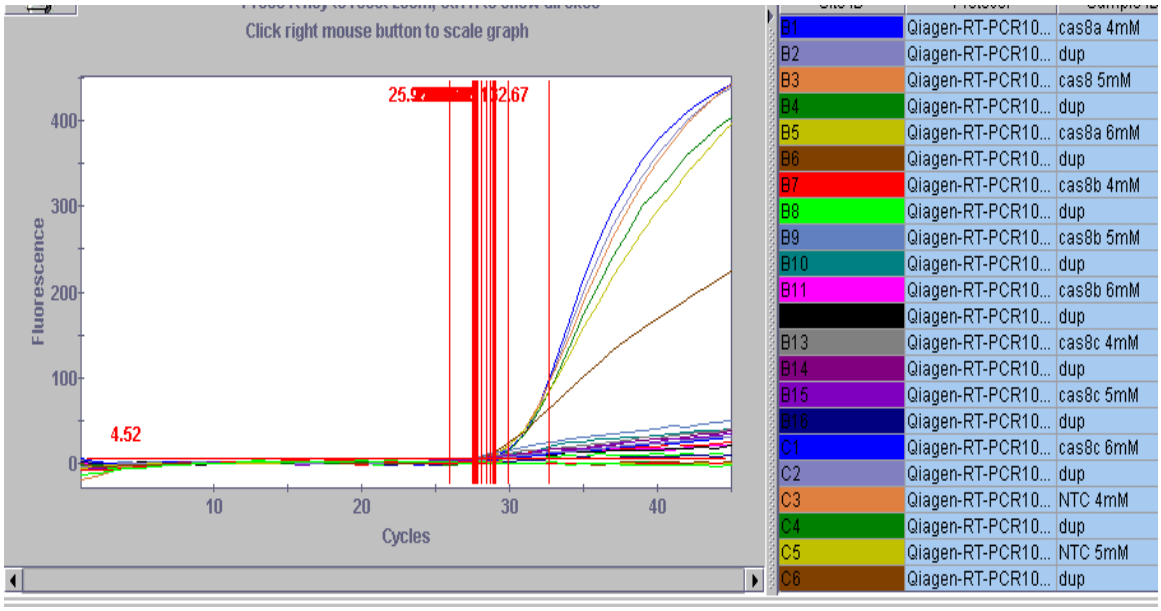

Figure 24. Supplemental Magnesium Titration and Multiple RT-PCR Primer/Probe Sets. Each gene target primer probe set was optimized for supplemental magnesium in PCR Master Mix. The cluster of markers cross the threshold between cycle 26-28. Prospective primer probe sets were identified by Primer Express™ software (Roche, Indianapolis, IN.)

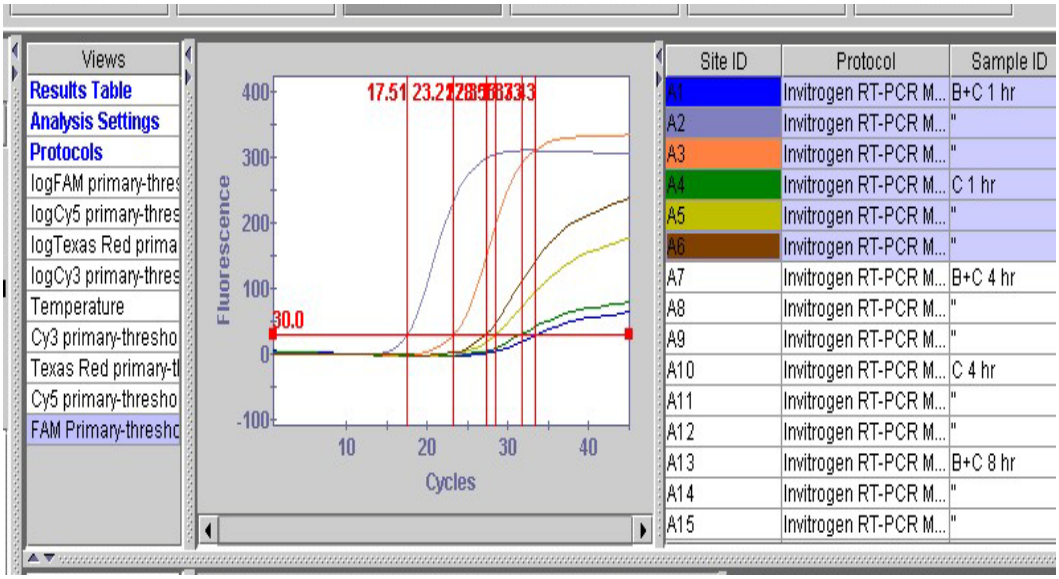

Figure 25. Reproducibility of Multiplex RT-PCR Requires tRNA. Real-time RT-PCR does not yield reproducible C_T values in the absence of stabilizing tRNA. Replicates of a single RNA template aliquot demonstrate a wide range of cycle-threshold (C_T) values

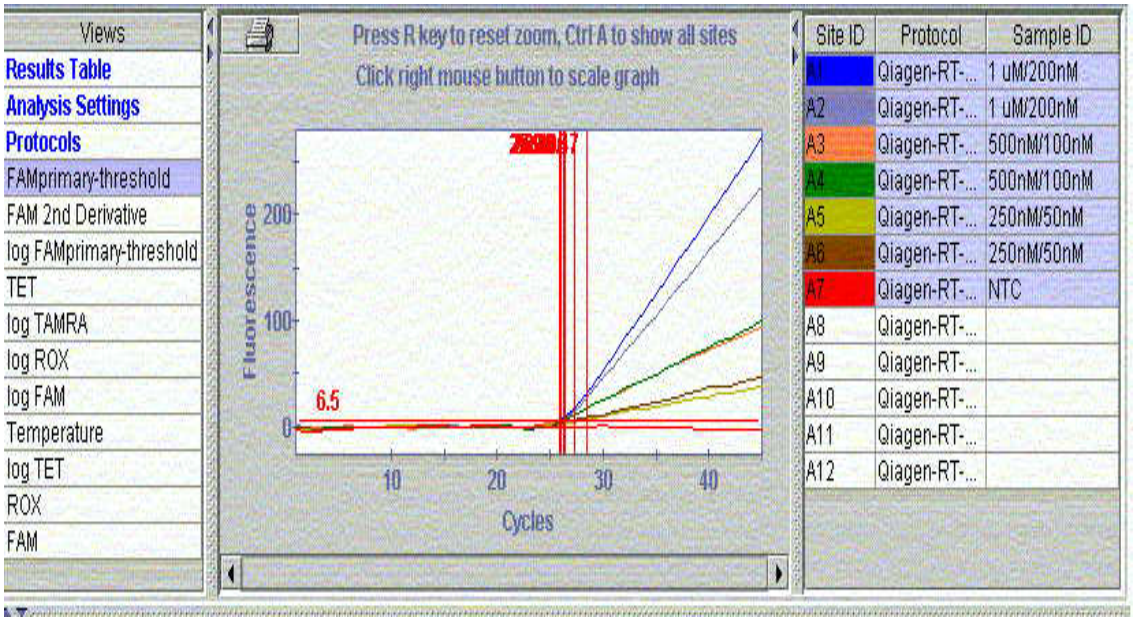

Figure 26. Primer and Probe Titration. A linear dilution of primer/probe were used to determine optimal primer/probe concentration. Optimal primer/probe concentrations were determined for each gene target (FADD primer/probe used as example).

Most test samples were >95% efficient for amplification. RNA templates from infected cells exhibited little variability in C_T values across all time points, as compared to a slightly broader variability in C_T values for cells treated with ceramide alone across all time points (data not shown).

Use of Multiplex Real-Time RT-PCR to Measure Relative Apoptotic Gene Expression for Early and Late Apoptotic Genes

Multiplex real-time RT-PCR provides a graphic and simultaneous representation of the gene expression for the gene-of-interest (GOI) and the reference house-keeping gene.

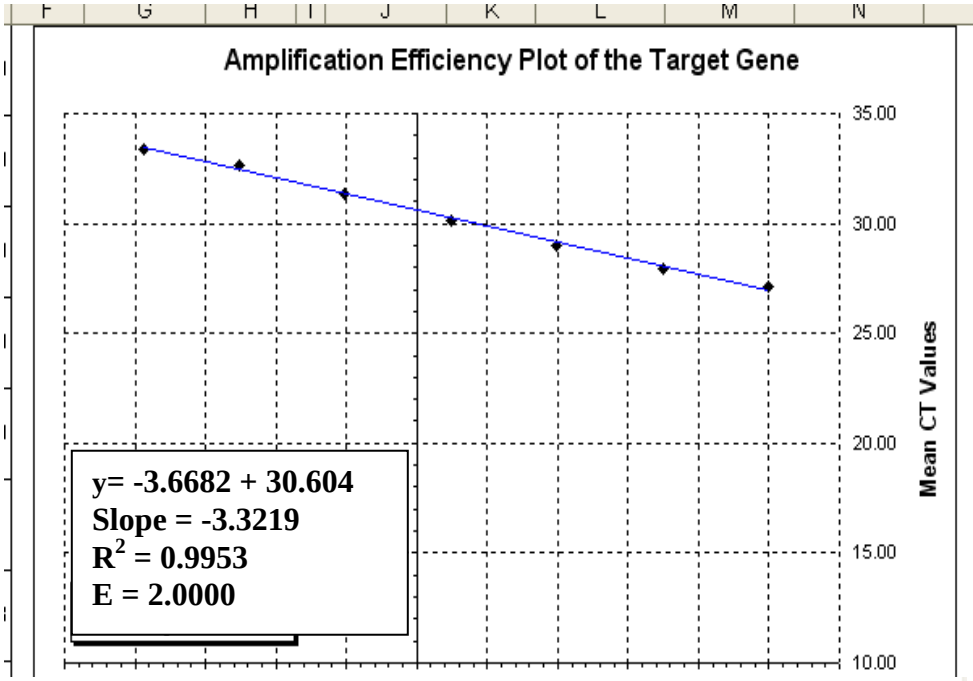

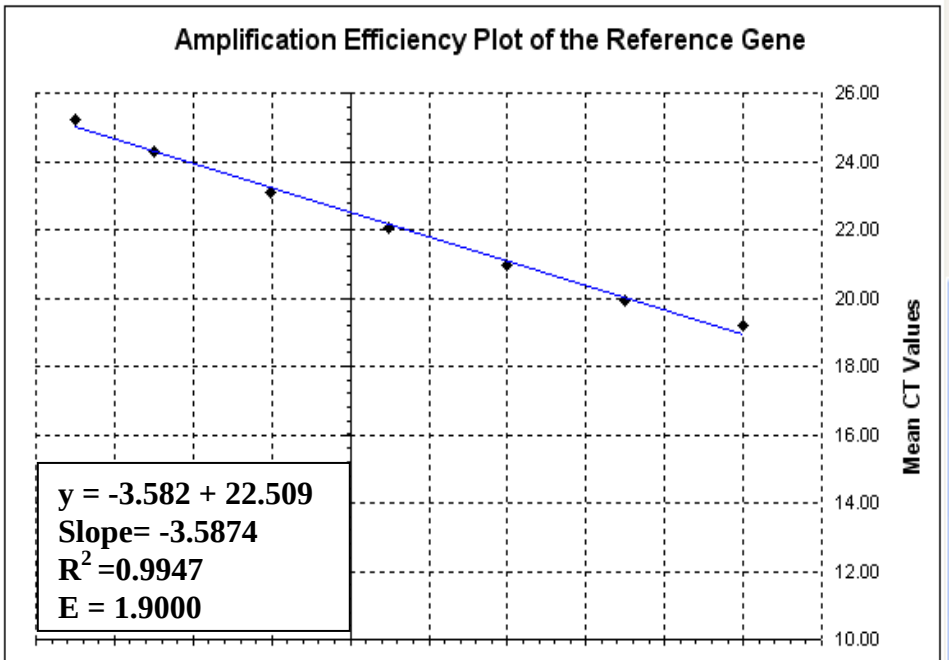

Figure 27. Standard Curve of TRADD Gene Expression. A comparison of standard curves for TRADD gene expression. RNA templates from control cells were diluted in a serial fashion. The curves demonstrate linear gene expression of TRADD as a function of serial dilution of gene template. Successive 2-fold dilutions of template yield corresponding increases in C_T values.

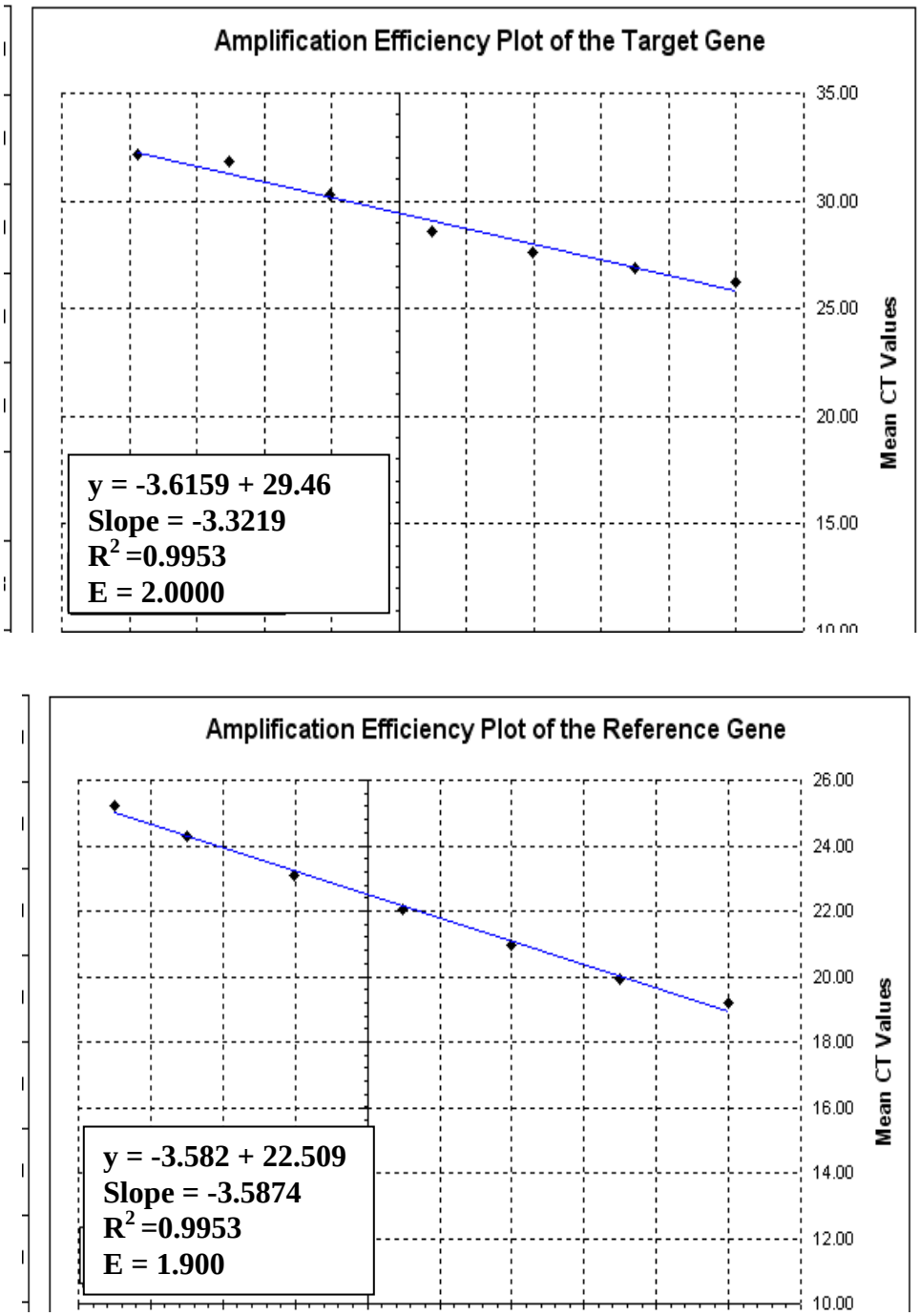

Figure 28. Standard Curve of FADD Gene Expression. A comparison of standard curves for FADD gene expression. RNA templates from control cells were diluted in a serial fashion. The curves demonstrate linear gene expression of FADD as a function of serial dilution of gene template. Successive 2-fold dilutions of template yield corresponding increases in C_T values.

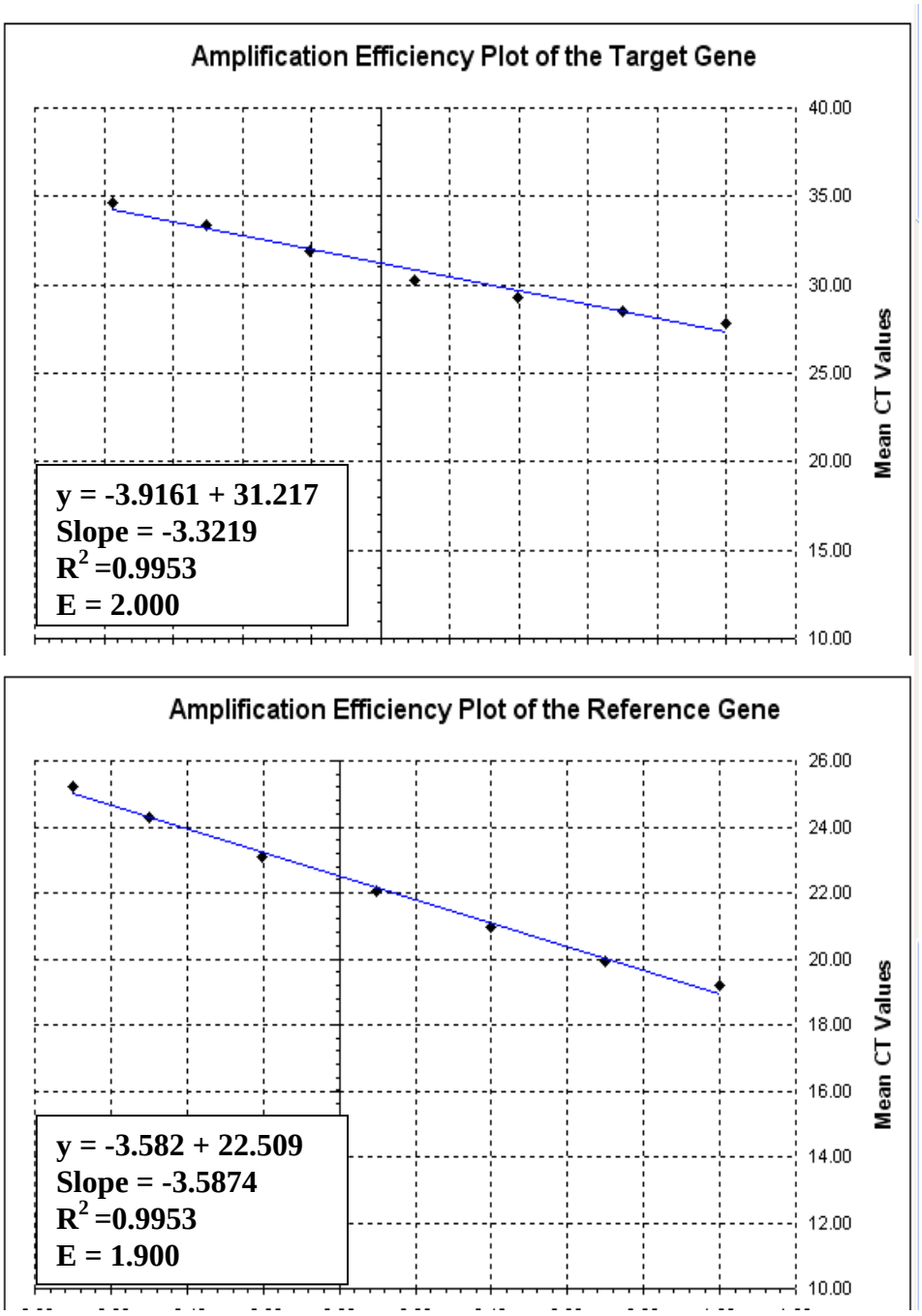

Figure 29. Standard Curve of Caspase-8 Gene Expression. A comparison of standard curves for Caspase-8 gene expression. RNA templates from control cells were diluted in a serial fashion. The curves demonstrate linear gene expression of Caspase-8 as a function of serial dilution of gene template. Successive 2-fold dilutions of template yield corresponding increases in C_T values.

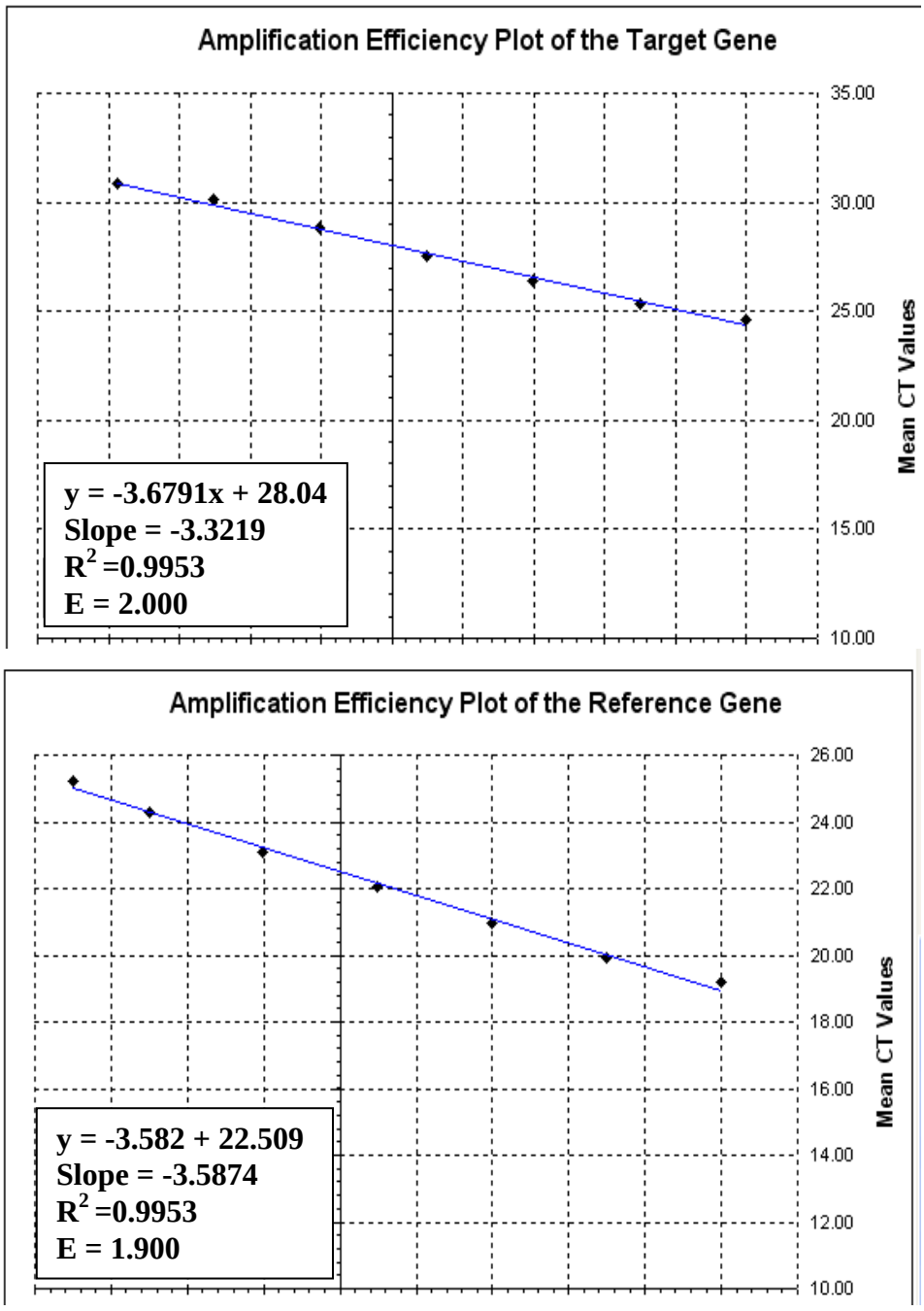

Figure 30. Standard Curve of Caspase-3 Gene Expression. A comparison of standard curves for Caspase-3 gene expression. RNA templates from control cells were diluted in a serial fashion. The curves demonstrate linear gene expression of Caspase-3 as a function of serial dilution of gene template. Successive 2-fold dilutions of template yield corresponding increases in C_T values.

In the analysis conducted here, the gene-of-interest (TRADD, FADD, Caspase-8, or Caspase-3) is normalized to the reference housekeeping gene (GADPH) for each sample by subtracting the average C_T value of the reference gene (GAPDH) from the average C_T value for the GOI, called ΔC_T. The normalized GOI from the sample of interest or focus sample, is then subtracted from the normalized GOI of the standardizing sample (Winer *et al.*, 1999; Livak and Schmittgen, 2001). The normalized gene expression of the reference sample is subtracted from the normalized gene expression of the test sample which is called the $\Delta\Delta C_T$. Specifically, relative gene expression (R.E.) is mathematically determined as follows:

R.E.= 2^(Normalized Gene Expression $_{\text{Test Sample}}$)-(Normalized Gene Expression $_{\text{Reference Sample}}$)
R.E=2^(GOI $_{\text{Test}}$-NG $_{\text{Test}}$)-(GOI $_{\text{Reference}}$-NG $_{\text{Reference}}$)

Ref. Sample= cell template used as “benchmark” reference or calibrator sample
Test Sample= sample where the gene expression level is desired.
GOI=gene of interest (target gene)
NG=Normalizing gene (GAPDH) or glyceraldehyde-6-phosphate dehydrogenase.

It is worth noting that by adjusting which sample is the test and which is the reference or calibrator one can determine the gene expression fold-increase as it relates to the reference sample.

Apoptosis was induced by ceramide treatment of uninfected and *B. henselae*-infected cells, and its effect on gene expression was monitored in a time-dependent manner. Gene expression was determined for the gene targets TRADD, FADD, caspase-8 and caspase-3 and the normalizing house-keeping gene, GAPDH, as described. Enhanced gene expression was defined as the net difference in transcript production for the uninfected cells and infected cell (Figures 27, 28, 29 and 30).

TRADD Gene Expression

Real-time RT-PCR revealed a time-dependent trend in enhanced TRADD gene expression for ceramide-treated cells. After a single hour of treatment, there was virtually no separation in TRADD C_T curves for RNA isolated from neither infected or uninfected cells, nor was there detectable separation of the GAPDH C_T curves (Figure 31A). After 2 hours, however, there was a significant increase in the separation in the GAPDH curves (Figure 31B, ~4.15 cycles) for Cer cells as compared to B+C cells with an average fold increase of 13.14 (Figure 32) and a $\Delta\Delta C_T$ of -3.72 (Table 3). Likewise at the same time-point the fold increase was 9.76 and 0.51 for Cer cells vs Controls and B+C cells vs. Controls, respectively (Figure 32; Table 2B and 2C). By 3 hour of ceramide treatment the fold-increase in TRADD gene expression was 3.91, 2.00 and 0.74 for Cer vs B+C, Cer vs Control and B+C vs Control, respectively (Figure 32; Table 3).

FADD Gene Expression

Real-time RT-PCR analysis reveals an enhancement of FADD expression similar to that which was observed with the TRADD gene. Following one hour of ceramide treatment, no separation of FADD C_T curves for templates derived from either infected or uninfected cells was detected (Figure 33A), but after two hours, there was a significantly higher level of the FADD transcript (relative to the GADPH standard) in the ceramide treated uninfected cells. The difference became even more pronounced after three hours (Figure 33B), with a 4.84 and 2.43 fold increase for Cer vs B+C and Cer vs Control, respectively (Figure 34; Table 4A and 4C). FADD gene expression returned to baseline by the 6-hour time point.

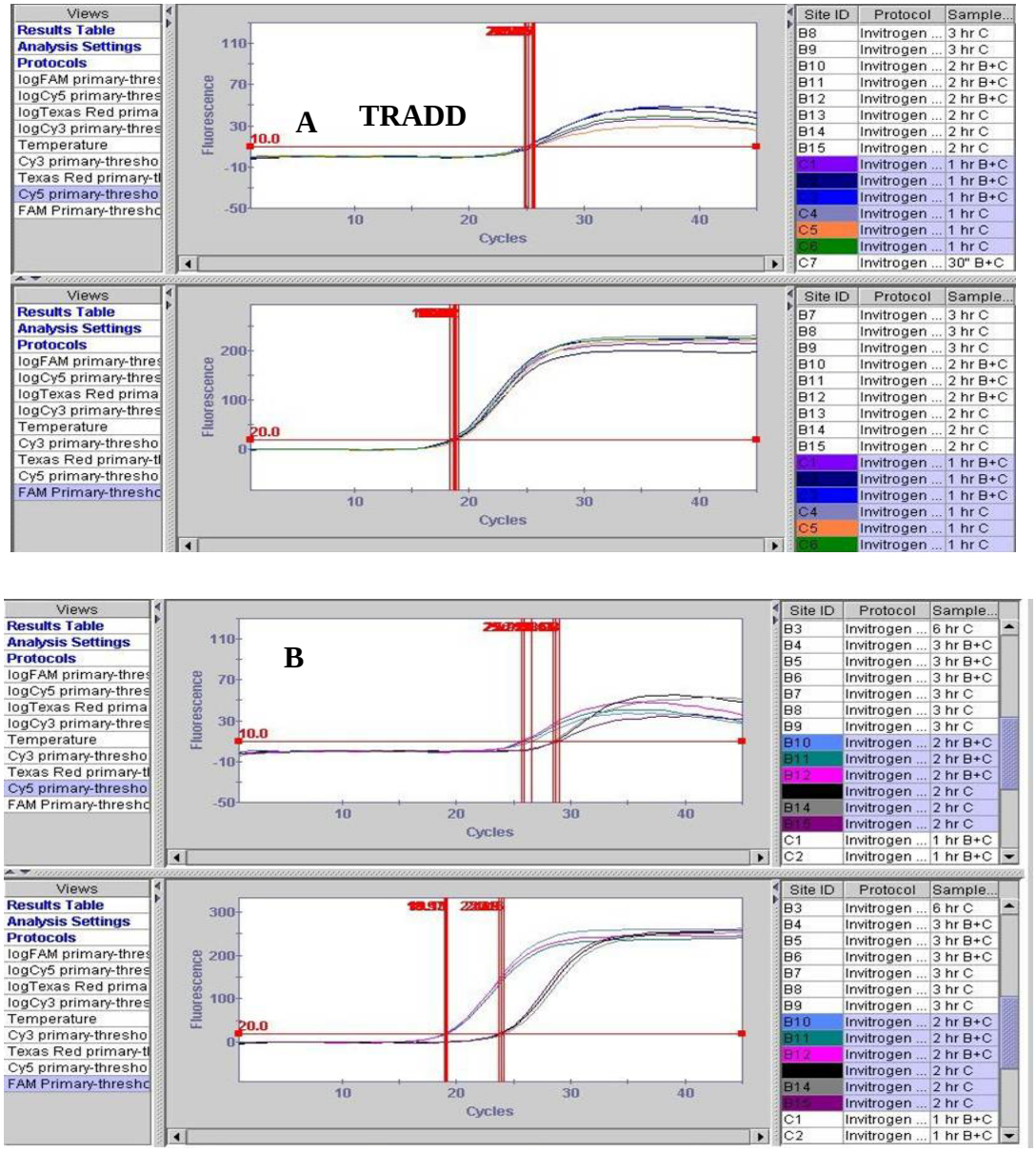

Figure 31. Multiplex Real-time RT-PCR for TRADD Gene Expression. TRADD gene expression (upper panel) is normalized to GAPDH gene expression (lower panel). Gene expression of TRADD is shown at 1 hour (Figure 31A) and 2 hour (Figure 31B). Ceramide treatment for 1 hour had no significant variation in gene expression between sample types. Two hour ceramide treatment demonstrates enhanced gene expression for TRADD (Figure 31B). Figure 31 is representative of multiple independent experiments (n=3). Experimental samples were run in triplicate

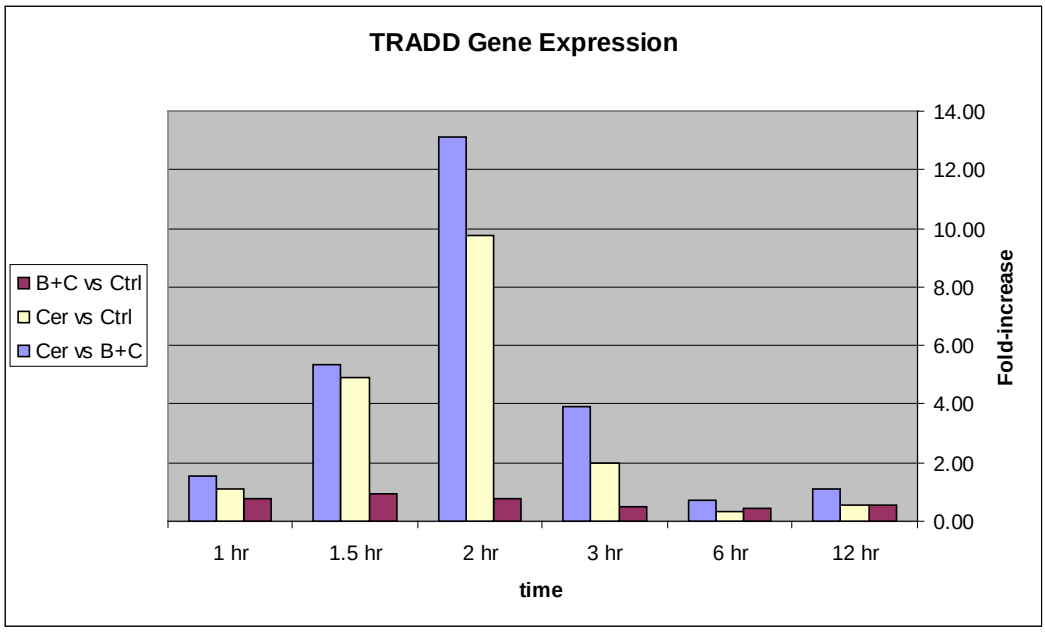

Figure 32. TRADD Gene Expression. Gene expression is represented as relative fold-increase for ceramide induced *B. henselae*-infected cells (B+C), ceramide treated uninfected cells (Cer) and control cells. Expression of apoptotic genes is normalized to GAPDH expression using the $\Delta\Delta C_T$ method. Values represent mean of fold-increase.

Caspase-8 and Caspase-3 Gene Expression

As with TRADD and FADD gene expression, the level of expression of the genes coding for Caspase-8 and Caspase-3 in *B. henselae*-infected cells following ceramide treatment was found to be significantly less than that of the uninfected control cells. The differences in gene expression became apparent at two hours post-ceramide treatment, reaching a peak at two hours for caspase-8 (4.45 fold-increase, Figure 36; Table 5) and caspase-3 (3.68 fold-increase, Figure 38; Table 6), then decreasing over the course of the next several hours (Figure 36 and 38; Table 5 and 6).

Table 3. TRADD Gene Expression Summary.

Cer vs B+C	**TRADD**	**1 hr**	**1.5 hr**	**2 hr**	**3 hr**	**6 hr**	**12 hr**
A	Fold-increase	1.56	5.34	13.14	3.91	0.74	1.09
	STDEV	0.43	0.59	0.69	2.39	0.02	0.03
	GOI (Test)	26.27	28.11	28.04	28.95	29.75	28.22
	Norm Gene (Test)	16.95	21.26	22.19	20.65	19.05	18.28
	ΔC_T	9.32	27.89	5.86	8.30	10.50	9.94
	GOI (Ref)	26.43	26.93	27.56	27.50	27.96	27.20
	Norm Gene (Ref)	16.86	17.72	17.99	17.38	17.68	17.13
	ΔC_T	9.94	9.27	9.57	10.12	10.28	10.07
	$\Delta\Delta C_T$	**-0.61**	**-2.41**	**-3.72**	**-1.82**	**0.43**	**-0.13**
B+C vs Ctrl	**TRADD**	**1 hr**	**1.5 hr**	**2hr**	**3 hr**	**6 hr**	**12 hr**
B	Fold-increase	0.52	0.45	0.51	0.74	0.92	0.75
	STDEV	0.15	0.08	0.01	0.08	0.12	0.22
	GOI (Test)	27.20	27.96	27.50	27.56	26.93	26.80
	Norm Gene (Test)	17.13	17.68	17.38	17.99	17.67	16.86
	ΔC_T	10.07	10.28	10.12	9.57	9.27	9.94
	GOI (Ref)	26.66	26.66	26.77	26.77	26.77	26.05
	Norm Gene (Ref)	17.56	17.56	17.63	17.63	17.63	16.56
	ΔC_T	9.10	9.10	9.14	9.14	9.14	9.49
	$\Delta\Delta C_T$	**0.96**	**1.18**	**0.98**	**0.43**	**0.13**	**0.45**
Cer vs Ctrl	**TRADD**	**1 hr**	**1.5 hr**	**2 hr**	**3 hr**	**6 hr**	**12 hr**
C	Fold-increase	1.12	4.89	9.76	2.00	0.33	0.58
	STDEV	0.03	0.09	0.57	1.26	0.07	0.18
	GOI (Test)	26.27	28.11	28.04	28.95	29.75	28.22
	Norm Gene (Test)	16.95	21.75	22.19	20.65	19.05	18.28
	ΔC_T	9.32	6.85	5.86	8.30	10.71	9.94
	GOI (Ref)	26.05	26.77	26.77	26.77	26.66	26.66
	Norm Gene (Ref)	16.56	17.63	17.63	17.63	17.56	17.56
	ΔC_T	9.49	9.14	9.14	9.14	9.10	9.10
	$\Delta\Delta C_T$	**-0.16**	**-2.29**	**-3.29**	**-0.84**	**1.61**	**0.84**

TRADD gene expression for ceramide treated unifected cells (Cer) versus ceramide treated *B. henselae*-infected cells (B+C), ceramide treated *B. henselae*-infected cells (B+C) versus control cells and ceramide treated unifected cells (Cer) versus control cells

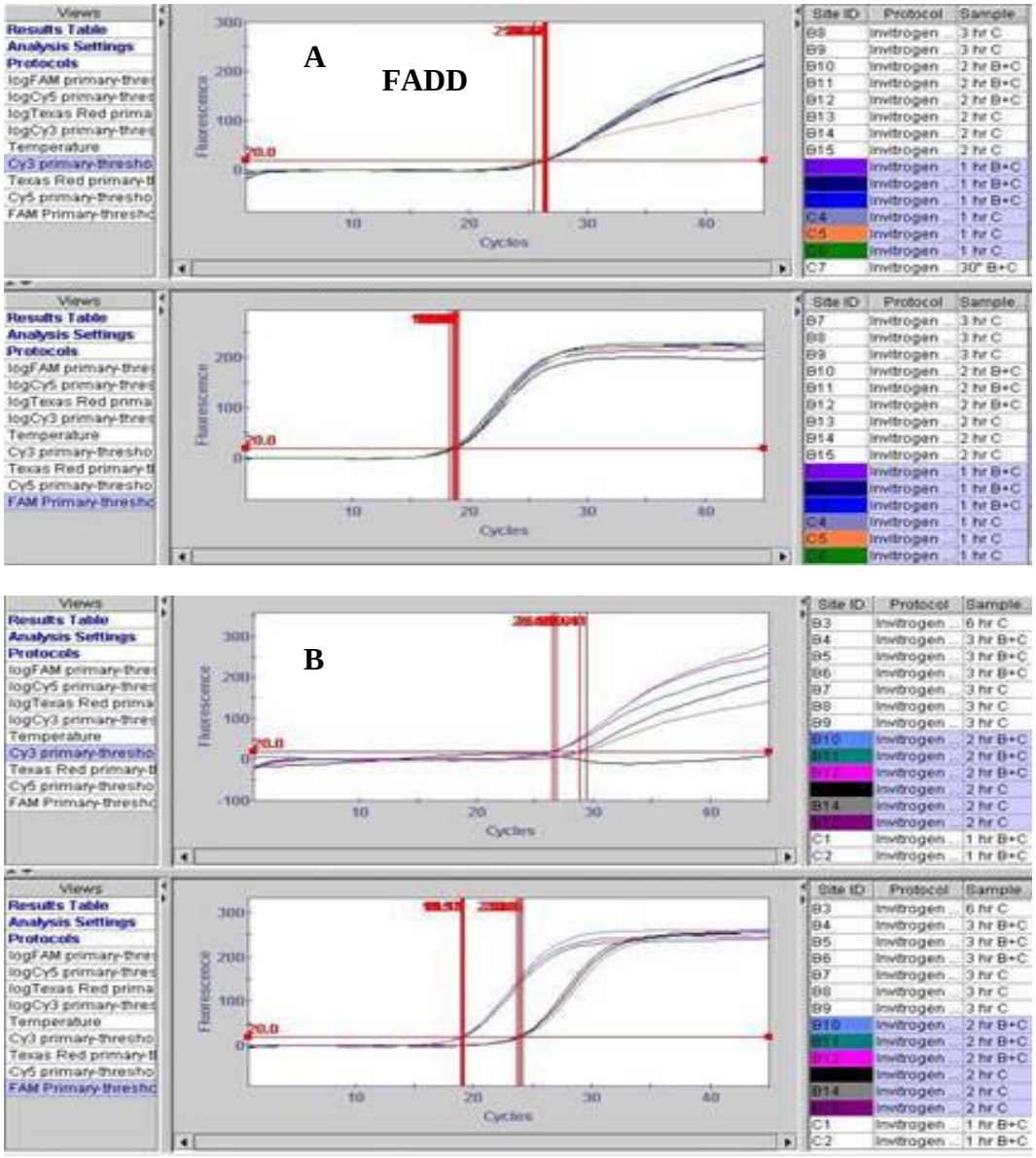

Figure 33. Multiplex Real-time RT-PCR for FADD Gene Expression. FADD gene expression (upper window) is normalized to GAPDH gene expression (lower window). Following 1 hour ceramide treatment, there was no significant variation in gene expression between sample types (Figure 33A). Two hour ceramide treatment demonstrates enhanced gene expression for FADD (Figure 33B). Figure 33 is representative of multiple independent experiments (n=3). Experimental samples were run in triplicate.

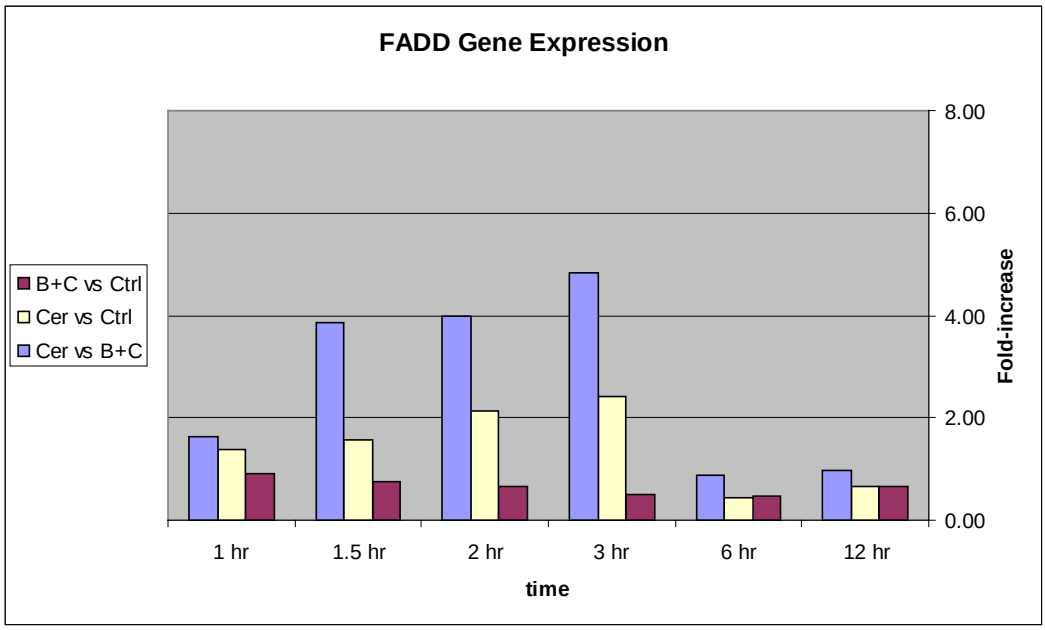

Figure 34. FADD Gene Expression. Gene expression is represented as relative fold-increase for ceramide induced *B. henselae*-infected cells (B+C), ceramide treated uninfected cells (Cer) and control cells. Expression of apoptotic genes is normalized to GAPDH expression using the $\Delta\Delta C_T$ method. Values represent the mean of the fold-increase. Enhanced expression levels were described is determined to be statistically significant ($p<0.05$). Gene expression is determined by multiple independent real-time RT-PCR experiments (n=3). Experimental samples were run in triplicate.

Use of Non-treated Control Cells As Normalizing Samples In Apoptotic Gene Expression Profiles

To generate a true baseline for gene expression in each of the experimental samples, we compared the fold-increase in apoptotic gene expression for uninfected and infected cells to the corresponding values for untreated uninfected and infected control cells (TRADD; Figure 39, FADD; Figure 40, Caspase-8; Figure 41 and Caspase-3; Figure 42). Following treatment of uninfected cells with ceramide, there was a significant increase in the expression of all four apoptotic genes tested relative to untreated control cells (Tables 3C, 4C, 5C and 6C)

Table 4. FADD Gene Expression Summary.

Cer vs B+C	FADD	1 hr	1.5 hr	2 hr	3 hr	6 hr	12 hr
A	Fold-increase	1.63	3.87	3.98	4.84	0.89	0.98
	STDEV	0.09	0.50	0.08	0.95	0.08	0.38
	GOI (Test)	26.27	27.67	27.30	27.10	27.57	26.57
	Norm Gene (Test)	16.86	17.67	17.99	17.38	17.68	17.13
	ΔC_T	8.70	8.06	7.68	7.46	10.06	9.53
	GOI (Ref)	25.65	29.32	29.87	28.11	29.10	27.81
	Norm Gene (Ref)	29.75	21.26	22.19	20.65	19.05	18.28
	ΔC_T	9.15	9.42	9.02	9.25	9.36	9.05
	$\Delta\Delta C_T$	**-0.70**	**-1.81**	**-1.63**	**-2.26**	**0.17**	**0.09**
B+C vs Ctrl	**FADD**	**1 hr**	**1.5 hr**	**2 hr**	**3 hr**	**6 hr**	**12 hr**
B	Fold-increase	0.92	0.74	0.66	0.50	0.48	0.66
	STDEV	0.12	0.08	0.01	0.03	0.00	0.11
	GOI (Test)	26.27	27.67	27.30	27.10	27.57	26.57
	Norm Gene (Test)	16.86	17.67	17.99	17.38	17.68	17.13
	ΔC_T	9.41	10.01	9.31	9.72	9.89	9.44
	GOI (Ref)	25.69	26.35	26.35	26.35	26.39	26.39
	Norm Gene (Ref)	16.56	17.63	17.63	17.63	17.56	17.56
	ΔC_T	9.13	8.72	8.72	8.72	8.83	8.83
	$\Delta\Delta C_T$	**0.28**	**1.29**	**0.59**	**1.01**	**1.06**	**0.60**
Cer vs Ctrl	**FADD**	**1 hr**	**1.5 hr**	**2 hr**	**3 hr**	**6 hr**	**12 hr**
C	Fold-increase	1.37	1.57	2.13	2.43	0.43	0.67
	STDEV	0.39	0.03	0.80	0.62	0.04	0.36
	GOI (Test)	25.65	29.32	29.87	28.11	29.10	27.81
	Norm Gene (Test)	16.95	21.26	22.19	20.65	19.05	18.28
	ΔC_T	8.70	8.06	7.68	7.46	10.06	9.53
	GOI (Ref)	25.69	26.35	26.35	26.35	26.39	26.39
	Norm Gene (Ref)	16.56	17.63	17.63	17.63	17.56	17.56
	ΔC_T	9.13	8.72	8.72	8.72	8.83	8.83
	$\Delta\Delta C_T$	-0.43	-0.66	-1.04	-1.26	1.22	0.69

FADD gene expression for ceramide treated unifected cells (Cer) versus ceramide treated *B. henselae*-infected cells (B+C), ceramide treated *B. henselae*-infected cells (B+C) versus control cells and ceramide treated unifected cells (Cer) versus control cells

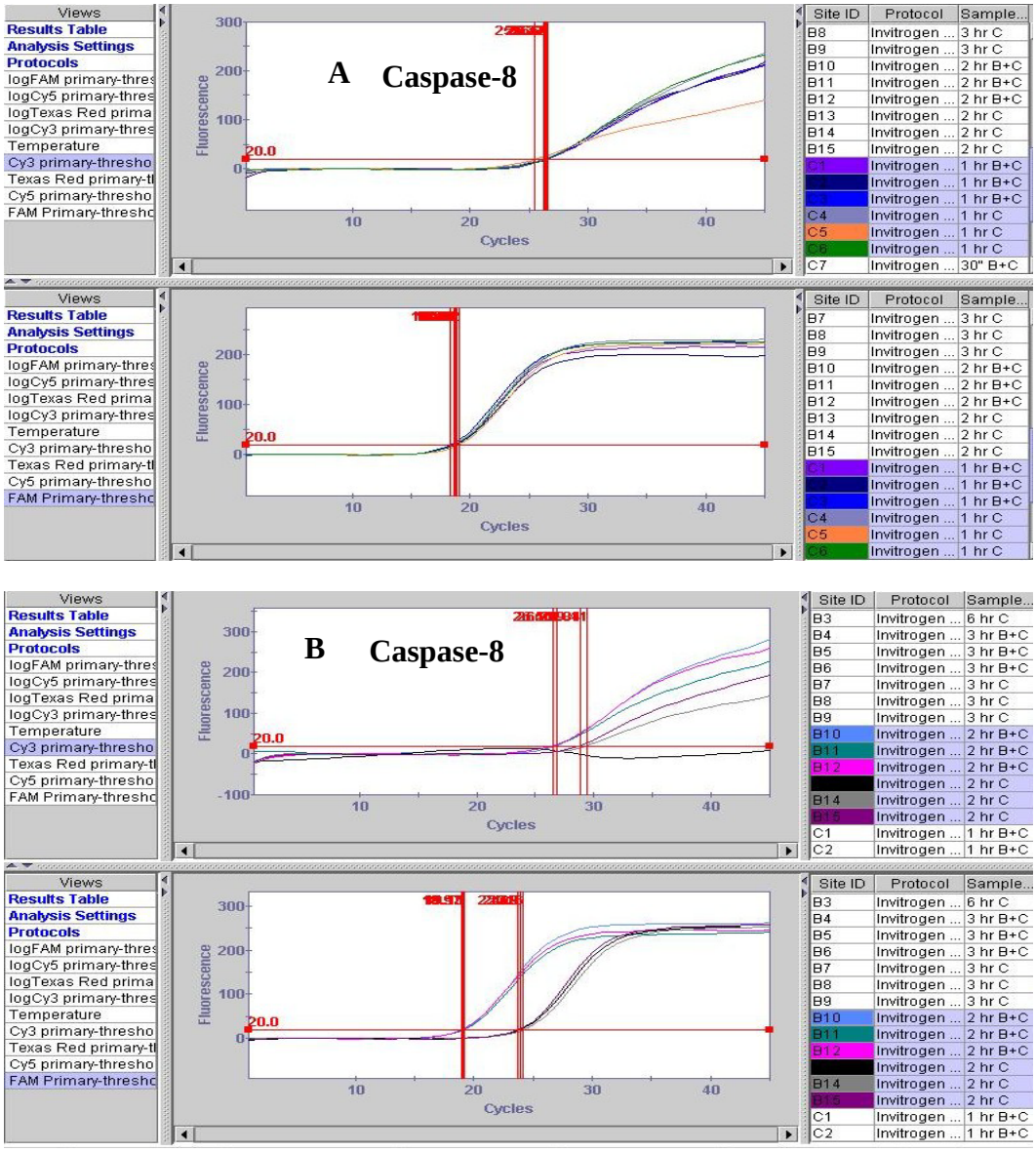

Figure 35. Multiplex Real-time RT-PCR for Caspase-8 Gene Expression. Caspase-8 gene expression (A, upper window) is normalized to GAPDH gene expression (B, lower window). Following 1 hour ceramide treatment, there was no significant variation in gene expression between sample types (Figure 35A). Two hour ceramide treatment demonstrates enhanced gene expression for Caspase-8 (Figure 35B). Figure 35 is representative of multiple independent experiments (n=3). Experimental samples were run in triplicate.

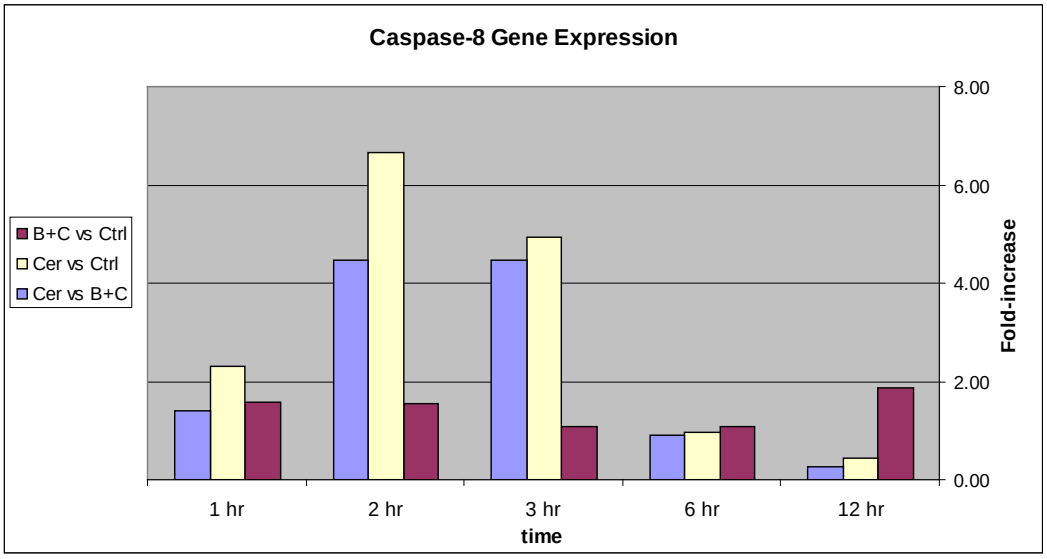

Figure 36. Caspase-8 Gene Expression. Gene expression is represented as relative fold-increase for ceramide induced *B. henselae*-infected cells (B+C), ceramide treated uninfected cells (Cer) and control cells. Expression of apoptotic genes is normalized to GAPDH expression using the $\Delta\Delta C_T$ method. Values represent mean of fold increase. Enhanced expression described is determined to be statistically significant ($p<0.05$).

In contrast, ceramide treatment has little or no effect on the expression of these genes in cells that have been infected with *B. henselae*. These results strongly suggest that *B. henselae* infection interferes with the expression of apoptotic genes.

Discussion

Real-time RT-PCR Assay Development

Microarray analysis and real-time RT-PCR both have the potential to generate large amounts of information about gene expression. In general, microarrays are considered to provide a more complete representation of cellular genome than real-time RT-PCR. However, the use of microarrays would have raised significant difficulties under the experimental parameters we employed.

Table 5. Caspase-8 Gene Expression Summary.

Cer vs. B+C	**Caspase-8**	**1 hr**	**2 hr**	**3 hr**	**6 hr**	**12 hr**
A	Fold-increase	1.40	4.45	4.47	0.91	0.28
	STDEV	0.14	1.31	0.57	0.17	0.13
	GOI (Test)	26.02	26.65	27.06	26.90	29.24
	Norm Gene (Test)	17.36	17.97	17.99	18.01	18.77
	ΔC_T	8.18	6.56	6.92	9.05	10.47
	GOI (Ref)	25.44	29.13	28.16	28.66	26.18
	Norm Gene (Ref)	17.26	22.57	21.25	19.61	17.67
	ΔC_T	8.67	8.68	9.07	8.89	8.52
	$\Delta\Delta C_T$	**-0.48**	**-2.11**	**-2.15**	**0.16**	**1.96**
B+C vs Ctrl	**Caspase-8**	**1 hr**	**2 hr**	**3 hr**	**6 hr**	**12 hr**
B	Fold-increase	1.59	1.53	1.07	1.08	1.86
	STDEV	0.85	0.66	0.45	0.98	1.24
	GOI (Test)	17.36	17.97	17.99	18.01	26.18
	Norm Gene (Test)	17.36	17.97	17.99	18.01	17.67
	ΔC_T	8.67	8.68	9.07	8.89	8.52
	GOI (Ref)	25.30	25.30	25.56	25.56	25.68
	Norm Gene (Ref)	16.09	16.09	16.47	16.95	16.47
	ΔC_T	9.21	9.21	9.09	8.61	9.21
	$\Delta\Delta C_T$	**-0.54**	**-0.53**	**-0.03**	**0.28**	**-0.69**
Cer vs Ctrl	**Caspase-8**	**1 hr**	**2 hr**	**3 hr**	**6 hr**	**12 hr**
C	Fold-increase	2.30	6.67	4.93	0.95	0.44
	STDEV	1.62	1.23	2.61	0.87	0.26
	GOI (Test)	25.44	29.13	28.16	28.66	29.24
	Norm Gene (Test)	17.26	22.57	21.25	19.61	18.77
	ΔC_T	8.18	6.56	6.92	9.05	10.47
	GOI (Ref)	25.30	25.30	25.56	25.56	25.68
	Norm Gene (Ref)	16.09	16.09	16.47	16.95	16.47
	ΔC_T	9.21	9.21	9.09	8.61	9.21
	$\Delta\Delta C_T$	**-1.02**	**-2.64**	**-2.18**	**0.44**	**1.26**

Caspase-8 gene expression for ceramide treated unifected cells (Cer) versus ceramide treated *B. henselae*-infected cells (B+C), ceramide treated *B. henselae*-infected cells (B+C) versus control cells and ceramide treated unifected cells (Cer) versus control cells.

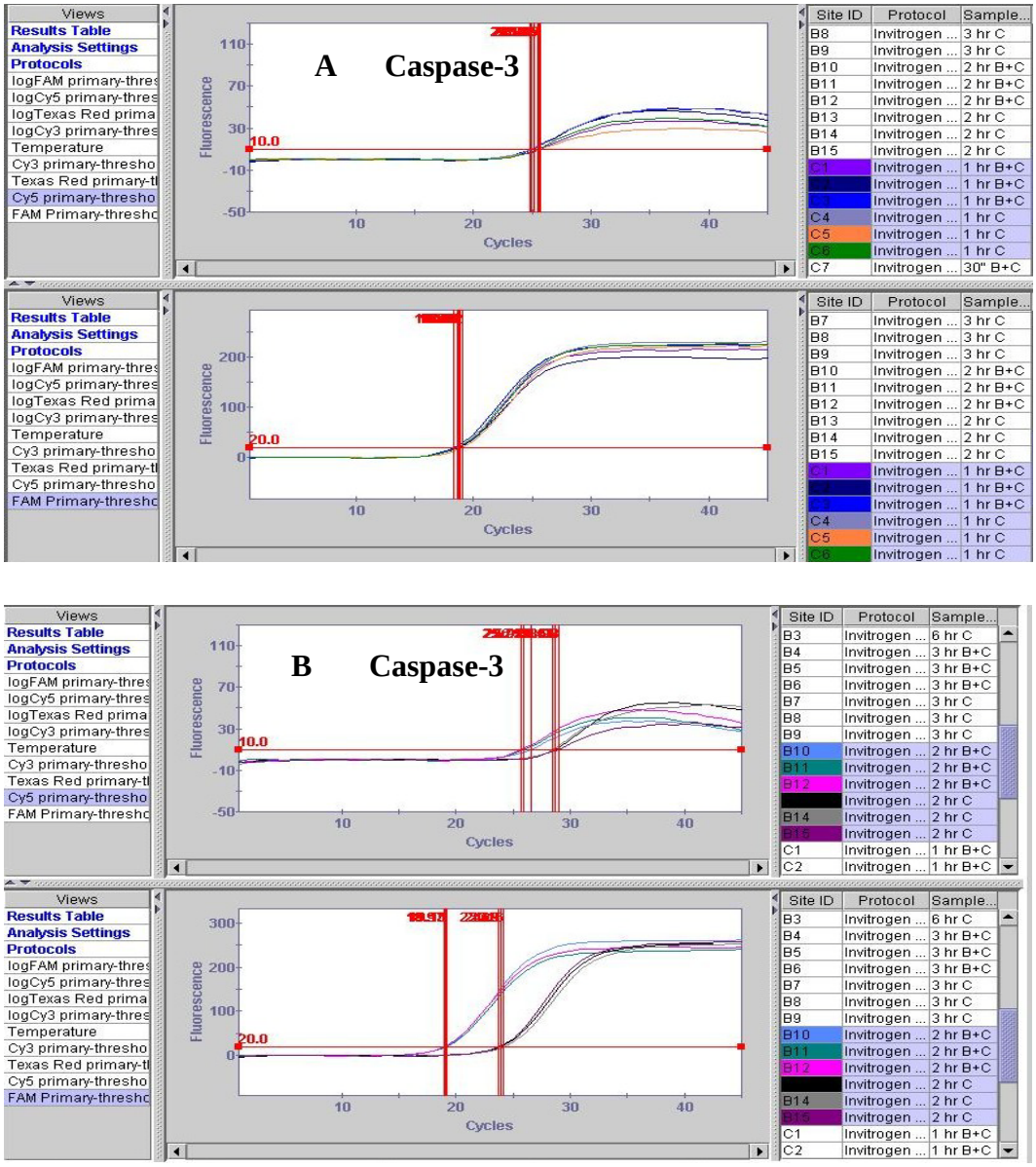

Figure 37. Multiplex Real-time RT-PCR for Caspase-3 Gene Expression. Caspase-3 gene expression (A, upper window) is normalized to GAPDH gene expression (B, lower window). Following 1 hour ceramide treatment, there was no significant variation in gene expression between sample types. Two hour ceramide treatment demonstrate enhanced gene expression for caspase-3 (Figure 37B). Figure 37 is representative of multiple independent experiments (n=3). Experimental samples were run in triplicate.

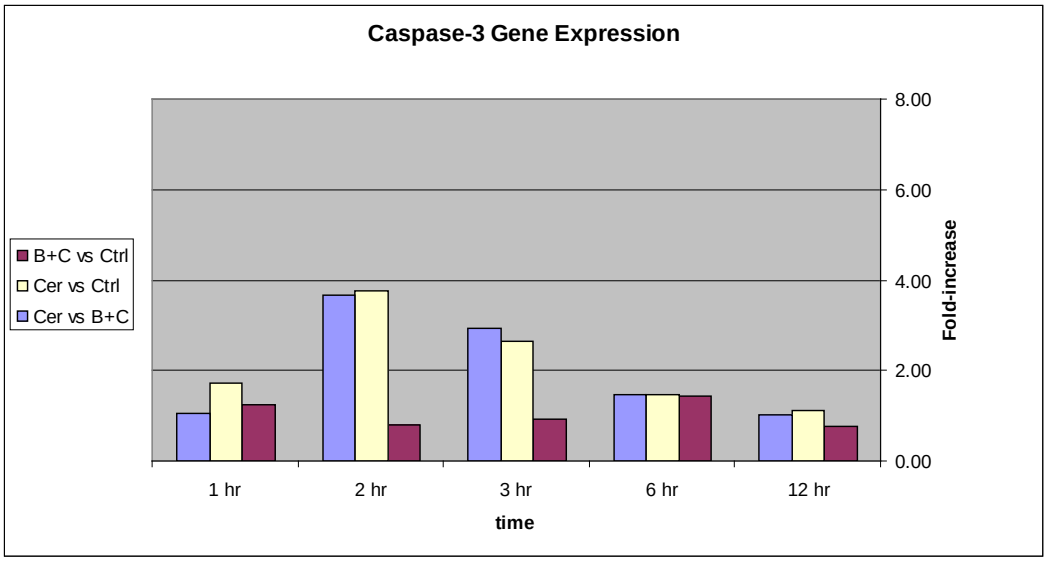

Figure 38. Caspase-3 Gene Expression. Gene expression is represented as relative fold-increase for ceramide induced *B. henselae*-infected cells (B+C), ceramide treated uninfected cells (Cer) and control cells. Expression of apoptotic genes is normalized to GAPDH expression using the $\Delta\Delta C_T$ method. Values represent mean of fold increase. Enhanced expression described is determined to be statistically significant ($p<0.05$). Gene expression is determined by multiple independent real-time RT-PCR experiments (n=3). Experimental samples were run in triplicate.

For instance, the amount of RNA template required for microarray analysis, derived from *in vitro* cell culture, would have been prohibitively large when considering multiple time points and other experimental conditions that we had to address. Moreover, the addition of C_2-ceramide, resulting as it does in large-scale cell death of uninfected cells, would seriously affect the ability to isolate RNA samples at levels high enough to analyze. To overcome these hurdles, real-time RT-PCR was used as it requires substantially less RNA template. In addition to its ability to optimize experimental parameters in ways that minimize the quantity of input template, real-time RT-PCR can be conducted at significantly lower cost than microarray analysis. The robustness of a real-time RT-PCR assay is dependent on the design of the primer/probe set. Primer/probe sets were designed using BLAST gene sequences available through GenBank.

Table 6. Caspase-3 Gene Expression Summary.

Cer vs Ctrl	**Caspase-3**	**1 hr**	**2 hr**	**3 hr**	**6 hr**	**12 hr**
A	Fold-increase	1.71	3.75	2.65	1.45	1.10
	STDEV	0.19	0.59	0.28	0.39	0.52
	GOI (Test)	23.61	27.79	26.73	25.51	25.21
	Norm Gene (Test)	17.26	22.57	21.25	19.61	18.77
	ΔC_T	6.36	5.22	5.48	5.90	6.44
	GOI (Ref)	23.21	23.21	23.35	23.35	22.92
	Norm Gene (Ref)	16.09	16.09	16.47	16.95	16.47
	ΔC_T	7.12	7.12	6.88	6.40	6.45
	$\Delta\Delta C_T$	**-0.76**	**-1.90**	**-1.40**	**-0.50**	**-0.01**
B+C vs Ctrl	**Caspase-3**	**1 hr**	**2 hr**	**3 hr**	**6 hr**	**12 hr**
B	Fold-increase	1.25	0.79	0.92	1.43	0.76
	STDEV	0.61	0.39	0.32	0.86	0.47
	GOI (Test)	23.78	25.07	25.03	24.46	24.10
	Norm Gene (Test)	17.26	22.57	21.25	19.61	18.77
	ΔC_T	-2.25	-1.58	-2.03	-2.45	-2.08
	GOI (Ref)	23.21	23.21	23.35	23.35	22.92
	Norm Gene (Ref)	16.09	16.09	16.47	16.95	16.47
	ΔC_T	-2.09	-2.09	-2.21	-2.21	-2.76
	$\Delta\Delta C_T$	**-0.16**	**0.51**	**0.19**	**-0.23**	**0.68**
Cer vs. B+C	**Caspase-3**	**1 hr**	**2 hr**	**3 hr**	**6 hr**	**12 hr**
C	Fold-increase	1.05	3.68	2.95	1.47	1.02
	STDEV	0.18	0.44	0.10	0.26	0.28
	GOI (Test)	23.61	27.79	26.73	25.51	25.21
	Norm Gene (Test)	17.26	22.57	21.25	19.61	18.77
	ΔC_T	1.17	0.38	0.52	0.87	1.30
	GOI (Ref)	23.78	25.07	25.03	24.46	24.10
	Norm Gene (Ref)	17.36	17.97	17.99	18.01	17.67
	ΔC_T	6.42	7.10	7.04	6.44	6.43
	$\Delta\Delta C_T$	**-0.06**	**-1.87**	**-1.56**	**-0.54**	**0.01**

Caspase-3 gene expression for ceramide treated unifected cells (Cer) versus ceramide treated *B. henselae*-infected cells (B+C), ceramide treated *B. henselae*-infected cells (B+C) versus control cells and ceramide treated unifected cells (Cer) versus control cells.

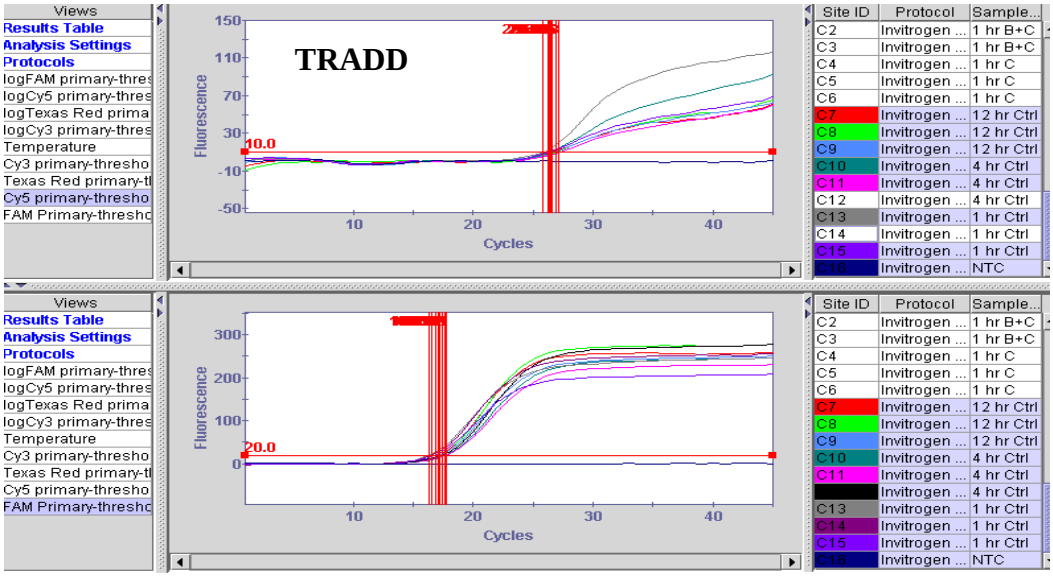

Figure 39. Multiplex Real-time RT-PCR for TRADD Controls. TRADD gene expression (upper window) as compared to GAPDH gene expression (lower window). RNA templates corresponding to 1, 4 and 12 hour ceramide-treatment time-points. TRADD gene expression demonstrates little variability in uninfected and non-apoptotic challenged cells at all time-points.

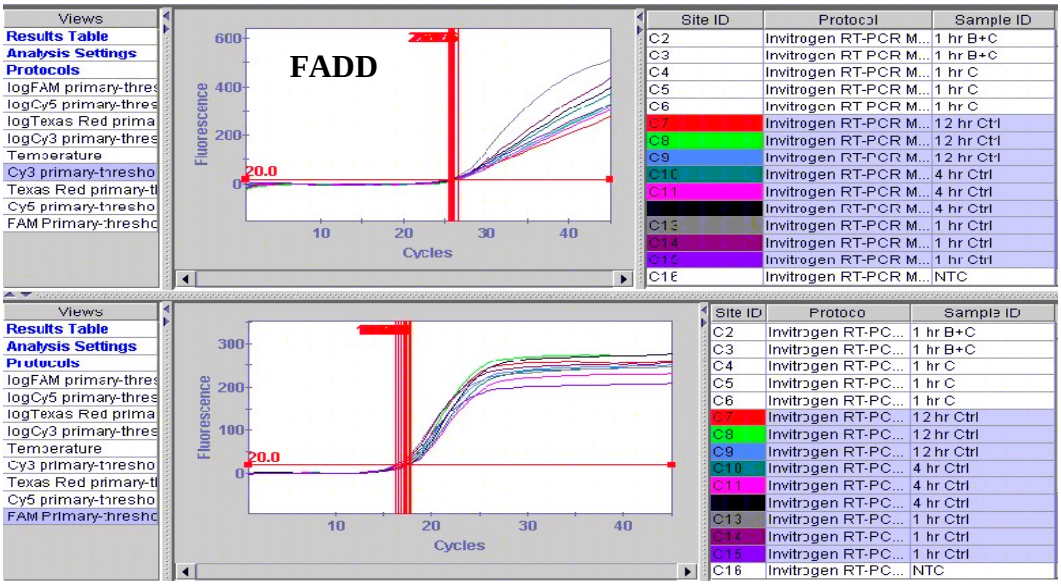

Figure 40. Multiplex Real-time RT-PCR for FADD Controls. FADD gene expression (upper window) as compared to GAPDH gene expression (lower window). RNA templates corresponding to 1, 4 and 12 hour ceramide-treatment time-points. FADD gene expression across a dynamic time-course demonstrates little variability in uninfected and non-apoptotic challenged cells.

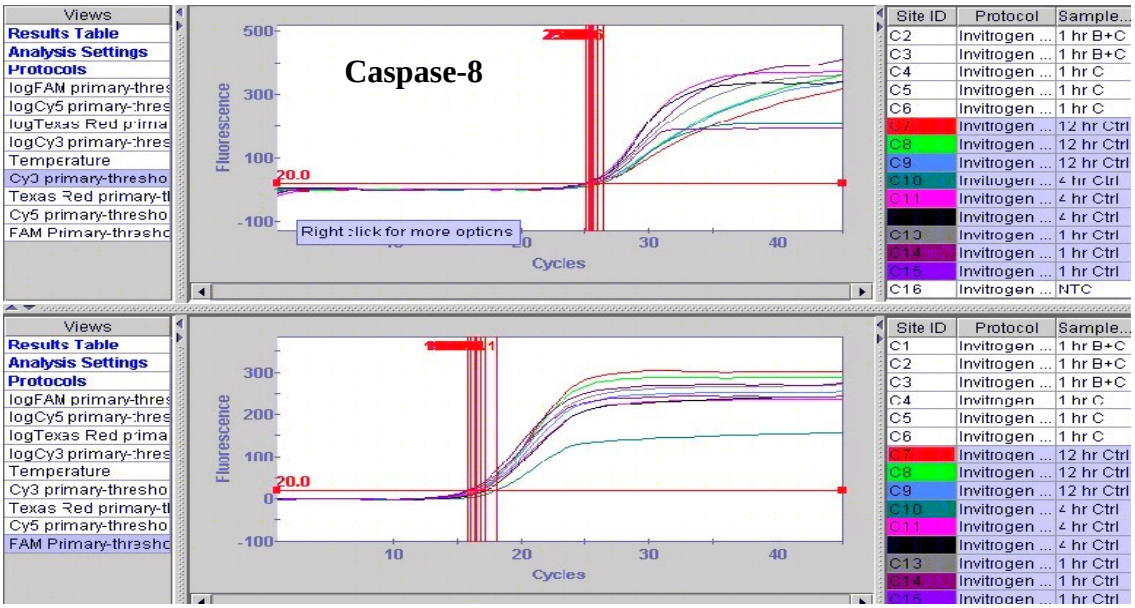

Figure 41. Multiplex Real-time RT-PCR for Caspase-8 Controls. Caspase-8 gene expression (upper window) as compared to GAPDH gene expression (lower window). RNA templates corresponding to 1, 4 and 12 hour ceramide-treatment time-points. Caspase-8 expression across a dynamic time-course demonstrates little variability in uninfected and non-apoptotic challenged cells.

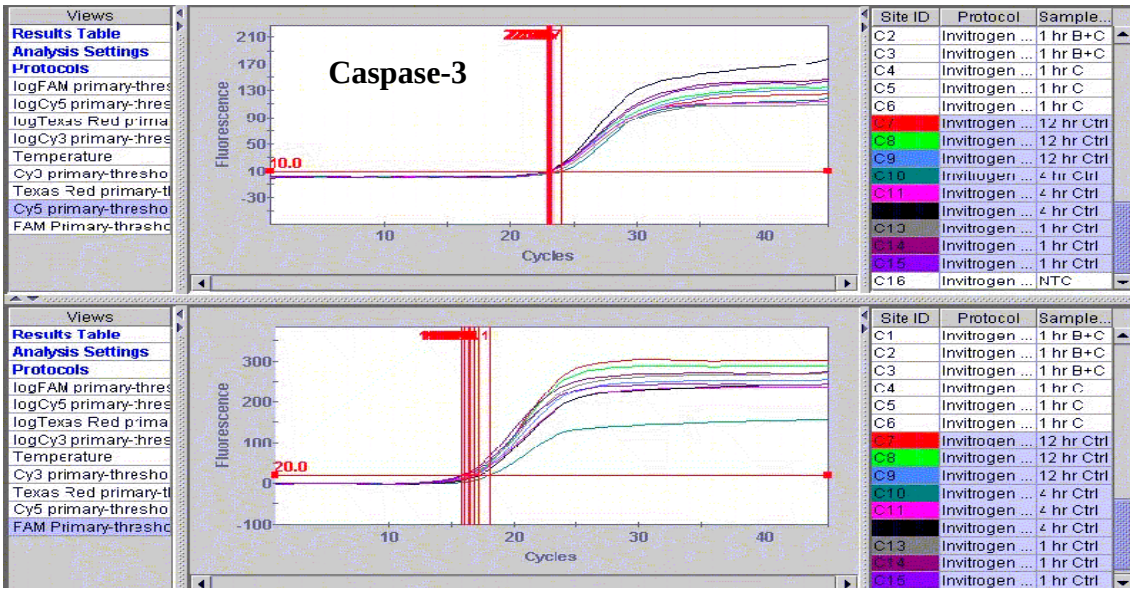

Figure 42. Multiplex Real-time RT-PCR for Caspase-3 Controls. Caspase-3 gene expression (upper window) as compared to GAPDH gene expression (lower window). RNA templates were generated from uninfected and untreated cells corresponding to 1, 4 and 12 hour ceramide-treatment time-points. Caspase-3 gene expression across a dynamic time-course demonstrates little variability in uninfected and non-apoptotic challenged cells.

BLAST sequences were used to design 5'-fluorogenic nuclease-assay primer and probe sets using Primer Express™ software. The target primer and probe sequences were screened for cross-reactivity using a silica-based system (courtesy of Lawrence Livermore National Laboratories). Primer/probe sets were further scrutinized by searching for overlap and self-binding sequences using Primer Express™ software. Lastly, primer and probe sequences were screened for near match "hits" using "NCBI near query". Primer and probe sequences that pass the software vetting, were subject to testing by wet chemistry.

Each primer probe set was tested for its specificity, sensitivity and overall performance in its ability to amplify the target gene. The proper ratio of primer/probe and cation concentration ensures that the appropriate start amplification conditions are achieved (Figure 24). Each individual primer/probe set may achieve optimal amplification with different cation concentrations. Subsequently, the addition of any necessary supplemental components is determined (Figure 25). It was previously demonstrated that multiplexed real-time PCR assays exhaust reagents when target sequences are present at different molar concentrations. The addition of Platinum Taq™ and additional dNTP's is required for equal amplification efficiency for target sequences (personal communication Dr. Jonas Winchell). The addition of supplemental yeast tRNA was determined necessary to ensure RNA stability and reproducible data. tRNA acts as a chaperone to stabilize RNA template and binds to the walls of plastic vessels ensuring that target template is not adsorbed (Sambrook, 1989).

Further, titration of the primer/probes within the normal range was necessary to determine the best minimal concentration without affecting signal intensity (Figure 26). Each gene marker was then tested for its amplification efficacy (Figures 27-30). Multiplexed assays allowed for assessing apoptotic genes while accounting for overall template concentration (Bustin and

Nolans 2004). Properly vetting primer/probe sets allow for selection of the most favorable primer/probe set for each target.

Use of Multiplexed Real-time RT-PCR to Assess Apoptotic Gene Expression

The major advantage of multiplexing the real-time RT-PCR assay is that it allows for the assessment of multiple genes in context with a normalizing house-keeping gene in a single reaction tube. Real-time RT-PCR has an added benefit in that it provides visual data for the genetic sequence of interest without further manipulation. The dynamics of 5'-fluorogenic nuclease chemistry adds an additional stringency to gene expression analysis by requiring two primers (both forward and reverse) and a target specific probe. All three independent events are necessary for generating a signal event. The lengths of real-time PCR amplicons are much shorter than conventional PCR and therefore are inherently less likely to be affected by secondary folding of synthesized product. The use of a single normalizing gene allows for relative gene expression levels to be measured. However, relative gene expression is only an approximation of true gene quantification (Suslov and Steindler, 2005).

Housekeeping Genes Used for Relative Apoptosis Gene Expression

Recently, there has been much debate about the use and reliability of conventional house-keeping genes for the purpose of normalizing gene expression. Some conventional house-keeping gene targets used for normalizing gene expression are: 18S ribosomal RNA, β-actin, RNAase P and GAPDH (Goncalves *et al.*, 2005). Much of this controversy stems from the debate over the reliability of gene expression across different cell types (Radonic *et al.*, 2004). Gene expression analysis across multiple tissue types does require the use of normalizing genes with low variability, but not necessarily robust expression. In addition, the use of multiple normalizing genes is essential to properly standardize the basal expression when comparing

different cell types (Vandesompele *et al.*, 2002). However, our experimental model is a homogenous stable cell line of a single cell type. This provides us genetic stability as opposed to primary cells or hybrid cells used in previous research (Kirby and Nekorchuck, 2002). Further, our interest focuses on analysis of a cluster of genes with complementary and non-competing function. Lastly, we are assessing relative gene expression and not quantitative gene expression.

Due to the fact that we are using a homogeneous host cell model, the house-keeping gene utilized herein provides a good reference for determining our best approximation of gene expression. The use of multiplexed real-time RT-PCR has novel value in that we are assessing the gene expression of a subset of desired genes between individual test and reference samples using small quantities of RNA template derived from a small experimental sample.

Apoptotic Gene Expression

What does gene expression highlight about *B. henselae*'s intracellulat survival strategy? When comparing gene expression for TRADD, FADD, Caspase-8 and Caspase-3, there are some striking differences for cells that are infected with *B. henselae* as opposed to cells that are not.

TRADD expression is induced in a like manner for both ceramide-treated uninfected cells (Cer) versus ceramide-treated *B. henselae*-infected (B+C) cells and Cer versus control (Ctrl) cells (Figure 32). TRADD demonstrates a rapid increase in the earliest ceramide treatment timepoints (1 and 2 hours), with a rapid decline thereafter, returning to baseline by 6 hours of ceramide treatment. In contrast, TRADD gene expression for B+C versus Ctrl is below baseline for all treatment time-points. The rapid induction of TRADD demonstrates that TRADD expression is induced by the presence of ceramide. The fact that TRADD expression for B+C cells compared to controls demonstrates that *B. henselae* is capable of suppressing TRADD gene expression

following ceramide challenge. This is the first account of *B. henselae's* ability to suppress the synthesis of TNF-1 receptor-death-domain protein following challenge by an apoptogenic agent.

Unlike TRADD, FADD gene expression maintains a modest ubiquitous expression in normal untreated cells. Following ceramide treatment, FADD increases from its normal expression level, peaking at 3 hour post-ceramide treatment. FADD expression returns to baseline thereafter. FADD expression appears to remain at baseline for B+C versus Ctrl during the duration of ceramide treatment. The fold increase in FADD gene expression is most impressive when comparing B+C versus Ctrl as compared to Cer versus Ctrl, where it appears that the presence of *B. henselae* suppresses FADD gene expression below that of control cells. This agrees with our preliminary finding that Western Blot analysis indicating that untreated HMEC-1 cells infected with *B. henselae* suppress FADD protein expression (Chapter 2, Figure 7).

Following our observation that *B. henselae* infection has a demonstrable effect on upstream TNF-dependent apoptosis modulators, we analyzed its effect on down-stream apoptosis modulators. Caspase-8 gene expression was induced in a time-dependent manner for both Cer versus B+C and Cer versus Ctrl (Figure 36). However, caspase-8 gene expression was observed to be more pronounced in Cer versus Ctrl than for Cer versus B+C. This suggests that intracellular *B. henselae* does suppress caspase-8 but not to levels below that of control cells. However, *B. henselae* does suppress caspase-8 gene expression in the presence of an apoptotic challenger.

Caspase-3 gene expression is consistent for Cer vs Ctrl and Cer vs B+C (Figure 36). Caspase-3 gene expression peaks rapidly following ceramide treatment and wanes slowly thereafter. The fold-increase of caspase-3 gene expression is modest at less than four-fold. In

opposition to caspase-8, caspase-3 does target a multitude of cellular targets and has the most abundant cellular pool and a long half-life of approximately 5.5 hours (Tan *et al.,* 2006). The C_T value of caspase-3 is not significantly lower than that of caspase-8. It does not appear that the presence of *B. henselae* has a dramatic effect on the gene expression of caspase-3, as compared to TRADD or FADD. However, considering the cellular reservoir of caspase-3 protein and the protein's half-life, disrupting caspase-3 gene expression may not be an expedient strategy of an intracellular pathogen.

CONCLUSION

Role of This Study

In this study, we demonstrated that *Bartonella henselae* circumvents host cell apoptotic mechanisms in order to survive as an intracellular pathogen of endothelial cells. *B. henselae* aids in the survival of their host cells following direct apoptogenic stimuli, thereby aiding their own intracellular survival. Previous researchers focused on the ability of *B. henselae* to stimulate host cell proliferation via cellular growth modulators as the means of surviving apoptotic challenge (Kempf *et al.,* 2004; Maeno *et al.,* 1999). Others concluded that *B. henselae* survive by abrogation of apoptotic intrinsic pathway proteolytic enzymes to ensure intracellular survival (Kirby and Nekorchuk, 2002). Recently, two groups claimed to have found the substrate responsible for *B. henselae*'s ability to disrupt apoptosis (Kempf *et al.*, 2005; Schmid *et al.*, 2006). Bartonella effector protein-A (BepA) has been described as the substrate that is translocated to the host cell where it functions to block apoptosis by increasing cellular cyclic-AMP (Schmid *et al.,* 2006). However, other research utilizing BadA- *B. henselae* confirmed that Bad A facilitates colonization of *B. henselae* and contributes a pre-formed effector molecule found on both viable and non-viable *B. henselae* bacterial cells. The presence of this pre-formed effector upregulates cellular inhibitor of apoptosis protein (IAP), which is regulated by NF-κB (Kempf *et al.,* 2005).

We assert that *B. henselae* achieve intracellular survival by redundant measures that involve modulation of both extrinsic and intrinsic apoptotic pathways. Preserving host cell viability is a consequence of infection with *B. henselae*, as well as with other related bacteria (Conley *et al.,* 1994). However, in contrast to previous research, we noted no significant increase

in host cell proliferation due to the presence of *B. henselae.* It is possible that this effect of *B. henselae* is not apparent within the time-frame of our experimental parameters. In addition, the experiments described here did not reveal any effect of intracellular *B. henselae* upon diminishing the cytotoxicity of RIP toxins (e.g., abrin and ricin) which have been shown to induce apoptosis by caspase upregulation (Rao, P.V. *et. al.,* 2005). Therefore, we conclude that *B. henselae* is not capable of abrogating all apoptotic mechanisms. Instead, our research results suggest that *B. henselae* exploits divergent apoptosis pathways to survive, such as suppression of extrinsic pathway modulators TRADD and FADD, and suppression of intrinsic pathway caspase-3 enzymatic activity. *Bartonella's* tropism for endothelial cells is indicative of its evolution toward host cells that are not induced to apoptosis by TNF-α (Faherty and Maurelli, 2008).

Gram-negative Bacterial Infection and LPS

The innate immune system is able to detect molecular patterns of most pathogens, including lipoloysaccharide (LPS) of gram-negative bacteria. The molecular pattern of these non-mammalian molecules is recognized by Toll-like receptors (TLR) and CD14 (Hansson and Edfeldt, 2005). LPS from Gram-negative bacteria bind to TLR-4 and CD14, which ultimately leads to the release of IκB from the nuclear factor NFκB. Among the genes activated by NFκB is TNF-α. Apoptosis induced by LPS from *Escherichia coli* in HMEC-1 cells was shown to be FADD-dependent. However, neither TNF-R1 nor Fas receptor plays a role in *E. coli* LPS-induced apoptosis using HMEC-1 cells (Kyong-Bok *et al.*, 1998). While *E. coli* LPS, which is a potent pyrogen, effectively induces apoptosis in HMEC-1 cells, not all Gram-negative endotoxins are apoptogenic.

B. henselae possesses an LPS that lacks O-chain carbohydrates, much like other bacteria capable of chronic infection such as Legionella spp. and Chlamydia. The result is that Toll-like receptors-2 (TLR-2) are not activated and TLR-4 are activated at levels nearly 1000-10,000 fold lower than that of other enteric bacteria (Zahringer *et al.,* 2004). Gene expression triggered by NF-kB causes ICAM-1 and E-selectin to be upregulated. However, in the case of *B. henselae*, ICAM-1 and E-selectin are upregulated by the presence of a *B. henselae* synthesized proteinaceous factor (Fuhrmann *et al.*, 2001). It has been suggested that the lipid A component of LPS can mimic the secondary messenger activity of ceramide. Using a cell permeable analog of ceramide, such as C_2-ceramide, induces many LPS-inducible genes (Barber *et al.,* 1996; van Bitterswijk *et al.,* 2003).

B. henselae **Infection**

Nearly a quarter of a century ago, *B. henselae* was identified as the causative agent of cat-scratch disease (Wear *et al.,* 1983; Slater *et al.,* 1993). Transmission between cats occurs horizontally through the arthropod vector *Ctencephalides felis*, the cat flea. Cats can maintain persistent infections, however, transmission of *B. henselae* in a cat colony occurs by infection of fleas from infected cats, which in turn infect other non-infected cats or re-infect a previously infected cat (Breitschwerdt and Kordick, 2000). During the persistent *B. henselae* infection in cats, the bacteria are harbored inside erythrocytes. Nearly 50% of domestic cats are seropositive for antibodies to *B. henselae*. Cat to human infection occurs by exposure to *B. henselae*-infected cat saliva or a scratch from an infected cat (Florin *et al.,* 2008). Upon entering the human host, *B. henselae* invade the hematopoetic progenitor cells but not erythrocytes. *B. henselae* have been shown to infect macrophages (Musso *et al.,* 2001; Kempf *et al.,* 2005) and endothelial progenitor

cells (Salvatore *et al.,* 2008). This would provide a means for *B. henselae* to traffic from the site of host introduction to their niche in the microvascular endothelium. *B. henselae* activate NF-κB gene products during the course of binding to the endothelial cell membrane and the formation of the invasome, a set of membrane protrusions that engulf the bacteria (Dehio *et al.,* 1999). However, invasome formation is found in umbilical vein endothelial cells such as HUVEC and not microvascular cells (Dehio, 2004). Upon entry into the microvascular endothelium, *B. henselae* induce the upregulation of cellular inhibitors of apoptosis (cIAP-1 and -2) and cellular adhesion molecule genes, ELAM-1 and ICAM-1 (Faherty and Maurelli, 2008).

Bartonella **Protein Factors and Their Role in Intracellular Survival**

Bartonella possess a variety of genes that are analogous to pathogenicity factors used by other bacteria that survive intracellularly in a similar manner (Foulongue *et al.,* 2000). Some of the proteins derived from these pathogenicity genes are used in an analogous manner to *B. henselae* to ensure its survival (Hacker and Fischer, 2002). The VirB/D4 gene cluster was discovered in *Bartonella* spp. following the identification of a 17kDa antigen with sequence similarity to the *virB7* gene of *Agrobacterium tumefaciens* (Padmalayam *et al.,* 2000). Many of the virulence properties of *B. henselae*, such as their entry into erythrocytic cells and their ability to promote cytoskeleton and adhesion molecule rearrangement (Schulein *et al.,* 2002), can be ascribed to the expression of the VirB/D4 operon, which codes for a Type IV secretion system (T4SS)(O'Callahan, *et al*., 1999). The induced operon functions to transfer Bartonella translocated effector proteins (Bep A-G) into the host cells. BepA has been proposed to have anti-apoptosis activity. Both BepA and BepD have also been proposed to have angiogenic activity, while BepG has been assigned an anti-angiogenic role (Molloy, 2009; Scheidegger *et*

al., 2009). BepA protein has been shown to translocate to the host cell membrane and increase the cyclic adenosine monophosphate (cAMP) levels in the cell. cAMP then activates a variety of protein kinases (PKA, ERK and MAPK) and inhibits the pro-apoptotic protein Bad. T4SS substrates with similar function have been identified in other bacterial systems (Couturier *et al.,* 2006).

Although BepA appears to play a significant role as an anti-apoptotic factor, it is unlikely that the BepA-induced pathway is the only mechanism used by *B. henselae* to prevent apoptosis of their host. In many cases, pathogens have evolved redundant strategies to ensure their survival. One example involves the F1 *Yersinia* antigen. *Yersinia* survival strategies and pathogenic factors bear many similarities to those of *Bartonella spp.* and other intracellular bacteria (de Jong *et al*., 2008). For many years, the F1 antigen has been considered to be the primary (and perhaps only) factor necessary for *Yersinia pestis* pathogenesis. However, the recent isolation of virulent F1 negative clinical isolates suggests that *Y. pestis* has other pathways available for maintaining virulence (Bashaw *et al*., 2007; Dr. Jeanine Petersen CDC, Fort Collins, CO personnal communication).

The *B. henselae* outer membrane protein adhesin A (BadA) has been identified as a Bartonella pathogenicity factor required for pathogen and host cell interaction (Reiss *et al.,* 2004). BadA is a non-fimbrial adhesion protein similar to its *Yersinia* counterpart YadA (Monack *et al.,* 1997). BadA appears to play a role in initiating an angiogenic response in host cells and inhibiting phagocytosis. However, a variant of the strain used for our studies (Houston-1: ATCC 49882) lacks expression of BadA and yet is capable of adhesion and entry into endothelial cells (Reiss *et al.,* 2004). While the search for the conclusive pathogenicity factor of a

particular pathogen is appealing, the reality is more likely to be that infectious agents have devised a versatile repertoire in order to successfully survive (Rajashekara *et al*., 2005).

B. henselae **Disrupts Gene and Protein Expression of Extrinsic and Intrinsic Apoptotic Pathway Modulators Following Apoptogenic Ceramide Treatment**

Our research has demonstrated that *B. henselae* targets apoptosis basically from the outside in. In short, *B. henselae* is capable of disrupting apoptotic modulators that function earlier in the cellular apoptotic pathway chain. Specifically, TRADD and FADD gene and protein expression are disrupted by the presence of *B. henselae*. Past researchers have largely focused on the enhanced proliferative activity of *B. henselae* factors as the mode of anti-apoptotic activity (Kempf *et al.*, 2001). Our studies differ in several ways. First, we used an experimental model and growth conditions that are consistent with natural disease and maintain the integrity of microvascular endothelial characteristics. In addition, we challenged the host cells with an apoptogenic agent that mimics a natural cellular messenger in response to Gram-negative bacteria.

We contend that serum starvation or protein synthesis inhibition (methods used by other investigators to induce apoptosis) adds an unnecessary bias by suppressing protein synthesis. The lack of serum simultaneously activates and suppresses multiple pathways and many of these mechanisms are poorly understood. Further, low serum concentration causes HMEC-1 cells to lose their microvascular endothelial characteristics (Ades *et al.*, 1992). Protein synthesis inhibitors provide two divergent biases. First, the lack of protein synthesis prevents any apoptotic or anti-apoptotic gene product which lacks sufficient cytoplasmic pools from being generated. This is not consistent with primary mechanisms of the natural disease state or the host immune

response. Secondly, previous researchers have demonstrated that protein synthesis inhibition disrupts the balance between typical caspase and c-FLIP proteins (Zimmermann *et al.*, 2001). Two apoptogenic agents which indeed disrupt protein synthesis, ricin toxin and abrin toxin, were tested in our model. The apoptogenic effect of these two agents on the host microvascular endothelial cell was not disrupted by the presence of *B. henselae* (data not shown).

The use of ceramide affords us an apoptogenic agent that mimics the cellular response to Gram-negative LPS (van Bitterswijk *et al.,* 2003). Ceramide has been characterized as causing induction of cellular kinases which leads to caspase induction in several experimental models. In fact, ceramide functions in at least four areas of the cell during apoptosis signaling. In the Golgi, ceramide contributes to lipid metabolism which helps generate lipid rafts (van Blitterswijk *et al.,* 2003). At the cell membrane, ceramide facilitates receptor clustering (Gulbins *et al.,* 2004), and alters mitochondria permeability (Kolsenick, 2002; Siskind *et al.,* 2002). Ceramide also contributes to the formation of membrane bound apoptotic bodies (van Blitterswijk *et al.,* 2003). Ceramide is released endogenously following extracellular stresses, such as treatment with lipopolysaccharide (LPS). However, we confirmed what others have observed that, *B. henselae* LPS is not cytotoxic by comparing the cytotoxic effect of like concentrations of endotoxin derived from both *B. henselae* and *E. coli* (Zahringer *et al.,* 2004). We have demonstrated that endothelial cells respond to exogenous ceramide in a dose-dependent apoptotic response.

B. henselae **Disrupts Extrinsic Pathway Receptor Mediated Apoptosis in Order to Ensure Its Survival**

TNF-receptor-1 (TNF-R1) clustering induces recruitment of TRADD to the TNF-R1 death domains (DD). This occurs in response to TNF-α-induced receptor clustering or lipid raft

induced clustering. In endothelial cells, the endogenous release of TNF-α would not necessarily signal theTNF-R1 clustering that would be expected to result in DISC formation. However, the addition of exogenous ceramide is known to result in lipid raft formation and the clustering of receptor proteins (Cuschieri *et al.,* 2006; Gulbins *et al.,* 2003). The clustering of TNF-R1 by ceramide would induce DISC formation, resulting in the accumulation of TRADD at the TNF-R1 DD. The recruited TRADD would recruit necessary downstream modulators (e.g., FADD). The rapid rise and fall of TRADD gene expression for ceramide treated endothelial cells would indicate that either 1) TRADD is stable and does not require prolonged translation,or 2) as the uninfected cell succumbs to ceramide treatment, the cell is diverting valuable resources to the production of new TRADD proteins. Infection by *B. henselae* precipitously suppresses both gene and protein induction of TRADD, indicating that there is a strong correlation between the presence of the bacteria and the signal(s) that trigger TRADD induction. By suppressing TRADD gene expression, *B. henselae* could cut off the cascade of events associated with the TNF-R1 extrinsic apoptosis pathways.

TRADD and FADD are sequential cellular modulators recruited by TNF-R1 in the TNF-dependent pathway. FADD recruitment has already been demonstrated to induce endothelial cell apoptosis specifically in HMEC-1 cells (Kyong-Bok *et al.*, 1998). As mentioned previously, our early observation that FADD protein expression declines following *B. henselae* infection suggested a preemptive and continuous anti-apoptotic strategy by *B. henselae*. It is important to remember the loss of detectable FADD by Western Blot following infection of *B. henselae* (Figure 7) occurred in the absence of any apoptosis agonist. The overall purpose of FADD in extrinsic pathway apoptosis is the recruitment of other downstream apoptotic modulators, namely

caspase-8, to the DISC. FADD is recruited by both TRADD and Fas as part of extrinsic apoptotic signaling pathways.

When examining gene expression as fold-increase, it is important to point out that expression levels are based on which sample type is being used as the benchmark and which is used as the illustration. Gene expression for TRADD is profoundly induced by ceramide. This is potentiated by the fact that the presence of *B. henselae* suppresses TRADD gene expression. FADD gene expression is only modestly induced by ceramide. *B. henselae*-infected cells suppress FADD gene expression, which makes FADD appear as a highly inducible gene following ceramide treatment. A different picture emerges when analyzing TRADD and FADD protein expression. TRADD protein expression is clearly inducible and is suppressed by the presence of *B. henselae.* The percentage of cells expressing TRADD is nearly 3 times lower in *B. henselae*-infected cells. Conversely, FADD protein is expressed in nearly half the cells regardless of *B. henselae*'s presence. But the presence of *B. henselae* does keep FADD expression from going any higher and slightly suppresses FADD protein expression. We demonstrated that *B. henselae* affects FADD protein expression both during the course of infection or following apoptogenic stimuli of *B. henselae*-infected cells. What is more pronounced is the profound effect *B. henselae* has on the gene and protein expression of TRADD. By abrogating TRADD signaling, *B. henselae* has subverted initiation of an entire apoptotic pathway.

***B. henselae* Suppresses Caspase-3**

Previous studies have indicated that *Bartonella*-infected cells suppress apoptosis induction by abrogating caspase activity (Kirby *et al.*, 2002). Our data indicate that *B. henselae* is capable of suppressing caspase-3 activity and caspase-8 and -3 gene expression. But the loss of

caspase-8 activity was not observed within our experimental parameters. Caspase-8 is the initial cysteine protease messenger in extrinsic (TNF-receptor-1 and Fas-dependent) apoptotic signaling pathways. Pools of capase-8 are maintained in the endoplasmic reticulum and translocated to the DISC complex following receptor signaling (Homlstrom *et al.*, 2000). As an initiator of the caspase cascade, caspase-8 present at high levels is not sufficient, nor required, to sustain apoptotic induction (Green, 2003). As an executioner, caspase-3 proteolytically cleaves many cellular substrates. Additionally, caspase-3 is necessary as an executioner for both intrinsic and extrinsic apoptotic pathways. This would require that either large pools of caspase-3 are maintained, or that caspase-3 is a rapidly inducible gene product. As mentioned earlier, caspase-3 is the most abundant caspase in the cell (Chickova *et al.*, 2004).

It is worthy to note the inherent flaws in relying upon caspase proteolytic activity assays as a true measurement of caspase involvement. First, the caspase specific target peptides are not actually specific, but rather preferential for a particular caspase. Second, enzymatic activity may not be an accurate measurement of a specific caspase activity. Historic dogma asserts that caspases are synthesized in a proform. The active "enzymatic" form is generated following proteolytic cleavage. Recent studies refute that assertion, especially with regard to caspase-8. Caspase-8 is active in its dimeric form (Green, 2003; Thorburn *et al.,* 2004). As mentioned earlier, caspase-8 has been shown to be "enzymatically" active in an unprocessed form. Thus, unprocessed caspase-8 may facilitate auto-proteolysis of caspase-3. Unlike caspase-8 and possibly caspase-6, caspase-3 is primarily a proteolytic enzyme.

What is clear is that ceramide treatment causes activation of caspase-3. Ceramide-induced activation of caspase-3 for uninfected cells occurs earlier, is maintained for a longer duration and is significantly more active as compared to ceramide treated *B. henselae*-infected, or control

cells. Our observation that caspase-3 is the only caspase of those we tested that is suppressed by the presence of Bartonella species is in direct conflict with previous observations (Kirby and Nekorchuck, 2002; Schmid *et al.*, 2006). We believe this is in part due to the cell line model used. Cell type variability in the use of different apoptosis mechanisms is an obstacle when comparing results using different model systems. Additionally, the use of an apoptogenic agent may produce different results than the use of serum starvation as the apoptogenic stimulus.

Summary

What we know about the strategies used by *B. henselae* to maintain host cells in numbers sufficient for successful infection is multifaceted. Previous research has demonstrated that *B. henselae* enhances proliferation (Slater *et al.*, 1994; Maeno *et al.*, 1999), that the cell cytoskeleton is rearranged during the course of infection (Dehio, 1999) and that adhesion molecules are upregulated that enhance *B. henselae* internalization (Fuhrmann *et al.*, 2001). Additionally, unlike those of other Gram-negative bacteria, the LPS molecules of *B. henselae* are not capable of inducing apoptosis (Zahringer *et al.*, 2004). The VirB/D4 operon provides a transport pilus that acts to translocate effector proteins, such as BepA, which are capable of "subverting" the host cell apoptosis mechanisms. Moreover, *B. henselae* generated modulators can affect caspase activity and thereby influence the cells' decision to enter an apoptotic pathway (Schmid *et al.*, 2006).

Our research provides evidence that *B. henselae* disrupts host cell gene and protein expression of the extrinsic apoptosis modulators TRADD and FADD. TRADD gene expression in particular is significantly suppressed by the presence of *B. henselae*. *B. henselae* also suppresses FADD gene expression. FADD protein is ubiquitously expressed under normal

cellular growth conditions. However, the presence of *B. henselae* minimizes FADD protein expression even following prolonged apoptogenic stimuli. In our experimental system caspase-8 and caspase-3 gene expression were modestly suppressed by *B. henselae.*

The proteolytic activity of either caspase-8 or caspase-6 was unaffected by the presence of *B. henselae*. However, the proteolytic activity of caspase-3 was suppressed significantly *B. henselae*. In fact, at some ceramide treatment time-points, *B. henselae*-infected cells had higher caspase-6 and caspase-8 activity than their uninfected counterparts. Lastly, the formation of apoptotic bodies and DNA fragmentation was dramatically reduced in *B. henselae*-infected cells. Enhanced host cell viability for *B. henselae*-infected cells was consistent with these results. We do know that *B. henselae* cannot disrupt the apoptogenic action of all apoptogenic stimuli, such as ricin and abrin toxins.

Future Directions

The means by which *B. henselae* migrate from their point of entry to their niche in the microvascular endothelium is not understood. Furthermore, the cellular proteins targeted by translocated effectors upon entry by the bacterium into the microvascular endothelium remain to be identified. Only a handful of apoptogenic agents have been used to challenge *Bartonella spp*; Hundreds of natural apoptogenic agents remain untested. Still, elucidation of the mechanism(s) by which *B. henselae* ensures its survival will enhance our understanding of pathogen-induced tumorgenesis. It will also help us to understand the processes used by evolutionarily similar intracellular bacterial pathogens.

BIBLIOGRAPHY

1. Abraham, N.G., Kushida, T., McClung, J., Weiss, M., Lafaro, R., D. Zbigniew and M. Wolin. 2003. Heme Oxygenase-1 Attenuates Glucose-Mediated Cell Growth Arrest and Apoptosis in Human Microvascular Endothelial Cells. *Circuation. Reserach*. **93**(6): 507-514.

2. Ades, E.W., Candal, F.J., Swerlick, R.A., George, V.G., Summers, S., Bosse, D.C. and T.J. Lawley. 1992. HMEC-1: Establishment of an Immortalized Human Microvascular Endothelial Cell Line. *Journal of Invetsigative Dermatology*. 1992. **99** :683 –690.

3. Ajenjo, N., Canon, E., Sanchez-Perez, I., Mastallanas, D., Leon, J., Perona, R. and P. Crespo. 2004. Subcellular Localization Determines the Protective Effects of Activated ERK2 against Distinct Apoptogenic Stimuli in Myeloid Leukemia Cells. *Journal of Biological Chemistry.* **279**(31): 32813-32823.

4. Apakama I, Robinson M.C, Walter N.M, Charlton R.G, Royds J.A, Fuller C.E, Neal D.E and F.C. Hamdy. 1996. Bcl-2 Overexpression Combined with p53 Protein Accumulation Correlates with Hormone-refractory Prostate Cancer. *British Journal of Cancer.* **74**(8): 1258-62.

5. B. Anderson. 2001. The Interaction of *Bartonella* with Endothelial Cells and Erythrocytes. *Trends in Microbiology.* **9**(11): 530 - 531

6. A. Ashkenazi. 2008. Directing Cancer Cells to Self-destruct with Pro-apoptotic Receptor Agonists. *Nature Review of Drug Discovery*. **12**:1001-12.

7. Ashkenazi, A. and V.A. Dixit. 1998. Apoptosis Control by Death and Decoy Receptors. *Current Opinions in Cell Biology*. **11**(2): 255-260.

8. Barber, S.A., Detore, G., McNally, R., and S. N. Vogel. 1996. Stimulation of the Ceramide Pathway Partially Mimics Lipopolysaccharide-Induced Responses in Murine Peritoneal Macrophages. *Infection and Immunity*. **64**(8): 3397-3400.

9. Bartee, E., Mohamed, M.R. and G. McFadden. 2008. Tumor Necrosis Factor and Interferon: Cytokines in Harmony. *Current Opinions in Microbiology*. **11**(4):378-83

10. Bashaw, J., Norris, S., Weeks, S., Trevino, S., Adamovicz, J.J. and S. Welkos. 2007. Development of In Vitro Correlate Assays of Immunity to Infection with *Yersinia pestis*. *Clinical Vaccine Immunology*. **14**(5): 605-606.

11. Bass, J. W., J. M. Vincent, and D. M. Person. 1997. The Expanding Spectrum of *Bartonella* Infections:II. Cat-scratch Disease. *Pediatric Infectious Disease Journal.* **16**:163-179.

12. Basu, S., Shariff, B., Zhang, Y., Lozano, J. and R. Kolesnick. 1998. BAD Enables Ceramide to Signal Apoptosis via Ras and Raf1. *Journal of Biological Chemistry*. **273**(46): 30419-30426.

13. Bird, B.A. and Francis T. Forrester. 1981. Basic Laboratory Techniques in Cell Culture. U.S. Department of Health and Human Services/Public Health Service/Centers for Disease Control, Atlanta, Georgia.

14. Belloc, F., M. A. Belaud-Rotureau, V. Lavignolle, E. Bascans, E. Braz-Pereira, F. Durrieu, and F. Lacombe. 2000. Flow Cytometry Detection of Caspase-3 Activation in Preapoptotic Leukemia Cells. *Cytometry*. 40:151-160.

15. Boatright, K.M. and G.S. Salvesen. 2003. Mechanisms of Caspase Activation. *Current Opinions in Cell Biology.* 15: 725-731.

16. Browne, D.A. and E. London. 1998. Functions of Lipid Rafts in Bological Mmbranes. *Annual Review of Cellular Development Biology.* **14**:111-136.

17. Breitschwerdt, E. B. and D. L. Kordick. 2000. Bartonella Infection in Animals: Carriership, Reservoir Potential, Pahogenicity and Zoonotic Potential for Human Infection. *Clinical Microbiology Review*. **13**: 428-438.

18. Bustin, S.A. and T. Nolan. 2004. Pitfalls of Quantitative Real-time Reverse-transcription Polymerase Chain Reaction. *Journal of Biomolecular Techniques*. **15** 155–166.

19. Burnette, W.N. 1980. "Western Blotting": Electrophoretic Transfer of Proteins from Sodium Dodecyl Sulfate-polyacrylamide Gels to Unmodified Nitrocellulose and Radiographic Detection with Antibody and Radioiodinated Protein A. *Analytical Biochemistry*. **112**(2): 195-202.

20. Candal, F.J., Rafii, S., Parker, J.T., Ades, E.W., Ferris, B.,Nachman, R. and K.L. Kellar. 1996. BMEC-1: A Human Bone Marrow Microvascular Endothelial Cell Line with Primary Cell Characteristics. *Microvascular Research*. 52:221-234.

21. Chichkova, N.V., Kim, S.H., Titova, E.S., Kalkum, M., Morozov, V.S., Rubtsov, Y.P., Kalinina, N.O., Taliansky, M.E. and A.B. Vartapetian. 2004. A Plant Caspase-Like Protease Activated during the Hypersensitive Response. *Plant Cell Preview*. **16**: 157-171.

22. Clifton, D.R., Goss, R.A., Sahni, S.K., vanAntwerp, D., Bagos, R.B., Marder, V.J., Silverman, D.J. and L.A. Sporn. 1998. NF-kB-dependent Inhibition of Apoptosis is Essential for Host Cell Survival During *Rickettsia rickettsii* Infection. *Proceedings of the National Academy of Science, USA*. **95**:4646-4651.

23. Conley, T., Slater, L. and K. Hamilton. 1994. *Rochalimaea* Species Stimulate Human Endothelial Cell Proliferation and Migration *In Vitro*. *Journal of Laboratory Clinical Medicine.* **124**: 521-528.

24. Cory, S. and J.M. Adams. 2002. The BCL2 Family: Regulators of the Cellular Life-or-Death Switch. *Nature Reviews*. **2**(9): 647-656.

25. Cory, S., Huang, D.C.S. and J.M. Adams. 2003. The Bcl-2 Family: Role in Cell Survival and Oncogenesis. *Oncogene* **22**:8590-8607.

26. Couturier, M.R., Tasca, E., Montecucco, C. and M. Stein. 2006. Interaction with CagF Is Required for Translocation of CagA into the Host via the *Helicobacter pylori* Type IV Secretion System. *Infection and Immunity*. **74**(1): 273–281.

27. Creagh, E.M., Conroy, H. and M. Seamus. 2003. Caspase Activation Pathways in Apoptosis and Immunity. *Immunological Reviews*. **193**(1):10-21.

28. Cuschieri, J., Billgren, J. and R.V. Maier. 2006. Phosphatidylcholine-specific Phospholipase C (PC-PLC) is Required for LPS-mediated Macrophage Activation Through CD14. *Journal of Leukocyte Biology.* **80**: 407-414.

29. Darby, A. C., Cho, N.H., H-H. Fuxelius, J. Westberg and Siv G.E. Andersson. 2007. Intracellular Pathogens Go Extreme: Genome Evolution in the Rickettsiales. *Trends in Genetics*. **23**(10):511-520.

30. Datta, S., Dudek, H., Tao, X., Masters, S., Fu, H., Gotoh, Y. and M.E. Greenberg. 1997. Akt Phosphorylation of BAD Couples Survival Signals to the Cell-Intrinsic Death Machinery. *Cell*. **91**(2): 231-241.

31. Dauphinee S.M., Karsan A. 2006. Lipopolysaccharide Signaling in Endothelial Cells. *Laboratory Investigations*. **86**(1):9-22.

32. Davis, C.N., Tabarean, I., Gaidarova, S., Behrens, M.M. and T. Bartfai. 2006. IL-1β Induces a MyD88-dependent and Ceramide-mediated Activation of Src in Anterior Hypothalmic Neurons. *Journal of Neurochemistry*. **98**: 1379-1389.

33. Day, T.W., Najafi, F., Wu, C-G and A.R. Safa. 2006. Cellular FLICE-like Inhibitory Protein (c-FLIP): Novel Target for Taxol-induced Apoptosis. *Biochemical Pharmacology*. **71**: 1551-1561.

34. de Jong, M., Sun, Y-H, den Hartigh, A.B., van Dijl, J.M. and R.M. Tsolis. 2008. Identification of VceA and VceC, Two Members of the VjbR Regulon that are Translocated into Macrophages by the Brucella Type IV Secretion System. *Molecular Microbiolog*y. **10**: 1365-2958.

35. C. Dehio. 1999. Interactions of *Bartonella henselae* with Vascular Endothelial Cells *Current Opinion in Microbiology*. **2**:78-82.

36. C. Dehio. 2001. *Bartonella* Interactions with Endothelial Cells and Erythrocytes. *Trends in Microbiology*. **9:**279-285.

37. C. Dehio. 2003. Recent progress in understanding *Bartonella*-induced Vascular Proliferation. *Current Opinion in Microbiology*. **6**(1): 61-65.

38. C. Dehio. 2004. Molecular and Cellular Basis of *Bartonella* Pathogenesis. *Annual Review of Microbiology*. **58**: 365-90.

39. de St Groth B.F. and A.L. Landay. 2008. Regulatory T Cells in HIV Infection: Pathogenic or Protective Participants in the Immune Response? *AIDS*. **30**(6):671-83

40. Dempsey, P.W., Doyle, S.E., He, J.Q. and G. Cheng. 2003. The Signaling Adaptors and Pathways Activated by TNF Superfamily. *Cytokine and Growth Factor Reviews* **14**(3-4): 193-209.

41. Desagher, S., Astrid Osen-Sand, A.N., Robert E., Sylvie M., Sandra L., Kinsey M., Bruno A. and J-C Martinou. 1999. Bid-induced Conformational Change of Bax is Responsible for Mitochondrial Cytochrome-c Release During Apoptosis. *Journal of Cell Biology*. **144**(5): 891-901.

42. D.W. Dickson. 2004. Apoptotic Mechanisms in Alzheimer Neurofibrillary Degeneration: Cause or Effect? *Journal of Clinical Investigations*. **114**(1):121-30.

43. Elzbieta B., Burfeind, P., Hsieh, T-Z, Wu, J.M., Aguero-Rosenfeld, M.E., Melamed, M.R., Horowitz, H.W., Wormser, G.P. and Z. Darzynkiewicz. 1998. Cell Cycle Effects and Induction of Apoptosis Caused by Infection of HL-60 Cells with Human Granulocytic *Ehrlichiosis* Pathogen Measured by Flow and Laser Scanning Cytometry. *Cytometry*. **33**:47-55.

44. Emmons, R.W., Riggs, J.L., Schachter J. 1976. Continuing the Search for the Etiology of Cat Scratch Disease. *Journal of Clinical Microbiology*. **4**:112-4.

45. Faherty, C.S. and A.T. Maurelli. 2008. Staying Alive: Bacterial Inhibition of Apoptosis During Infection. Trends in Microbiology. **16**(4): 173-180.

46. E. Farrando-May. 2005. Nucleocytoplasmic transport in apoptosis. *Cell Death and Differentiation.* **12**:1263-1276.

47. Faust, E. C. and P. F. Russell (1964) in *Craig and Faust's Clinical Pathology* (Faust, Ernest C. and Paul F. Russell, eds), pp. 871-872. Lea and Febiger, Philadelphia.

48. Feng, Y., Hu, J., Xie, D., Zhong, Y., Li, X., Xiao, W., Wu, J., Tao, D., Zhang, M., Zhu, Y., Song, Y., Reed, F., Li, Q. Q. and J. Gong. 2005. Subcellular Localization of Caspase-3 Activation Correlates with Changes in Apoptotic Morphology in MOLT-4 Leukemia Cells Exposed to X-ray Irradiation. *International Journal of Oncology*. **27**(3): 699-704.

49. Fillet, M., Beintires-Ali, M., Deregowski, V., Gielen, J., Piette, J., Bours, V. and M-P. Merville. 2003. Mechanisms Involved in the Exogenous C_2- and C_6-ceramide-induced Cancer Cell Toxicity. *Biochemical Pharmacology*. **65**(10):1633-1642.

50. Florin, T., Zaoutis, T.E. and L.B. Zaoutis. 2008. Beyond Cat Scratch Disease: Widening Spectrum of *Bartonella henselae* Infection. *Pediatrics.* **121**(5):1413-1425.

51. Foulongne, V., Bourg, G., Cazavieille, C., Michaux-Charachon, S. and D. O'Callaghan 2000. Identification of *Brucella suis* Genes Affecting Intracellular Survival in an In Vitro Human Macrophage Infection Model by Signature-tagged Transposon Mutagenesis. *Infection and Immunity*. **68**:1297-1303.

52. Franchi, L., Malisan, F., Test, T. and R. Test. 2006. Ceramide Catabolism Critically Controls Survival of Human Dendritic Cells. *Journal of Leukocyte Biology*. **79**:166-172

53. Fuhrmann, O., M. Arvand, A. Gohler, M. Schmid, M. Krull, S. Hippenstiel, J. Seybold, C. Dehio, and N. Suttorp. 2001. *Bartonella henselae* Induces NF-kB-Dependent Upregulation of Adhesion Molecules in Cultured Human Endothelial Cells: Possible Role of Outer Membrane Proteins as Pathogenic Factors. *Infection and Immunity* **69**: 5088-5097.

54. Gao, L.-Y., and Y. A. Kwaik. 2000. The Modulation of Host Cell Apoptosis by Intracellular Bacterial Pathogens. *Trends in Microbiology.* **8**:306-311.

55. Gebran, S J, Newton, C A, Yamamoto, Y, Klein, T W and H.A. Friedman. 1994. Rapid Colorimetric Assay for Evaluating *Legionella pneumophila* Growth in Macrophages *In Vitro*. *Journal of Clinical Microbio*logy. **32**:127–130

56. M. Giacca. 2005. HIV-1 Tat, Apoptosis and the Mitochondria: A Tubulin Link. *Retrovirology*. **2**:7-11.

57. Gomez-Angelats, M., and J. A. Cidlowski. 2003. Molecular Evidence for the Nuclear Localization of FADD. *Cell Death and Differentiation*. **10**:791-97.

58. Goncalves, S., Cairney, J., Maroco, J., Oliveiral, M. M. and C. Miguell. 2005. Evaluation of Control Transcripts in Real-time RT-PCR Expression Analysis During Maritime Pine Embryogenesis. Planta **3**:556-63

59. Goping, I. S., Gross, A., Lavoie, J.N., Nguyen, M., Semmerson, R., Roth, K., Korsmeyer, S.J. and G. C. Shore. 1998. Regulated Targeting of BAX to Mitochondria. *Journal of Cell Biology* **143**(1):207-215.

60. Grassme, H., Andreas, J., Riehle, A., Schwartz, H., Berger, J., Sandhoff, K. and E. Gulbins. 2001. CD95 Signaling Via Ceramide-rich Membrane Rafts. *Journal of Biological Chemistry*. **276**(23):20589-20596.

61. Grassme, H., Cremesti, A., Kolesnick, R. and E. Gulbins. 2003. Ceramide-mediated Clustering is Required for CD95-DISC Formation. *Oncogene.* **22***(*35*)*:5457-70.

62. D. R. Green. 2003. Overview: Apoptotic Signaling Pathways in the Immune System. *Immunological Reviews*. **193**(1):5-9.

63. Grinberg, M., Sarig, R., Zaltsman, Y., Frumkin, D., Grammatikakis, N., Reuveny, E. and A. Gross. 2002. tBid Homooligomerizes in the Mitochondrial Membrane to Induce Apoptosis. *Journal of Biological Chemistry*. 277:12237-12245.

64. E. Gulbins. 2003. Regulation of Death Receptor Signaling and Apoptosis by Ceramide. *Pharmacological Research* **47**(5):393-399.

65. Gulbins, E., Dreschers, S., Wilker, B. and H. Grassme. 2004. Ceramide, Membrane Rafts and Infections. *Journal of Molecular Medicine.* **82**(6):357-63.

66. Gulbins, E. and P.L. Li. 2006. Physiological and Pathophysiological Aspects of Ceramide. *American Journal of Physiological Regulation and Intergrated Comparitive Physiol*ogy. **290**:R11-R26.

67. Gulbins, E., Jekle, A., Ferlinz, K., Grassme, H. and F. Lang. 2000. Physiology of Apoptosis. *American Journal of Renal Physiology*. **279**:F605-615.

68. C. Guoquing and D. V. Goeddel. 2002. TNF-R1 Signaling: A Beautiful Pathway. *Science*. 296(5573): 1634-1635.

69. Häcker, G. and S.F. Fischer. 2002. Bacterial anti-Apoptotic Activities. *FEMS Microbiology Letters.* **211**(1):1-6.

70. Haimovitz-Friedman A., Kolesnick R.N. and Z. Fuks. 1997. Ceramide Signaling in Apoptosis. *British Medical Bulletin*. **53**(3):539-553.

71. Hansson, G. K. and K. Edfeldt. 2005. Toll To Be Paid at the Gateway to the Vessel Wall. *Arteriosclerosis, Thrombosis, and Vascular Biology.* **25**:1085-1088

72. Harper, N., Hughes, M., MacFarlane, M. and G.M. Cohen. 2003. Fas-associated Death Domain Protein and Caspase-8 Are Not Recruited to the Tumor Necrosis Factor Receptor 1 Signaling Complex during Tumor Necrosis Factor-induced Apoptosis. *Journal of Biological Chemistry.* **278**(28): 25534-25541.

73. Hentschel, U., Steinert, M. and Hacker, J. 2000. Common Molecular Mechanisms of Symbiosis and Pathogenesis. *Trends in Microbiology* **8**(2): 226-230.

74. Hirata, H., Takahashi, A., Kobayashi, S., Yonehara, S., Sawai, H., Okazaki, T., Yamamoto, K. and M. Sasada. 1998. Caspases are Activated in a Branched Protease Cascade and Control Distinct Downstream Processes in Fas-induced Apoptosis. *Journal of Experimental Medicine.* **187**(4):587-600.

75. Holmström, T. H., Schmitz, I., Söderström, T.S., Poukkula, M., Johnson, V.L., Chow, S.C., Krammer, P.H. and J. E. Eriksson. 2000. MAPK/ERK Signaling in Activated T Cells Inhibits CD95/Fas-mediated Apoptosis Downstream of DISC Assembly. *The EMBO Journa**l***. **19**(20): 5418-5428.

76. Hotchkiss, R. S., Tinsley, K.W., Swanson, P.E and I. E. Karl. 2002. Endothelial Cell Apoptosis in Sepsis. *Critical Care Medicine.* **30**(5):S225-S228.

77. Hu, X., Yee, E., Harlan, J. M., Wong, F. and A. Karsan. 1998. Lipopolysaccharide Induces the Antiapoptotic Molecules, A1 and A20, in Microvascular Endothelial Cells. *Blood*. 92(8): 2759-2765

78. Huggett, A. St. G. and S. F. Suffolk. 1936. TheTrypanocidal Action of Azo Dyes. *Journal of Pharmacological Experimental Therapy.* **56**:188-193.

79. Hull, C., McLean, G., Wong, F., Patrick, J.D. and A. Karsan. 2002. Lipopolysaccharide Signals an Endothelial Apoptosis Pathway Through TNF Receptor-Associated Factor 6-Mediated Activation of c-Jun NH_2-Terminal Kinase. *Journal of Immunology.* **169**: 2611-2618.

80. Imaizumi, T., Itaya, H., Fujita, K., Kudoh, D., Kudoh, S., Mori, K., Fujimoto, K., Matsumiya, T.,Yoshida, H. and K. Satoh. 2000. Expression of Tumor Necrosis Factor-α in Cultured Human Endothelial Cells Stimulated With Lipopolysaccharide or Interleukin-1-α. *Vascular Biology*. **200**:410-414.

81. Karsan, A., E.Yee and J. M. Harlan. 1996. Endothelial Cell Death Induced by Tumor Necrosis Factor-α Is Inhibited by the Bcl-2 Family Member, A1. *Journal of Biological Chemistry*. **44**(1): 27201-27204.

82. Kataoka, T. 2005. The Caspase-8 Modulator c-FLIP. *Critical Review in Immunology*. **25**(1): 31-58.

83. Karvinen J, P. Hurskainen, S. Gopalakrishnan, D. Burns, U. Warrior and I. Hemmila. Homogeneous time-resolved fluorescence quenching assay (LANCE) for caspase-3. 2002. *Journal of Biomolecular Screening*. **7***:223-231*

84. Kempf, V. A. J., Volkmann B., Schaffer, M., Sander, C.A., Alitalo, K., Reiss, T. and I.B. Autenrieth. 2001. Evidence of a Leading Role for VEGF in Bartonella henselae-induced Endothelial Cell Proliferation. *Cell Microbiology*. **3**(9):623-32.

85. Kempf, V. A.J., Hitziger, N., Reiss, T. and I. B. Autenrieth. 2002. Do Plants and Human Pathogens Have Common Pathogenicity Strategy? *Trends in Microbiology.* **10**(6):269-275.

86. Kempf, V.A.J.; Lebiedziejewski, M., Alitalo, K., Wälzlein, J-H, Ehehalt, U., Fiebig, J., Huber, S., Schütt, B., Sander, C. A., Müller, S., Grassl, G., Yazdi, A. S., Brehm, B. and I. B. Autenrieth. 2004. Activation of Hypoxia-Inducible Factor-1 in Bacillary Angiomatosis Evidence for a Role of Hypoxia-Inducible Factor-1 in Bacterial Infections. *Circulation*. **111**: 1054-1062.

87. Kempf, V. A.J., Schairer, A., Neumann, D., Grassl, G.A., Lauber, K., Lebiedziejewski, M., Schaller, M., Kyme, P., Wesselborg, S. and I. Autenrieth. 2005. *Bartonella henselae* inhibits apoptosis in Mono Mac 6 cells. *Cellular Microbiology.* **7**(1): 91-104.

88. M.A. King. 2005. Antimycin A-Induced Killing of HL60 Cells: Apoptosis Initiated Within Mitochondria Does Not Necessarily Proceed Via Caspase-9. *Cytometry* **63A**: 69-76.

89. J.E. Kirby. 2004. In Vitro Model of *Bartonella henselae*-Induced Angiogenesis. *Infection and Immunity*. **72**(12):7315-7317

90. Kirby, J.E., and D.M. Nekorchuk. 2002. *Bartonella*-associated Endothelial Proliferation Depends on Inhibition of Apoptosis. *Proceedings of the National Academy of Science, USA.* **99**: 4656-4661.

91. Kluck, R.M., Bossy-Wetzel, E., Green, D.R. and D.D. Neumeyer. 1997. The Release of Cytochrome c from Mitochondria: A Primary Site for Bcl-2 Regulation of Apoptosis. *Science*. **275**(5303):1132-1136.

92. Kolsenick, R. 2002. The Therapeutic Potential of Modulating the Ceramide/Sphingomyelin Pathway. *Journal of Clinical Investigation.* **110**(1):38.

93. Kottke, T.J., Blajeski, A.L., Meng, X.W., Svingen, P.S., Ruchard, S., Mesner, P.W. Jr., Boerner, S.A., Samejima, K., Henriquez, N.V., Chilcote, T.J., Lord, J., Salmon, M., Earnshaw, W.C. and S.H. Kaufmann. 2001. Lack of Correlation Between Caspase Activation and Caspase Activity Assays in Paclitaxel-treated MCF-7 Breast Cancer Cells. *Journal of Biological Chemistry*. **277**(1): 804-815.

94. Korcheva, V., Wong, J., Lindauer, M., Jacoby, D.B., Iordanov, M.S. and B. Magun. 2007. Role of Apoptotic Signaling Pathways in Regulation of Inflammatory Responses to Ricin in Primary Murine Macrophages. *Molecular Immunology*. **44**(10): 2761-2771.

95. Krutzik, P. O. and G.P. Nolans. 2003. Intracellular Phospho-protein Staining Techniques for Flow Cytometry: Monitoring Single Cell Signalling Events. *Cytometry* Part A. **55A**: 61-70.

96. Kyong-Bok, C., Wong, F., Harlan, J.M., Chaudhary, P.M., Hood, L. and A. Karsan. 1998. Lipopolysaccharide Mediated Endothelial Apoptosis by a FADD-Dependent Pathway. *Journal of Biological Chemistry.* **273**(32): 20185-20188.

97. A. J. Lax and W. Thomas. 2002. How Bacteria Could Cause Cancer: One Step at a Time. *Trends in Microbiology.* **10**(6):293-299.

98. Lee A.K. and S. Falkow. 1998. Constitutive and Inducible Green Fluorescent Protein Expression in *Bartonella henselae*. *Infection & Immunity.* **66**(8):3964-7.

99. Liberto, M.C., Giovanni M., Lamberti, A.G., Barreca, G.S., Quirino, A. and A. Foca. 2003. *In vitro* Bartonella Quintana Infection Modulates the Programmed Cell Death of Endothelial Cells. *Diagnostic Microbiology and Infectious Diseases.* **45**(2):107-115.

100. Lidington E. A, Moyes D. L, McCormack A. M and M. L. Rose. 1999. A Comparison of Primary Endothelial Cells and Endothelial Cell Lines for Studies of Immune Interactions. *Transplant Immunology*. **7**:239–246.

101. K. J. Livak and T. D. Schmittgen. 2001. Analysis of Relative Gene Expression Data Using Real-Time Quantitative PCR and $2^{-\Delta\Delta C}{}_{T}$ Method. *Methods*. **25**: 402-408.

102. Lessene G., Czabotar P.E. and P. M.Colman. 2008. BCL-2 Family Antagonists for Cancer Therapy. *Nature Review of Drug Discovery*. **12**:989-1000.

103. Longley, D.B., Wilson T.R., McEwan M., Allen W.L., McDermott U., Galligan, L. and P.G. Johnston. 2006. c-FLIP Inhibits Chemotherapy-induced Colorectal Cancer Cell Death. *Oncogene*. **25**(6):838-48.

104. MacLachlan, T. K. and W.S. El-Deiry. 2002. Apoptotic Threshold is Lowered by p53 Transactivation of Caspase-6. *Proceedings of the National Academy of Science, USA.* **99**(14): 9492-9497.

105. Maeno, M., Oda, H., Yoshiie, K., Wahid, M.R., Fujimura, T. and S. Matayoshi. 1999. Live Bartonella henselae Enhances Endothelial Cell Proliferation Without Direct Contact. *Microbial Pathogenesis*. **27**:419-427.

106. Molloy, S. 2009. Type IV Secretion System: A Sprouting Interest in *Bartonella. Nature Review Microbiology.* 7(406):

107. McCord, A., Burgess, A., Whaley, W.O., Anderson, M. J. and B. E. Anderson. 2005. Interaction of Bartonella henselae with Endothelial Cells Promote Monocyte/Macrophage Chemoattractant Protein 1 Gene Expression and Protein Production and Triggers Monocyte Migration. *Infection and Immunity*. **73**(9): 5735-5742.

108. Mehock, J.R., Greene, C.E., Gherardini, F.C., Hahn, T-W and D.C. Krause. 1998. Bartonella henselae Invasion of Feline Erythrocytes In Vitro. *Infection and Immunity*. **66**(7): 3462-3466.

109. Micheau, O. and J. Tschopp. 2003. Induction of TNF Receptor 1-mediated Apoptosis via Two Sequention Signaling Complexes. *Cell*. **114**:181-190.

110. Minnick, M. F. and B. E. Anderson. 2000. *Bartonella* Interactions with Host Cells, p. 97-122. *In* O. a. Hacker (ed.), Sub-Cellular Biochemistry: Bacterial Invasion into Eukaryotic Cells, vol. **33**. Plenum, New York.

111. Minnick, M.F., Smitherman, L.S. and D. S. Samuels. 2003. Mitogenic Effect of *Bartonella bacilliformis* on Human Vascular Endothelial Cells and Involvement of GroEL. *Infection and Immunity*. **71**(12): 6933-6942.

112. Monack, D.M., Mecsas, J., Ghori, N. and S. Falkow. 1997. *Yersinia* Signals Macrophages to Undergo Apoptosis and YopJ is Necessary for This Cell Death. *Proceedings of the National Academy of Science, USA.* **94**(19): 10385-10390.

113. Moreira, M.E.C. and M.A. Barcinski. 2004. Apoptotic Cellular and Phagocytic Interplay Recognition and Consequences in Different Cell Systems. *Anais de Academia Brasileria de Ciencias*. **76**(1): 93-115.

114. Morgan, M., Thorburn, J., Pandolfi, P.P. and A. Thorburn. 2002. Nuclear and Cytoplasmic Shuttling of TRADD Induces Apoptosis Via Different Mechanisms. *Journal of Cell Biology*. **157**(6): 975-984.

115. Musso, T., Badalato, R., Ravarino, D., Stornello, S., Panzanelli, P., Merlino, C., Savoia, D., Carvallo, D., Ponzi, A.N. and M. Zucca. 2001, Interaction of *B. henselae* With the Murine Macrophage Cell Line J774: Infection and Proinflammatory Response. *Infection and Immunity*. **69**(10): 5974-5980.

116. Nagata, S., H. Nagase, K. Kawane, N. Mukae and H. Fukuyama. 2003. Degradation of chromosomal DNA during apoptosis. *Cell Death & Differentiation.* **10**(1): 108-116.

117. Nakazawa, Y., Kamijo, T., Koike, K. and T. Noda. 2003. ARF Tumor Suppressor Induces Mitochondrial-dependent Apoptosis by Modulation of Mitochondrial Bcl-2 Family Proteins. *Journal of Biological Chemistry*. **278** (30): 27888-27895.

118. Nanobashvili, J., Alicja Jozkowicz, Ch. Neumayer, A. Fügl, E. Sporn, P. Polterauer and I. Huk. 2003. Comparison of Angiogenic Potential of Human Microvascular Endothelial Cells and Human Umbilical Vein Endothelial Cells. *European Surgery*. **35**(4): 214-218.

119. R. Nunez. 2001. DNA Measurement and Cell Cycle Analysis by Flow Cytometry. *Current Issues in Molecular Biology.* **3**(3): 67-70.

120. Obeid, L. M., Linardic, C. M.., Karolak, L.. and Y. A. Hannun. 1993. Programmed Cell Death Induced by Ceramide. *Science.* **259**:1769-1771.

121. O'Callaghan, D., C. Cazaevieille, A. Allardet-Servent, M. L. Boschiroli, G. Bourg, V. Foulongne, P. Frutos, Y. Lulakov, and M. Ramuz. 1999. A Homologue of the Agrobacterium tumefaciens VirB and *Bordetella pertussis* Ptl Type-IV Secretion Systems is Essential for Intracellular Survival of *Brucella suis Molecular Microbiology*. **33**:1210-1220.

122. Ogretmen, B. and Y.A. Hannun. 2004. Biologically Active Sphingolipids in Cancer Pathogenesis and Treatment. *Nature Reviews Cancer*. **4**: 604-616.

123. Padmalayam, I., Karem, K., Baumstark, B. and R Massung. 2000. The Gene Encoding the 17-kDa Antigen of Bartonella henselae is Located Within a Cluster of Genes Homologous to the VirB Virulence Operon. *DNA Cell Biol*ogy. **19** (6):377-82.

124. Qu, X. and L. Qing. 2004. Abrin Induces HeLa Cell Apoptosis by Cytochrome *c* Release and Caspase Activation. *Journal of Biochemistry and Molecular Biology*. **37**(4): 445-453.

125. Rao, P.V. Lakshmana, Jayaraji, R., Bhaskar, A.S.B, Kumar, Om, R. Bhattacharya, R., Saxena, Parag, Dash, P.K.and R. Vijayaraghavan. 2005. Mechanism of Ricin-induced Apoptosis in Human Cervical Cancer Cells. *Biochemical Pharmacology*. **69**(5): 855-865.

126. Radonic, A., Thulke, S., Mackay, I.M., Landt, O., Seigert, W. and A. Nitsche. 2004. Guideline to Reference Gene Selection for Quantitative Real-time PCR. *Biochemical and Biophysical Research Communication.* **313**:856-862.

127. Rajashekara, G., Glover, D. A., Krepps, M. and G. A. Splitter. 2005. Temporal Analysis of Pathogenic Events in Virulent and Avirulent Brucella melintensis Infections. *Cellular Microbiology*. **7**(10): 1459-1473.

128. Rath, G., Schneider, C., Langlois, B., Sartelet, H., Morjani, H., Btaouri, H.E.L., Dedieu, S. and L. Martiny. 2008. De novo Ceramide Synthesis is Responsible for the Anti-tumor Properties of Camptothecin and Doxorubicin in Follicular Thyroid Carcinoma. 2008. *International Journal of Biochemistry & Cell Biology*. ePub November 5 2008.

129. Resto-Ruiz, Sandra I., MIchael Schmeiderer, Debra Sweger, Catherine Newton, Thomas W. Klein, Herman Friedman and Burt E. Anderson. 2002. Induction of a Potential Paracrine Angiogenic Loop between Human THP-1 Macrophages and Human Microvascular Endothelial Cells during *Bartonella henselae* Infection. **70**(8): 4564-4570.

130. Reiss, T., Andersson, S. G.E., Lupas, A., Schaller, M., Schafer, A., Kyme, P., Martin, J., Walzlien, J-H, Ehehalt, U., Lindroos, H., Schirle, M., Nordheim, A., Autenrieth, I. B. and V. A. J. Kempf. 2004. Bartonella Adhesin A Mediates a Proangiogenic Host Cell Response. *Journal of Experimental Microbiology* (JEM). **200**(10): 1267-1278.

131. Rodriquez, J. and Yuri Lazebnik. 1999. Caspase-9 and APAF-1 form an Active Holoenzyme. *Genes and Development*. **13**:3179-3184.

132. Rudiger, A., Stotz, M. and M. Singer. 2008. Cellular Processes in Sepsis. *Swiss Medical Weekly*. **138**(43-44): 629-634.

133. P. P. Ruvolo. 2001. Ceramide Regulates Cellular Homoeostasis Via Diverse Stress Signaling Pathways. *Leukemia*. **15**:1153-1160.

134. P. P. Ruvuolo. 2003. Intracellular Signal Transduction Pathways Activated by Ceramide and Its Metabolites. *Pharmacological Research*. **47**(5): 383-392.

135. Salvatore, P., Casamassimi, A., Sommese, L., Fiorito, C., Ciccodicola, A., Rossiello, R., Avallone, B., Grimaldi, V., Costa, V., Rienzo, M., Colicchio, R., Williams-Ignarro, S., Pagliarulo, C., Prudente, M.E., Abbondanza, C., Lambert, F., Baroni, A., Bucommino, E., Farzati, B., Antonietta, M., Ignarro, L.J. and C. Napoli. 2008. Detrimental Effects of *B. henselae* are Counteracted by L-Arginine and Nitric Oxide in Human Endothelial Progenitor Cells. *Proceedings of the National Academy of Science, USA*. **105**(27): 9427-9432.

136. Salvesen, G. and V.M. Dixit. 1999. Caspase Activation: The Induced Proximity Model. *Procedings of the National Academy of Science, USA.* **96**: 10964-10967.

137. Saini, L. S., Galsworthy, S.B., John, M.A. and M.A. Valvano. 1999. Intracellular Survival of Burkholderia cepacia Complex Isolates in the Presence of Macrophage Cell Activation. *Microbiology.* **145**:3465-3475.

138. A. Samadi. 2007. Ceramide-induced Cell Death in Lens Epithelial Cells. *Molecular Vision*. **13**:1618-26.

139. Screaton, R. A., Kiessling, S., Sansom, O. J., Millar, C. B., Maddison, K., Bird, A., Clarke, A. R. and S. M. Frisch. 2003. Fas-associated Death Domain Protein Interacts With Methyl-CpG Binding Domain Protein 4: A Potential Link Between Genome Surveillance and Apoptosis. *Proceedings of the National Academy of Science, USA.* **100**(9): 5211-5216.

140. Scheidegger, F., Ellner, Y., Guye, P., Rhomberg, T.A., Weber, H., Augustin, H. G. and C. Dehio. 2009. Distinct Activities of *Bartonella henselae* Type IV Secretion Effector Proteins Modulate Capillary-like Sprout Formation. *Cellular Microbiology*. **11**(7): 1088-1101.

141. Schmid, M.C., Schulein, R., Dehio, M., Denecker, G., Carena, I. and C. Dehio. 2004. The VirB Type IV Secretion System of *Bartonella henselae* Mediates Invasion, Proinflammatory Activation and Antiapaoptotic Protection of Endothelial Cells. *Molecular Microbiology*. **52**(1): 81-92.

142. Schmid, M.C., Scheidegger, F., Dehio, M., Balmelle-Devaux, N., Schulein, R., Guye, P., Chennakesava, C.S., Biederman, B. and C. Dehio. 2006. A Translocated Bacterial Protein Protects Vascular Endothelial Cells from Apoptosis. *PLoS Pathogen.* **2**(11): 1083-1097.

143. Schubert, K.M., Scheid, M.P. and V. Duronia. 2000. Ceramide Inhibits Protein Kinase B/Akt by Promoting Dephosphorylation of Serine 473. *Journal of Biological Chemistry.* **18**:13330-13335.

144. J. B. Schulz. 2008. Update on the Pathogenesis of Parkinson's Disease. *Journal of Neurology*. **255** Suppl 5:3-7.

145. Schulein, R. and C. Dehio. 2002. The VirB/VirD4 Type IV Secretion System of *Bartonella* is Essential for Establishing Intraerythrocytic Infection. *Molecular Microbiology*. **46**(4):1053-1057.

146. Y. Shi. 2002. Mechanisms of Caspase Activation and Inhibition during Apoptosis. *Molecular Cell*. **9**:459-470.

147. Singer, S.J. and G.L. Nicolson. 1972. The Fluid Mosaic Model of the Structure of Cell Membranes. *Science.* **175**(23):720-31.

148. Siskind, L.J., Kolsenick, R.N. and M. Colombini. 2002. Ceramide Channels Increase the Permeability of the Mitochondrial Outer Membrane to Small Proteins. *Journal of Biological Chemistry*. 277(30): 26796-26803.

149. Slater, C.T., Hamilton, L. and K. Hamilton. 1994. Rochalimaea Species Stimulate Human Endothelial Cell Proliferation and Migration In Vitro. *Journal of Laboratory Clinical Medicine*. **124**:521–528

150. Slater L.N, Welch D.F, Hensel D., Coody D.W. 1993. A New Recognized Fastidious Gram-negative Pathogen as a Cause of Fever and Bacteremia. *New England Journal of Medicine*. **323**:1587-93.

151. Slee, E.A., Harte, M.T., Luck, R.T., Wolf, B.B., Caisano, C.A., Neumeyer, D.D., Wang, H-G, Reed, J.C., Nicholson, D.W., Alnemri, E.S., Green, D.R. and S. J. Martin. 1999. Ordering the Cytochrome c-initiated Caspase Cascade: Hierarchical Activation of Caspases-2, -3, -6, -7, -8 and -10 in a Caspase-9-dependent Manner. *Journal of Cell Biology*. **144**(2): 281-292.

152. Slee, E. A., Adrian, C. and S. J. Martin. 2001. Executioner Caspase-3, -6, and -7 Perform, Distinct, Non-redundant Roles during the Demolition Phase of Apoptosis. *Journal of Biological Chemistry*. **276**(10): 7320-7326.

153. Smith, E. L. and E.H. Schuchman. 2008. The Unexpected Role of Acid Sphingomyelinase in Cell Death and the Pathophysiology of Common Diseases. *FASEB Journal*. **22**: 3419-3431.

154. Sohn, D., Gudrum, T.Essmann, Frank, Schulze-Osthoff, Klauss, Levkau, Bodo and Reiner U. Janicke. 2006. The Proteosome is Required for Rapid Initiation of Death-Receptor-Induced Apoptosis. *Molecular and Cellular Biology*. **26**(5): 1967-1978.

155. Suslov. O. and D.A. Steindler. 2005. PCR Inhibition by Reverse Transcriptase Leads to an Overestimation of Amplification Efficiency. *Nucleic Acids Research*. **33**(20): e181.

156. Tao, F., Hang, L., Hu, H., Shi, L., McCarty, G.A., Nance, D.M., Greenberg, A.H. and G. Zhong. 1998. Inhibition of Apoptosis in Chlamydia-infected Cells: Blockade of Mitochondrial Cytochrome c Release and Caspase Activation. *Journal of Experimental Medicine*. **187**(4): 487-96.

157. Tang, D., Lahti, J. M. and V. J. Kidd. 2000. Caspase-8 Activation and Bid Cleavage Contribute to the MCF-7 Cellular Execution in a Caspase-3-dependent Manner during Staurosporine-mediated Apoptosis. *Journal of Biological Chemistry.* **275**(13): 9303-9307.

158. A. Thorburn. 2004. Death Receptor-Induced Cell Killing. *Cellular Signalling*. **16**(2): 139-144.

159. Thorburn, J., Bender, L.M., Morgan, M. J. and A. Thorburn. 2003. Caspase- and Serine Protease-dependent Apoptosis by the Death Domain of FADD in Normal Epithelial Cells. *Molecular Biology of the Cell*. **14**(1): 67-77.

160. Torrecillas, Alejandro, Aroca-Aguilar, J. Daniel, Aranda, Francisco J., Gajate, Consuelo, Mollinedo, Faustino, Corbalán-García, Senena , de Godos, Ana and Juan C. Gómez-Fernández. 2006. Effects of the Anti-neoplastic Agent ET-18-*O*CH_3 and some Analogs on the Biophysical Properties of Model Membranes. *International Journal of Pharmeceuticals*. **318**(1-2): 28-40.

161. True, A. L., A. Rahman, and A. B. Malik. 2000. Activation of NF-kB Induced by H_2O_2 and TNF-a and Its Effects on ICAM-1 Expression in Endothelial Cells. *American Journal of Physiology-Lung Cellular & Molecular Physiology*. **279**:L302-11.

162. van Bitterswijk, Wim J., van der Luit, A.H., Veldman, R.J., Verheij, M. and J. Borst. 2003. Ceramide: Second Messenger or Modulator of Membrane Structure and Dynamics? *Biochemistry Journal*. **15**(369Pt2):199-211.

163. van Engeland, M., Nieland, L J. Ramaekers, F C. Schutte, B. Reutelingsperger, C P. 1998. Annexin V-affinity Assay: A Review on an Apoptosis Detection System Based on Phosphatidylserine Exposure. *Cytometry*. **31**(1):1-9, 1998.

164. Vandesompele, J., De Preter, K., Pattyn, F., Poppe, B., Van Roy, N., De Paepe, A. and F. Speleman. 2002. Accurate Normalization of Real-time Quantitative RT-PCR Data by Geometric Averaging of Multiple Internal Control Genes. *Genome Biology*. **3**(7): 34.1-34.11.

165. Walsh, C.M., Luhrs, K.A. and A.F. Arechiga. 2003. The "Fuzzy Logic" of the Death-Inducing Signaling Complex in Lymphocytes. *Journal of Clinical Immunology*. **23**(5): 333-353.

166. Wang. X. 2001. The Expanding Role of Mitochondria in Apoptosis. *Genes and Development*. **15**(22): 2922-2933.

167. Ware, C.F. 2003. The TNF Family. *Cytokine and Growth Factor Reviews*. **14**(3-4):181-184.

168. Wear, D.J., Margileth, A.M., Hadfield, T.L., Fischer, G.W., Schlagel, C.J. and F.M. King. 1983. Cat-scratch Disease: A Bacterial Infection. *Science*. **221**(4618): 1403-1405.

169. Wesche-Soldato D.E, Swan, R.Z., Chung, C.S. and A. Ayala. 2007. The Apoptotic Pathway as a Therapeutic Target in Sepsis. *Current Drug Targets*. **8**(4):493-500.

170. Winer, J., Kwang, C., Jung, S., Shackel, I and P.M. Williams. 1999. *Analytical Biochemistry*. **270**:41-49.

171. Xia, Y., Wang, J., Liu, T.J., Yung, W.K., Hunter, T. and Z. Lu. 2007. c-Jun Downregulation by HDAC3-dependent Transcriptional Repression Promotes Osmotic Stress-Induced Cell Apoptosis. *Molecular Cell.* **25**(2): 219-232.

172. Xu Y, Swerlick RA, Sepp N, Bosse D, Ades EW, Lawley TJ. 1994. Characterization of Expression and Modulation of Cell Adhesion Molecules on An Immortalized Human Dermal Microvascular Endothelial Cell Line (HMEC-1). *Journal of Investigative Dermatology.* **102**(6):833-7.

173. Yang, J., Xuesong L., Bhalla, K., Kim, C.N., Ibrado, A.M., Cai, J., Peng, T-I, Jones, D.P. and X. Wang. 1997. Prevention of Apoptosis by Bcl-2: Release of Cytochrome c from Mitochondria Blocked. *Science.* **275**(5303): 1129-1132.

174. Zahringer, Ulrich, Buko, L., Knirel, Y.A., van der Akker, W.M.R., Hiestand, R., Heine H. and C. Dehio. 2004. Structure of Biological Activity of the Short-chain Lipopolysaccharide from *Bartonella henselae* ATCC 49882. *Journal of Biological Chemistry*. **20**: 21046-21054.

175. Zhang, X.D., Gillespie S.K. and Peter Hersey. 2004. Staurosporine Induces Apoptosis of Melanoma by Both Caspase-dependent and -independent Apoptotic Pathways. Molecular Cancer Therapy. **3**: 187-197.

176. Zhang D.X., Zou A.P. and P.L. Li. 2002. Ceramide-induced Activation of NADPH Oxidase and Endothelial Dysfunction in Small Coronary Arteries. *American Journal of Physiology and Heart Circulation Physiology*. **284**(2):H605-12

177. Zimmermann, K.C. and D.R. Green. 2001. How Cells Die: Apoptosis Pathways. *Journal of Allergy and Clinical Medicine.* **108**(4):S99-S103.